System Design and Performance Analysis of Wireless Body Area Networks

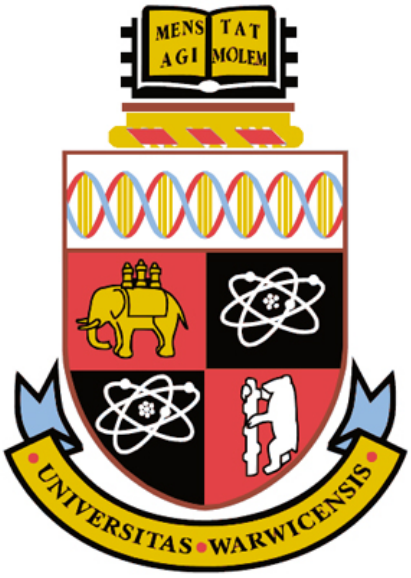

Yangzhe Liao

A thesis submitted to the University of Warwick in partial fulfilment of the requirements for the degree of

Doctor of Philosophy

School of Engineering

June 2017

Table of Contents

List of Tables

List of Figures

Acknowledgements

First and foremost, I would like to express my deepest thanks to my first supervisor Dr Mark Leeson, whose guidance and inspiration have given me the confidence for the development of the work. I would also like to thank Dr Matthew Higgins for his suggestive advice and help.

Many thanks to the School of Engineering for the financial support. My live experience at the University of Warwick has been really enjoyable thanks to the people of different nationalities and research interests. I would also like to thank all members of the Communication Networks Laboratory for providing wonderful research environment and the fruitful discussions. Moreover, I would express my sincere appreciation to my PhD viva examiners Dr Yunfei Chen (Warwick) and Dr Pavlos Lazaridis (Huddersfield), for their insightful and suggestive guidance in the thesis.

Moreover, it is my pleasure to express my thanks to my fiancee who was always stand by my side. Finally, I would express my special thanks to my parents and family members for their support, encouragement and love.

Declaration

This thesis is submitted in partial fulfilment for the degree of Doctor of Philosophy under regulations formulated by the School of Engineering, University of Warwick.

I herewith declare that this thesis contains my own research performed under the supervision of Dr Mark Leeson and Dr Matthew Higgins, without the assistance of third parties. The research materials have not been submitted in any previous application for a degree at any other university.

List of Publications

Journal publications

[1] **Y. Liao**, M. S. Leeson, M. D. Higgins, and C. Bai, "Analysis of in-to-out wireless body area network systems: towards QoS-aware health Internet of Things applications," *Electronics*, Special Issue on Wearable Electronics and Embedded Computing Systems for Biomedical Applications, vol. 5, Article 28, 26 pages, 2016.

[2] **Y. Liao**, M. S. Leeson, and M. D. Higgins, "A communication link analysis based on biological implant wireless body area networks," *Applied Computational Electromagnetics Society Journal*, Special Issue on Bio-Electromagnetic Methods and Applications Vol. 31, pp. 619-628, 2016.

[3] **Y. Liao**, M. S. Leeson, and M. D. Higgins, "Flexible quality of service model for wireless body area sensor networks," *IET Healthcare Technology Letters*, Special Issue on Decision Support for Person-Centred Healthcare, Vol. 3, pp. 12-15, 2016.

Conference publications

[1] **Y. Liao**, M. S. Leeson, M. D. Higgins, and C. Bai, "An Incremental Relay Based Cooperative Routing Protocol for Wireless In-body Sensor Networks," in *IEEE 8th International Conference on Wireless and Mobile Computing, Networking and Communications (WiMob)*, New York, USA, pp. 1-6, 2016.

[2] **Y. Liao**, M. S. Leeson, and M. D. Higgins, "Analysis of PC and SGA models for an ultra wide-band ad-hoc network with multiple pulses," in *IEEE 20th International*

Workshop on Computer Aided Modelling and Design of Communication Links and Networks (CAMAD), Guildford, UK, pp. 246-250, 2015.

[3] **Y. Liao**, M. S. Leeson, and M. D. Higgins, "An in-body communication link based on 400 MHz MICS band wireless body area networks," in *IEEE 20th International Workshop on Computer Aided Modelling and Design of Communication Links and Networks (CAMAD)*, Special Session on Body Centric Wireless Communication and Networking from Meter to the Nano-scale, Guildford, UK, pp. 152-155, 2015.

Abstract

One key solution to provide affordable and proactive healthcare facilities to overcome the fast world population growth and a shortage of medical professionals is through health monitoring systems capable of early disease detection and real-time data transmission leading to considerable improvements in the quality of human life. Wireless body area networks (WBANs) are proposed as promising approaches to providing better mobility and flexibility experience than traditional wired medical systems by using low-power, miniaturised sensors inside, around, or off the human body and are employed to monitor physiological signals. However, the design of reliable and energy efficient in-body communication systems is still a major research challenge since implant devices are characterised by strict requirements on size, energy consumption and safety. Moreover, there is still no agreement regarding QoS support in WBANs.

The first part of this work concentrates on the design and performance evaluation of WBAN communication systems involving the ‘in-body to in-body’ and ‘in-body to on-body’ scenarios. The essential step is to derive the statistical WBAN path loss (PL) models, which characterise the signal propagation energy loss transmitting via intra-body region. Moreover, from the point of view of human body safety evaluation, the obtained specific absorption rate (SAR) values are compared with the latest Institute of Electrical and Electronics Engineers (IEEE) 802.15.6 Task Group technical standard and the International Commission on Non-Ionizing Radiation Protection (ICNIRP) safety guidelines. Link budget analysis is then presented using a range of energy-efficient modulation schemes, and the results are given including the

transmission distance, data rate and transmitting power in individual sections. On the other hand, major quality of service (QoS) support challenges in WBANs are discussed and investigated. To achieve higher lifetime and lower network energy consumption, different data routing protocol methods, including incremental relaying and the two-relay based routing technique are taken into account. A set of key QoS metrics for linear mathematical models is given along with the related subjective functions. The incremental relaying routing protocol promises significant enhancements in in-body WBAN network lifetime by minimising the overall communication distance while the two-relay based routing method achieves better performance in terms of emergency data transmission and high traffic condition, QoS-aware WBANs design. Moreover, to handle real-time high data transmission applications such as capsule endoscope image transmission, a flexible QoS-aware wireless body area sensor networks (WBASNs) model is proposed and evaluated that can bring novel solutions for a realistic multi-user hospital environment regarding information packet collision probability, manageable numbers of sensor nodes and a wide range of data rates.

Abbreviations

AWGN: additive white Gaussian noise

BER: bit error rate

BPSK: binary phase-shift keying

ECG: electrocardiograms

EEG: electroencephalography

EMC: electromagnetic compatibility

FCC: Federal Communication Commission

FDTD: finite-difference time domain

I2O: In-to-out

ICNIRP: International Commission on Non-Ionizing Radiation Protection

IEEE: Institute of Electrical and Electronics Engineers

ISM: industrial, scientific and medical

MAC: media access control

MICS: medical implant communication service

MIDA: multimodal imaging-based detailed anatomical

MUI: multi-user interference

P2P: peer to peer

PAM: pulse amplitude modulation

PC: pulse collision

PDF: probability density function

PEC: perfect electric conducting

PL: path loss

PPM: pulse position modulation

QoS: quality of service

QPSK: quadrature phase shift keying

RF: radio frequency

Rx: The receiver

SAR: specific absorption rate

SGA: standard Gaussian approximation

TDMA: time division multiple access

THMA: time hopping multiple access

TH: time hopping

Tx: The transmitter

UWB: ultra wide-band

WMTS: wireless medical telemetry services

WPAN: wireless person area network

WSN: wireless sensor network

3D: three-dimensional

16PSK:16 phase shift keying

16QAM: 16-quadrature amplitude modulation

CHAPTER 1.

Introduction

1.1 Background

There is a rapidly accelerating global trend towards population ageing and average life expectancy has increased significantly from an estimated 67.6 years in 2000 to around 73.3 years in 2019; the total number of population aged 65 and above is anticipated to more than 604 million worldwide in 2020 [1-2]. Moreover, the current amount of people who have chronic diabetes, cardiovascular disease, Parkinson's disease or asthma is higher than 387 million, and this figure is expected to increase to 592 million by 2035 [3]. Furthermore, current trends in healthcare, and medical expenditure are such that it is estimated to consume above 20% of gross domestic product in 2022, which is a huge risk to the world economy [4].

The motivation for future healthcare systems from the increasing medical applications is that the majority of diseases can be preserved or treated under the condition that they can be sensed or detected in their early stages [1, 4]. The modern healthcare systems are widely based on wired centralised networks where patients are only able to receive diagnostic or treatment by physicians or doctors in hospitals. However, current information and communications technology (ICT) enabled networking in hospital monitoring services suffer from a lack of privacy and bring low-mobility to the patients. As indicated in [5], this commonly used method will become unsustainable with the future trends because of the overloaded demand, slow data rate

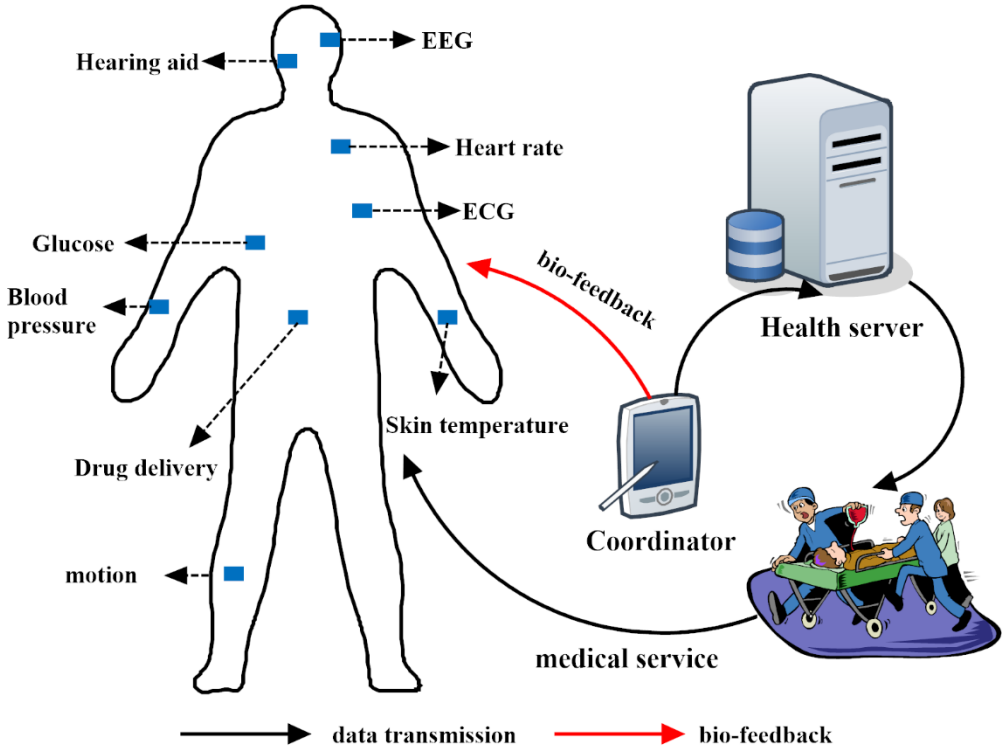

Figure 1.1 Example of a simple health monitoring system network architecture.

and high costs. On the other hand, the authors in [6] state that the characteristics of future medical systems should evolve from the centralised model to a pervasive model and decentralised provision customised healthcare services.

1.2 Research motivations

Technology-driven improvements to current healthcare practices have prompted the wireless nature of the communication system, and the wide range of body sensors offer many novel, useful and innovative applications to improve the people's life quality [2, 6]. As stated earlier, patients experience extremely low physical mobility because of the wired distributed healthcare systems. To overcome this technical challenge, wireless communication healthcare systems that can be applied to monitor physiological parameters for different diseases are recommended as an emerging technique. As shown in Figure 1.1, a wireless healthcare system allows for continuous

monitoring of patients' physiological attributes not only for implanted scenarios such as drug delivery, cardiovascular disease detection and glucose, but also for measurement in on-body applications of parameters via electrocardiograph (ECG), electroencephalography (EEG), heart rate, blood pressure, motion detection and skin temperature [4]. Body area communications are required to support a broad range of data rates for multiple kinds of applications. In particular, in-body medical applications such as video surveillance systems and drug delivery requiring high data rates up to a few Mbps, while on-body signals such as ECG and EEG require relative low data rates of within the kbps range because their parameters are varying very slowly. The healthcare system should also be able to transmit the medical information to the external coordinator, which is capable of forwarding the collected data to the health server or offering timely bio-feedback to the patient under emerging situations. Moreover, [6] reported that substantial contributions to remote telemedicine support systems that make patients' health status monitoring feasible by doctors/nurses via the health Internet of Things (IoT) [2].

As an emerging short-range wireless communication technology, a wireless body area network (WBAN) is mainly expected to be beneficial and convenient for high-quality healthcare services. It also capable of supporting new possibilities for entertainment, sports training and many other areas, by networking various body sensors to establish a WBAN to monitor personal health information [7-8]. The first step to designing the WBAN system is to select the proper transmission frequency band and networking technologies [4]. In-body channel models are included in the IEEE 802.15.6 technical report, but they only refer to the frequency band between 402 MHz and 405MHz and it has been reported in [9] that this cannot satisfy medical application requirements. Deploying the human body as the signal transmission medium, the safety concern of

the human body and tissues has the highest priority compared with other wireless communication techniques. IEEE 802.15 Task Group has established the wireless communication standardisation of WBAN to optimise network energy consumption and safety guidelines for medical and non-medical applications [4, 11]. In [4], it has been shown that signal energy absorption leads to the body temperature increase. Once the body temperature is above the normal values, adverse biological effects may result in irreversible tissue damage and human health damage [4]. It is, therefore, crucial to limit the signal transmission power to ensure human safety in body area communications.

WBAN communication systems support should include not only wearable data transmission, but also cover in-body communication links [12]. To date, there is very limited research work on propagation loss or channel modelling within the human body [13-16]. Hence, advanced and accurate in-body communication link modelling efforts are of considerable significance as this is the essential step to the characteristics of the in-body WBAN propagation. The past efforts in this research work area focus on semi-empirical in-body path loss (PL) and simply investigated the human body models as a multi-layer structure [4, 13-15].

Another major challenge is the modelling. The communication system performance of implant WBANs is significantly influenced by the transmission environment and frequency band [13, 17-18]. The bit error rate (BER) performance evaluation can then be obtained by the static in-body channels. A series of communication parameters can be derived including the link budget, data rate, transmission distance and the minimum required transmitting power [4]. Due to technical challenges and specific WBAN safety requirements, numerous proposed ad hoc or wireless sensor network (WSN) routing protocols are not applicable to in-body WBAN communications [19-22]. The

key objective of the protocols is to prolong the WBAN communication system lifetime. This can be achieved by employing a relay-based routing scheme, which is capable of reducing the overall data transmission distance [22]. However, it has been demonstrated that the current single relay and two relay-based schemes offer low-energy efficiency and thus have difficulty in supporting quality of service (QoS) data transmission requirements [20].

QoS techniques in WBANs have distinctive requirements for a series of target-specific healthcare applications. Considering extremely high data rate applications such as video transmission, the ultra wide-band (UWB) wireless communication method is proposed as an effective solution to offer more than the 30 Mbps data rate requirement [17]. As demonstrated in [23], pulse position modulation is commonly adopted for impulse radio UWB systems and outperforms other modulation methods. Another technique is the time hopping (TH) coding approach, which can be applied to handle network multiple user identity issues within the same WBAN. The pulse collision probability should be controlled to be low enough in order to assure that medical sensors within the same WBAN communication system achieve satisfactory performance [24]. The design of a flexible QoS-aware WBAN communication model can be considered for extremely high data transmission rate and to efficiently overcome multi-user interference requirements [6, 25].

1.3 Research objectives

Recent technological developments of advanced very low power consumption microelectronics, combined with improvements in wireless communications, is resulting in a rapidly increasing demand for wireless communications in the human body area [4]. Differing from numerous existing short-range communication

techniques such as Bluetooth and ZigBee, a WBAN concentrates on data collection and transmission just in the human body area [7].

In a scenario of body area communication systems, different types of body sensor nodes that are either located inside or near the human body are organised in a small-scale network to collect physiological signals and promise reliable data transmission to the medical professionals via the Internet or other network connections [13]. The demand for those requirements is promoting health research institute and manufacturer to design affordable, and energy efficient means to enhance healthcare information delivery. The aim of WBANs also encompasses supporting remote medical services and cost reduction by enabling patient and health systems to be connected anytime and anywhere to support the management of chronic care outside traditional settings [12].

In this thesis, statistical in-body PL models that describe the signal transmission distance between the transmitter and receiver are obtained by using advanced electromagnetic solver from Computer Simulation Technology (CST[1]), based on different heterogeneous and innovative three-dimensional (3D) virtual human body models. Furthermore, it should be noted that all other simulation cases throughout this thesis are implemented employing the mathematical computing software MATLAB[2].

1.4 Research contributions

The effort of this PhD thesis is to focus on wireless body area communications, in-body channel modelling, system performance and data routing design. As demonstrated in the last section, the selections are motivated by some fundamental aspects: (a) as will be presented in Chapter 2, the WBAN technology is proposed as a

[1] CST is a user-friendly electromagnetic simulation software.
[2] MATLAB is a mathematical computing software developed by MathWorks.

particular type of WSN and has been recommended as the most promising type of body area communications among different communication modes discussed in the literature [4]; (b) to provide a comprehensive review of this state-of-art in the field of current technology standards, available frequency bands and safety guidelines. As described in Sections 2.1 and 2.2, traditional communication models and outcomes in WSNs are not applicable to the design of in-body communication systems and routing protocols; (c) to investigate implant WBAN system performance, which consists of numerous parameters such as transmission energy attenuation, network power consumption, data rate, channel reliability and transmission distance [1-5]. The research objectives addressed in this thesis have been identified to meet this requirement, and are summarised in the following.

The first research task is to investigate the communication system performance based on a detailed, comprehensive multi-modal imaging-based anatomical human head model. Since the human cephalic region is an area in which future implants are likely, WBAN system design is thus worthy of attracting significant attention. Moreover, suitable curve fitting approaches for the PL model have been considered. The BER performance is demonstrated based on the obtained fading channel by employing binary phase shift keying (BPSK) and pulse-amplitude modulation (PAM). Additionally, possible transmission distances for a broad range of data transmission rates for predetermined acceptable BERs are accomplished.

The second research objective is to analyse the communication system performance based on a human frontal thorax model. The in-to-out (I2O) WBAN communication channel suffers significant power attenuation due to human body/tissues energy absorption. The path loss model can be used for health IoT communication channel

design as well as determining the system link budget. The system performance for the I2O WBAN is ascertained using a series of energy efficient modulation methods.

Owing to the existing technical constraints of the in-body sensor node design, the third research objective of this thesis is to analyse high energy efficient routing protocols to reduce the overall power consumption and prolong the network lifetime. Relay-based protocol techniques have been considered to decrease the power consumption of the implanted sensor nodes by minimising the transmission distance [21]. An incremental routing protocol is thus proposed and compared with the existing two relay-based routing technique.

Finally, another significant contribution focuses on an extremely high date rate UWB-based WBASN model. Instead of using the previously presented RF signals for analysing the system performance, the thesis extends a new technique proposed by IEEE 802.15.6 as a potential short-range high data-rate communication technology in WBANs [17]. Also, it addresses the question of flexible QoS management regarding data rate, the number of users and the transmission reliability. The results demonstrate that higher data rates can support fewer users within the same WBAN network. Also, the results demonstrate that UWB-based technology is a suitable candidate to overcome multi-user interference (MUI) [23].

1.5 Thesis outline

The PhD thesis is organised into seven chapters. The first chapter is the introduction chapter, and the last chapter summarises the entire thesis along with future research plans, and the remaining five chapters each demonstrate an individual task that was accomplished. The highlights of those chapters are listed as follows.

In Chapter 1, the introduction, the motivation, the research objectives and the contributions of this thesis are outlined.

In Chapter 2, a detailed demonstration of WBAN technology is presented. In contrast to WSNs, WBANs have two main types of communication systems: implant and wearable communication networks. Multiple technical requirements are demonstrated, followed by the research aspects and potential medical and non-medical applications and services that may benefit from WBANs.

In Chapter 3, the design of a wireless in-body WBAN system is given, based on a high-resolution human head model. An in-body channel PL model is obtained by using an advanced 3D human head model in conjunction with CST software. Moreover, the relationship between link budget and the transmission distance is presented.

In Chapter 4, the design of a wireless I2O WBAN system is demonstrated which is based on the advanced human frontal thorax model. The BER evaluation for this communication channel employing numerous energy efficient modulation schemes is investigated. The results show that the BPSK offers 1.6 cm of reliable transmission distance at a high data rate of 30 Mbps.

In Chapter 5, an incremental relaying routing protocol is given, which aims to minimise the overall communication distance. The linear mathematical formulas are given along with a series of constraints functions. This relay-based cooperative QoS-aware routing scheme for the I2O WBAN channel is investigated regarding network lifetime, transmission delay, average network energy consumption and the number of transmission packets. In addition, an existing two-relay based routing technique is reviewed.

In Chapter 6, a flexible QoS-aware model for wireless body area sensor networks WBASNs is presented, followed by a description of the proposed UWB communication technology. Moreover, numerous existing communication models are investigated and compared. The proposed WBASN is capable of supporting fast data transmission, adaptive schedule medium access control (MAC), and effectively overcome MUI.

Chapter 7 summarises and concludes the entire thesis, and presents future research topics that can be considered.

References

[1] D. T. Jamison *et al.*, "Global health 2035: a world converging within a generation," *The Lancet*, vol. 382, no. 9908, pp. 1898-1955, 2013.

[2] S. R. Islam, D. Kwak, M. H. Kabir, M. Hossain, and K. S. Kwak, "The internet of things for health care: a comprehensive survey," *IEEE Access*, vol. 3, pp. 678-708, 2015.

[3] L. Guariguata, D. Whiting, I. Hambleton, J. Beagley, U. Linnenkamp, and J. Shaw, "Global estimates of diabetes prevalence for 2013 and projections for 2035," *Diabetes research and clinical practice*, vol. 103, no. 2, pp. 137-149, 2014.

[4] H. B. Li and K. Y. Yazdandoost, *Wireless body area network*: River Publishers, 2010.

[5] R. Spanjers, W. Hasselbring, R. Peterson, and M. Smits, "Exploring ICT enabled networking in hospital organisations," in *Proceedings of the* IEEE *Annual Hawaii International Conference on System Sciences*, Hawaii, USA, pp. 1-10, 2001.

[6] Y. Liao, M. S. Leeson, M. D. Higgins, and C. Bai, "Analysis of in-to-out wireless body area network systems: towards QoS-aware health Internet of Things applications," *Electronics,* vol. 5, no. 3, p. 38, 2016.

[7] R. Cavallari, F. Martelli, R. Rosini, C. Buratti, and R. Verdone, "A survey on wireless body area networks: technologies and design challenges," *IEEE Communications Surveys & Tutorials,* vol. 16, no. 3, pp. 1635-1657, 2014.

[8] S. Ullah *et al.*, "A comprehensive survey of wireless body area networks," *Journal of Medical Systems,* vol. 36, no. 3, pp. 1065-1094, 2012.

[9] H. Cao, V. Leung, C. Chow, and H. Chan, "Enabling technologies for wireless body area networks: A survey and outlook," *IEEE Communications Magazine,* vol. 47, no. 12, pp. 84-93, 2009.

[10] R. Chávez-Santiago *et al.*, "Propagation models for IEEE 802.15.6 standardization of implant communication in body area networks," *IEEE Communications Magazine,* vol. 51, no. 8, pp. 80-87, 2013.

[11] M. M. Alam and E. B. Hamida, "Surveying wearable human assistive technology for life and safety critical applications: standards, challenges and opportunities," *Sensors,* vol. 14, no. 5, pp. 9153-9209, 2014.

[12] A. Darwish and A. E. Hassanien, "Wearable and implantable wireless sensor network solutions for healthcare monitoring," *Sensors,* vol. 11, no. 6, pp. 5561-5595, 2011.

[13] Y. Liao, M. S. Leeson, and M. D. Higgins, "A communication link analysis based on biological implant wireless body area networks," *Applied Computational Electromagnetics Society Journal,* vol. 31, no. 6, pp. 619-628, 2016.

[14] A. Kiourti and K. S. Nikita, "Miniature scalp-implantable antennas for telemetry in the MICS and ISM bands: design, safety considerations and link budget analysis," *IEEE Transactions on Antennas and Propagation,* vol. 60, no. 8, pp. 3568-3575, 2012.

[15] A. Kiourti, K. A. Psathas, and K. S. Nikita, "Implantable and ingestible medical devices with wireless telemetry functionalities: A review of current status and challenges," *Bioelectromagnetics,* vol. 35, no. 1, pp. 1-15, 2014.

[16] J. Shi, D. Anzai, and J. Wang, "Diversity performance of UWB low band communication over in-body to on-body propagation channel," in *European Conference on Antennas and Propagation (EUCAP),* Prague, Czech, pp. 535-539, 2012.

[17] K. S. Kwak, S. Ullah, and N. Ullah, "An overview of IEEE 802.15. 6 standard," in *International Symposium on Applied Sciences in Biomedical and Communication Technologies (ISABEL 2010),* Roma, Italy, pp. 1-6, 2010.

[18] Q. Wang, K. Masami, and J. Wang, "Channel modeling and BER performance for wearable and implant UWB body area links on chest," in *IEEE International Conference on Ultra-Wideband,* Vancouver, Canada, pp. 316-320, 2009.

[19] M. Quwaider and S. Biswas, "DTN routing in body sensor networks with dynamic postural partitioning," *Ad Hoc Networks,* vol. 8, no. 8, pp. 824-841, 2010.

[20] K. Deepak and A. V. Babu, "Improving energy efficiency of incremental relay based cooperative communications in wireless body area networks," *International Journal of Communication Systems,* vol. 28, no. 1, pp. 91-111, 2015.

[21] A. Ahmad, N. Javaid, U. Qasim, M. Ishfaq, Z. A. Khan, and T. A. Alghamdi, "RE-ATTEMPT: a new energy-efficient routing protocol for wireless body area

sensor networks," *International Journal of Distributed Sensor Networks*, vol. 2014, 2014.

[22] Y. Liao, M. S. Leeson, M. D. Higgins, and C. Bai, "An incremental relay based cooperative routing protocol for wireless in-body sensor networks," in *IEEE International Conference on Wireless and Mobile Computing, Networking and Communications (WiMob)*, New York, USA, pp. 1-6, 2016.

[23] Y. Liao, M. S. Leeson, and M. D. Higgins, "Analysis of PC and SGA models for an ultra wide-band ad-hoc network with multiple pulses," in *IEEE International Workshop on Computer Aided Modelling and Design of Communication Links and Networks (CAMAD)*, Guildford, UK, pp. 246-250, 2015.

[24] Y. Liao, M. S. Leeson, and M. D. Higgins, "Flexible quality of service model for wireless body area sensor networks," *Healthcare Technology Letters*, vol. 3, no. 1, pp. 12-15, 2016.

[25] E. Ibarra, A. Antonopoulos, E. Kartsakli, J. J. Rodrigues, and C. Verikoukis, "QoS-aware energy management in body sensor nodes powered by human energy harvesting," *IEEE Sensors Journal*, vol. 16, no. 2, pp. 542-549, 2016.

CHAPTER 2.

Wireless Body Area Networks

WBAN applications and services have emerged as one of the most important research subjects within WSNs. WBANs are concentrated on short-range wireless data transmission and have received considerable attention as a significant development for wireless communications in the human body area [1-3]. In general, WBANs require extremely miniaturised and noninvasive body sensor nodes as well as a smaller number of nodes in comparison with conventional WSNs. Those requirements lead to various technical challenges such as in-body sensor node battery design and a very limited power supply in a WBAN. Also, WBANs should be capable of enabling a multitude of medical and health services, which necessitate different data rates and network lifetime requirements [4].

The key feature of a WBAN in the medical field is to provide real-time and reliable healthcare monitoring facilities employing both implanted and wearable sensors [4]. As reported in [5], the energy consumption of a medical system at relatively low data rates should be far smaller than an average WSN thus lengthening network lifetime. For example, a medical implantable cardioverter defibrillator is only available to provision collected data within 12 seconds at 200 kbps, while the network lifetime would considerably increase to 96 seconds when operating at 25 kbps. Moreover, the communication distance is another vital concern when designing wireless medical communication systems. A longer transmission range generally in a WBAN consumes

higher energy when using the same data rates [5-6]. Physiological signals such as heart rate and ECG could change state rapidly based on the status of the patients, and thus relatively high data rate communication links are required. Furthermore, within the same WBAN system, improving the channel transmission quality will result in significantly more power consumption and reduce the network lifetime [6]. Thus, the trade-offs between various parameters need careful investigation when designing WBAN-based communication systems.

WBAN technology standards analysis is a crucial issue owing to the distinct, strict requirements in terms of information transmission reliability, network energy consumption, and operational system flexibility. The IEEE 802.15 Task Group was appointed to recommend the technical standards for wireless personal area networks (WPANs) along with other short-range wireless networks related to body area communications [7-8]. Among all IEEE 802.15 published standards, the most promising candidate suggested was the IEEE 802.15.6 technical standard [7]. This approach has been recommended to support low power, short range and highly reliable wireless communications for the human body area and to offer a broad range of data transmission rates by employing different communication technologies. Moreover, WBAN frequency band selection has a high influence on communication system performance due to the dielectric properties of human body tissues [7, 9-11]. As demonstrated in [10], there exist numerous research difficulties in this area. Firstly, technological requirements of WBAN applications are generally target-specific and vary from one application to another. Also, WBAN communication system design is still a major research challenge because the IEEE 802.15.6 Task Group has not defined the exact meaning of QoS issues in the latest draft [1].

Body area communications can be categorised into wearable channels and implant channels depending on the positions of the transmitter and receiver sensor nodes. Recently, the majority of research work has been published in on-body WBANs, while a very limited amount of work has been focused on in-body WBAN communication systems [12-15]. An essential step to study implant WBAN data transmission characteristics is to develop the in-body path loss (PL) model. This is a crucial issue in channel design and can help to determine the maximum distance that can be covered. However, due to the natural lossy environment of the intra-body region, most published in-body channel models are investigated based on homogeneous human models or single-layer tissue patterns [14]. In order to obtain an accurate in-body WBAN communication channel model and evaluate the system performance, it is vital to study the wireless radio signal propagation mechanism of the intra-body region using advanced electromagnetics software and high-resolution human models [14-15].

WBAN technologies have enormous potential to revolutionise a wide variety of medical and non-medical applications. WBANs enable continuous monitoring of one's vital signals in healthcare systems such as blood pressure, heartbeat and body temperature; they are also capable of detecting abnormal conditions, which results in effective enhancements of life quality in the patients [16]. Additionally, since human emotion detection can be realised by initiating the physical manifestations through several types of in-body sensors such as ECG and heart rate, the collected data can also be used to a series of non-medical applications such as virtual reality, sports training and fitness monitoring [16-17].

This Chapter consists of six sections. Section 2.1 discusses the development of WBAN technology. Section 2.2 demonstrates a series of existing technical standards and wireless communication technology candidates. Section 2.3 reports various critical

requirements in WBAN system design, and Section 2.4 describes two commonly used WSN-based topologies that can be considered for WBANs design. Section 2.5 and 2.6 represent several research challenges and a collection of future promising applications, respectively.

2.1 From WSNs to WBANs

2.1.1 Development of WBANs

In general, a WSN consists of a large number of spatially distributed sensors that are capable of detecting, collecting and processing numerous physical activities and environmental conditions in applications such as food security, traffic controlling, weather prediction, and industry [1, 8]. Moreover, the collected WSN data can be delivered through multi-hop routing from individual wireless sensors to the sink [18-19]. However, the use of WSNs is reported incapable of deployment in human body area applications because of the large sensor nodes size, low network power utilisation, high transmission delay and so forth [1]. Besides, the human safety in body area communications has a higher priority than for other wireless communication systems [4].

WBANs have specific features and strict technical requirements when compared with WSNs regarding energy consumption, size, data transmission reliability, and node density [1, 6]. WSN sensor nodes are usually replaceable and accessible which benefits in sensor node replacement and the disposal of the node. In-body sensor nodes are typically surgically implanted inside the human body, power recharge or battery replacement of such nodes is difficult and could cause damage to human organs [1, 4, 20]. The WSN sensor nodes are informed by the operational environment, and nodes' locations are regarded as fixed; context awareness is not the key concern in WSNs.

However, due to the mobility of the human body, context awareness in WBAN is still an emerging research topic [14, 20]. Moreover, WSNs employ redundant sensor nodes to accommodate the failure of any sensor node whereas all sensor nodes in WBAN implement multiple tasks with node redundancy available [5]. Table 2.1 summarises the key features of WBANs and WSNs.

Table 2.1 Comparison of key features with WBANs and WSNs.

Types	WSNs	WBANs
Network size	up to few kilometres	within a few metres
Node number	from few and up to 1000	< 256 nodes
Functionality	-nodes dedicated to a target -redundant nodes are available	-no redundant sensors -multiple tasks available
Accuracy	redundant nodes help to compensate for inaccuracy	high accuracy required
Resources	much more energy resources than WBANs	-very limited source -low computational capacity
Mobility	fixed or static positions	-implant sensors are fixed -on-body sensors are mobile
Context awareness	sensor nodes receive environmental information	highly required

2.1.2 Description of WBANs

The communication techniques behind WSNs are still under progress and development and at present research results obtained for WSNs are not applicable to the challenges associated with the human body area. As a consequence, a new generation of WSNs for body area communication systems has been proposed by many researchers. The concept of ‘WBANs’ was first introduced by Yang in 2006

[21]. In [22], it is reported that WBANs are capable technologies that can provide the prospect of early disease detection, pervasive healthcare monitoring, and telemedicine design in the near future. Those applications can be achieved by employing various wireless communication technologies and networking both wearable and implanted sensors in the vicinity and inside the human body. As demonstrated in Figure 2.1, body area channels are commonly categorised into in-body to in-body (A→B), in-to-out body (A→C) and on-body to off-body (C→D) data transmission scenarios. Moreover, signal transmission inside the human body regions (A→B and A→C) is extremely complex and suffers significant energy attenuation [14]. According to the sensor nodes' location inside, on or off the human body where it operates, WBANs can be divided into wearable WBANs and implant WBANs [7]. The former primarily offers RF communication system between on-body sensor nodes and a coordinator for numerous kinds of vital signs monitoring such as ECG, skin temperature, etc. The implementation of such wearable communication channels is widely by adoption of UWB technology, and the energy attenuation mainly occurs by shadow fading due to diffraction around the human body as well as large amounts of radiation energy absorbed by the body. On the other hand, due to the heterogeneous nature of body tissue, data transmission via implant WBANs inside the human body experiences significant energy attenuation due to the energy absorption in human tissues [4].

2.2 WBANs technology standards

2.2.1 IEEE 802.15 Task Group

An international standardisation IEEE 802.15 Task Group has proposed various communication technology standards for wireless personal area networks (WPANs)

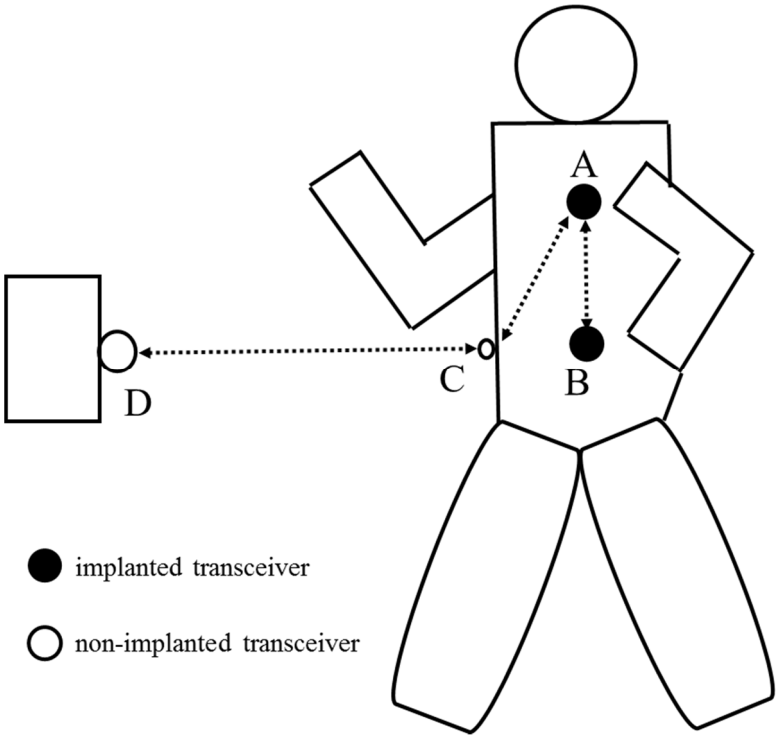

Figure 2.1 Introduction of the WBAN system.

and WBANs [4, 8, 11]. WPANs employ communication technologies that support personal area data transmission and a connectively range of up to 10 metres. WPANs are the most commonly employed to communicate with on-body sensors (wearable devices) and to interactively transfer data to other body area sensors, employing the human body as a data transmission network. A WBAN can be seen as a special generation communication technique of a WPAN, which enables numerous ubiquitous applications for both medical and non-medical services. Table 2.2 demonstrates the available frequencies bands for WBANs and WPANs. The most important WPANs and WBANs technical standards are now given in this section.

-**IEEE 802.15.1**: This technology is only available to Bluetooth applications and consists of MAC and physical layer specification [23]. It has been reported that this approach only supports a data rate of up to 3 Mbps and thus it is highly unlikely to be adopted for future WPANs applications.

Table 2.2 Frequencies bands for WBANs and WPANs.

Frequency band	Band [MHz]	Region
MICS	402-405	Global
ISM	433.1-434.8	Europe only
ISM	868-868.6	Europe only
ISM	2400.0-2483.5	Global
ISM	5725.0-5875.0	Global
WMTS	608-614	USA only
WMTS	1395-1400	USA only
WMTS	1427-1432	USA only
UWB	100-960	USA only
UWB	3100-10600	Global

-IEEE 802.15.2: This standard was proposed for the coexistence mechanism of WPANs when different types of wireless technology-based devices that are functioning in numerous unlicensed frequency bands [24].

-IEEE 802.15.3: This technical standard was designed for high data rate communication applications. For instance, the IEEE 802.15.3a was proposed to support high data rates UWB services such as real-time imaging and multimedia transmission. The IEEE 802.15.3c was projected for high-speed WPAN applications utilising millimetre waves [8].

-IEEE 802.15.4: This technical standard was proposed for low data rate applications with very long lifetime and low complexity requirements. IEEE 802.15.4c was designed for Chinese WPANs, and the IEEE 802.15.4d was intended for Japanese

WPAN applications [24]. Other IEEE 802.15.4 technical standards such as IEEE 802.15.4m, IEEE 802.15.4n and IEEE 802.15.4p are still in progress and have not achieved agreement [2, 24].

-IEEE 802.15.5: This was responsible for the specification of mesh networking for WPANs and consists of low data rate WPAN mesh and high rate WPAN mesh [25].

-IEEE 802.15.6: This is a new technical standard for body area communications that is accepted worldwide. It is focused on WBAN technologies regarding short-range data QoS-aware data transmission inside, on or off the human body region [3]. In addition, this standard provides the specific absorption rate (SAR) regulations to avoid human body and tissue damage [5].

2.2.2 Frequency selection

Generally, more than 60% of the intra-body environment is composed of water, this may lead to considerable power attenuation when transmitting data from in-body to in-body, and in-body to on-body [19]. According to the IEEE 802.15 Task Group technical standards for WPANs and WBANs, numerous frequency bands have been proposed by different authorities to meet different healthcare application needs [22]. It should be noticed that frequency selection is highly influenced by a series of factors such as implant antenna design, network energy consumption and available transmission distance. The main features of the various frequency bands are shown in Table 2.3. The proposed frequency bands are listed as follows:

-Medical implanted communication service (MICS): The MICS frequency band was suggested for medical implant applications and services. This was reported as a promising approach to accommodate WBAN high data rate applications. It was also suitable for multiple signal transmission scenarios such as in-body to in-body, in-body

to on-body, and on-body to off-body scenarios. According to the Federal Communication Commission (FCC), the transmission power of MICS standard should be not more than 25μW to avoid electromagnetic effects that are potentially hazardous to the human body [8].

-Industrial, scientific and medical (ISM): ISM frequency bands were proposed for the commercial use of the RF spectrum. According to the International Radio Communication and other authorities, only 2.4 GHz to 2.4835 GHz frequency bands are globally accepted and worthy of attracting significant attention for further research [14].

-Wireless medical telemetry services (WMTS): these frequency bands were proposed by the FCC for remote healthcare services. However, such frequency bands are only applicable in the USA and not available in other countries [23].

-Ultra wide-band (UWB): A UWB frequency band is employing extremely short pulses to achieve high data rate transmission. The FCC has authorised the unlicensed frequency range from 3.1 to 10.6 GHz and is now accepted worldwide [5, 10].

Table 2.3 Key features of the various frequency bands.

Type	**MICS**	**WMTS**	**ISM**	**UWB**
medical	Yes	yes	yes	yes
non-medical	No	no	yes	yes
data rate	Low	medium	medium	very high
bandwidth utilization	<300 KHz	<6 MHz	scalable	>500 MHz

2.3 Requirements in WBANs

The main objectives of WBANs are monitoring vital signs and providing real-time information to clinicians to support the health decision-making process in hospitals. Technical difficulties and challenges in WBANs reach beyond the technically constrained resources of the WSN and other existing wireless communication technologies [5]. Also, energy management of WBAN healthcare services varies from one application to another mainly because of the complex intra-body environment and target-specific technical requirements [14]. This section demonstrates various key elements of implant WBAN technical challenges.

2.3.1 Power consumption

Although enormous efforts have been devoted to decreasing the energy necessities of wireless communication, it is still the most power consuming module in an implanted WBAN sensor node [3, 26]. The in-body sensor node must be extremely noninvasive, and the total number of in-body sensors within a WBAN should be carefully studied to minimise interference. Additionally, due to the technical constraints of the in-body sensor battery, the power supply of the WBAN is still a major bottleneck, and the power consumption of the communication module should be limited.

In [14], it was reported that decreasing the data transmission rate would lead to reducing the power consumption of WBAN systems. Bradai *et al.* [27] stated that a typical WBAN-based medical network is specified to have few sensor nodes with a scalable range that includes up to 256 sensor nodes. The WBAN requirements indicated in [28-30] mention that the operating range for WBANs should be limited to within 3 metres. In order to expand the lifetime of the in-body sensors, the external coordinator is expected to allocate transmission frames and prohibit data

retransmission at all time slots according to the IEEE 802.15.6 standard [14, 20, 31]. The authors in [20] stated that limiting the communication distance would decrease a WBAN system power consumption. Lowering the WBAN communication system frequency band could significantly lower the transmitting signal energy attenuation. Those mentioned characteristics create tradeoffs between the WBAN power consumption and a host of factors and should be taken into account when designing customised WBAN communication systems [4].

2.3.2 Data rate

Currently, an international common WPAN-based solution is the Bluetooth technique because of ease of use and security features. The disadvantage comes with the fact that this technique suffers considerable delay and only promises data transmission rates ranging from 1 to 3 Mbps [23]. IEEE 802.15.6 is the latest technology standardisation and aims to offer a global technical standard for low-power, short distance wireless communication and supporting a broad range of data rates from 1 kbps to nearly 10 Mbps for different applications [28].

On the other hand, the reliability of the communication channel is measured using the total number of unsuccessfully transmitted bits or bit error rate (BER). In [14, 26], the authors demonstrated that the channel reliability significantly depends on the data transmission rate. In [28], different kinds of medical devices were considered: it was reported that low data rate sensors could deal with high BER scenarios of approximately 10^{-3}, whereas higher data rate sensors required a lower BER at around 10^{-6}. Also, due to the human safety requirements, the relationship between the data rate and the required transmitting power should be taken into consideration when designing the security of WBAN architectures [5].

2.3.3 QoS

QoS in traditional communication networks and WSNs is mainly investigated from two perspectives, namely the application/user level and the network level [28]. From the networking point of view, the main aim is to offer the QoS to ensure maximum utilisation of the network resource while QoS denotes to an assurance to provide a list of measurable service attributes to the user or application regarding data rate, communication link quality and so forth. The IEEE 802.15.6 standard has proposed numerous types of communication channel models for the transmission environment and frequency bands [28]. However, it does not offer any QoS support information in WBANs.

For WBANs there is thus a need to analyse the application requirements and deploy various network QoS mechanisms [14]. As stated in [14], there is still no agreement as to the concept of QoS in WBAN system design. Reference [20] reported that the important target of QoS is to enhance the data transmission quality at any time by optimising the number of in-body sensors. The authors in [29] illustrated that QoS is the right concept for measuring and maintaining the quality of communication network characteristics such as link quality. Also, WBAN QoS techniques are required to satisfy some target-specific healthcare settings. For example, physiological signals such as heart rate and ECG demand relatively high data rate wireless communication paths because those parameters change and reach peak values fast on the status of the patients. Hence, the main QoS parameters such as bandwidth, reliability, and delay should be comprehensively studied when designing WBAN communication systems. The details of the QoS support in different layers can be found in [28].

2.3.4 Electromagnetic compatibility

Generally, implant WBAN communication systems utilise an electromagnetic field source inside the human body to monitor parts of the body health, and thus biological effects and human safety issues may cause by exposure to RF fields [14]. Electromagnetic radiation from an implanted sensor also leads to energy absorption in the human body and produces interference with other medical devices. The distribution of the internal fields is related to a few parameters, including the frequency band, human tissue dielectric properties, and the in-body antenna type. A WBAN system should be capable of minimising radiation emission and temperature.

Another important factor involves the calculation of energy absorption in the human body. In the intra-body region, the saline-water nature of the human body environment contributes significantly to the absorption of the electromagnetic wave transmission [1, 28]. One practical solution to calculate the SAR values is to use advanced computational electromagnetics methods and compare the calculation results with the authorities' safety guidelines or national guidelines [5]. SAR is the absorbed power per unit mass and can be expressed as [28]:

$$SAR = \frac{\sigma |E|^2}{\rho} \tag{2.1}$$

where E and σ denote the electric field caused by radiation and the conductivity of human tissues, respectively, and ρ represents the human tissue density. Morevoer, tissue damage may happen because of the human body's inability to deal with the excessive heat. Hence, it is essential to determine the appropriate transmitting power to guarantee human body safety [28].

2.4 WBAN topologies

Topologies are commonly used to define the interconnected structure for data communication between different sensors in the same WBAN. Since in-body sensor nodes are of extremely small size with limited energy resources, one key aspect of configuration management for WBANs is topology management [21]. The authors in [22] reported that star and mesh topologies are widely employed in standalone WBAN system, and a hybrid method is a capable technique to support both competition-oriented and schedule-oriented conditions. The promising candidates, peer-to-peer, star, mesh, and hybrid topologies are listed in this section.

2.4.1 Peer-to-peer topology

The peer-to-peer (P2P) topology was proposed for high data rate transmission with a medium density networking at a distance of 1 to 10 metres [28]. An illustration of the P2P topology is given in Figure 2.2. This technique has been widely used for the IEEE802.15.4 standard where full function sensor nodes can implement P2P communication without any routing capability such as real-time imaging transmission [30].

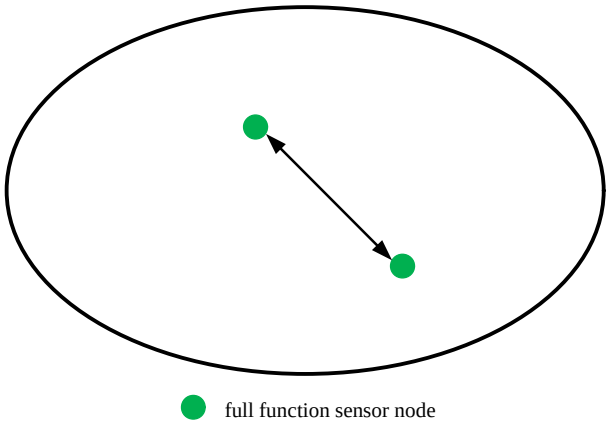

Figure 2.2 Peer-to-peer topology.

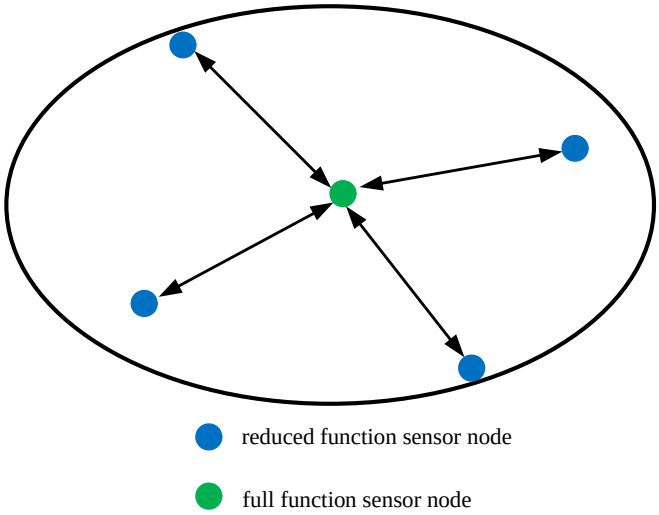

Figure 2.3 Star topology.

2.4.2 Star topology

Star topologies have been commonly employed in numerous wearable technologies such as Zigbee. As can be seen from Figure 2.3, sensor nodes are divided into two types: reduced function sensors and full function sensors. In a star topology, all body sensor nodes connect to the external coordinator, which achieves high throughput and supports data fusion with simple data routing methods [31]. The advantages of the star topology are its simple architecture and high bandwidth utilisation. However, the topology has some drawbacks such as its high probability of transmission failure, poor scalability and high energy waste. It should be noticed that a series of star topologies are able to organise a cluster tree topology as demonstrated in [22]. The sensor nodes within a star topology can transmit data to the nodes in other star topologies via the coordinators. However, it has been demonstrated in [28] that a cluster topology achieves very low data transmission reliability, high latency, low bandwidth utilisation, and is thus not applicable for future WBAN topology design.

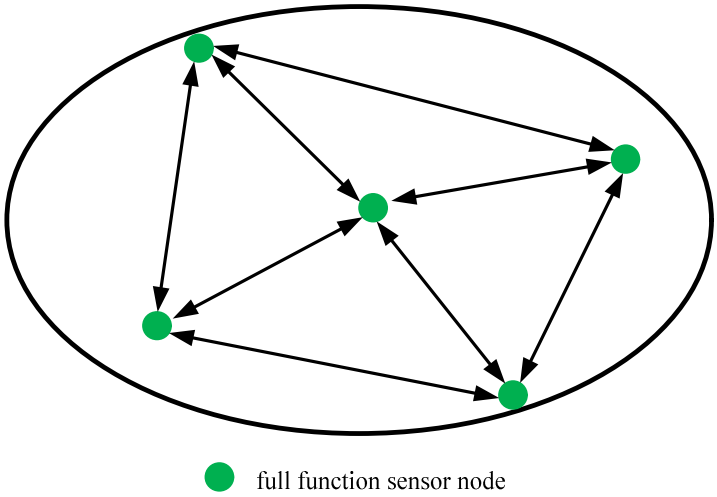

Figure 2.4 Mesh topology.

2.4.3 Mesh topology

As shown in Figure 2.4, all sensor nodes in mesh topology are capable of performing all the routing operations and data transmission. This technique is a promising candidate to support high-reliability on-body physiological signal monitoring applications [28]. The main advantage of this topology is the multiple communication paths provided to each node which contributes to achieving reliable information transfer and significantly improve the network fault tolerance performance. However, mesh topologies are not widely employed since they have relatively high energy consumption and need complex routing protocols [32].

2.4.4 Hybrid topology

As mentioned in the star and mesh topology sections above, only one coordinator in a WBAN implies the high possibility of data transmission failure. As shown in Figure 2.5, a hybrid topology is proposed to handle this technical weakness by extending the star or mesh topologies and can be seen as a combination of star and mesh topologies.

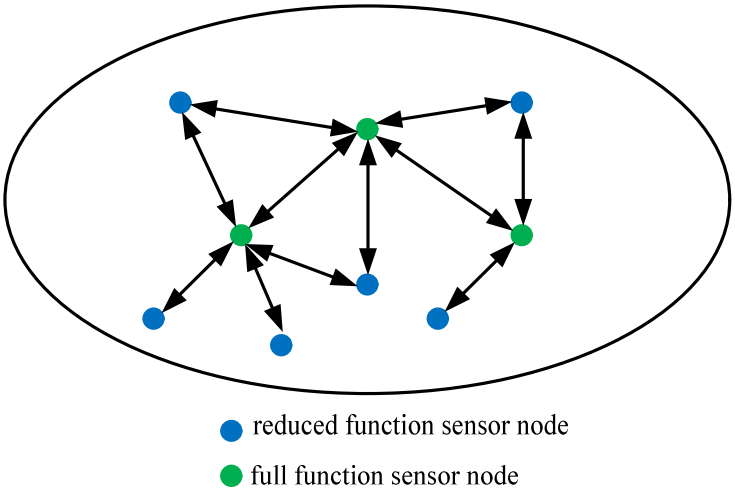

Figure 2.5 Hybrid topology.

The sensor nodes in a hybrid topology can be added at any time, thus significantly enhancing the network fault-tolerant capability. In addition, hybrid topologies can achieve data gathering speeds and can bridge systems from the body area to a large range or wider area. However, a hybrid topology still faces several critical technical challenges such as high complexity and a significant amount of network energy consumption [32].

2.5 WBAN research challenges

2.5.1 Propagation channel modelling

A crucial step in the analysis of WBAN system performance is to derive the in-body communication channel PL model [28]. However, in this respect, a very limited number of research articles have initiated channel modelling investigations [4-5, 8-9]. The main reason for this research challenge involves the fact that signal propagation measurement inside a human body is prohibited by the majority of countries due to health and safety legislation [14]. Moreover, an in-body WBAN channel PL model cannot be easily obtained due to the complex structure of the human body shape and

tissues. Numerous alternative approaches have been proposed [9, 14-15] to explore WBAN communication channel characteristics in recent years. Among all those proposed approaches, high-resolution human body models in conjunction with advanced computational electromagnetics methods are reported as promising options to derive the statistical WBAN channel PL models [14-15]. Those results can be realised by determining the electromagnetic field at selected predetermined locations of the transmitter inside the body. In [14], the authors concluded that diffraction is the main propagation mechanism, and the channel modelling performance showed good correspondence with FDTD simulation results. Other approaches such as Method of Moments have been also applied to investigate the radio signal propagation characteristics inside the human body. However, those methods are only applicable for multi-layer cylinders and spheres human body models, and therefore undesirable in the achievement of accurate PL models [15].

2.5.2 QoS challenges

As stated in 2.3.3 above, QoS is traditionally seen from the perspective of the application or user and from the perspective of the network. In terms of the latter, QoS provision needs to ensure maximisation of network utilisation whereas for the latter, QoS refers to a set of measurable attributes. The network design is required to satisfy the application requirements and deploy various network QoS mechanisms to achieve those aims [1].

To date, there is still no agreement regarding the concept of QoS in WBAN system design [14]. Literature such as [17] proposed that a key aim of the QoS is to provide an optimum number of in-body sensor nodes to support critical medical information transmission at any given time.The authors in [28] reported that QoS is a task for

measuring and maintaining the quality of communication network characteristics such as link quality. In practice, QoS-aware support in WBANs have some strict technical requirements and vary from one application to another. Physiological signals such as heart rate and ECG are changing very fast, and relatively high data rate wireless communication links are needed, which entails the disadvantage of significantly increased power consumption [1-2, 28]. So far the majority of published work has concentrated on the wearable sensor devices in WBANs. There is thus significant scope for in-body WBAN research regarding QoS-awareness; this is of vital importance in implant WBANs and can be suggested for future WBAN system design to include high data transmission rate support, energy consumption minimization and packet loss handling. The trade-offs of various factors should also be studied carefully.

Due to the limited in-body sensor node power source, one approach capable of prolonging the WBASN in-body sensor node lifetime is to employ highly energy efficient routing protocols [14, 20]. As reported in [18], WBAN energy consumption is related to the overall data transmission distance between in-body sensor nodes and the external coordinator. Thus it is essential to realise and perform the most energy efficient route selection by minimising the transmission distance. In the current research into WBAN protocol design, relay-based routing solutions have been considered as effective methods to minimise the communication distance. This is achieved by employing relay nodes to receive data from in-body sensors and then forward those data to the coordinator, thus significantly shortening the communication length and reducing the energy consumption of in-body sensor nodes. Cooperative communication techniques have also attracted attention as an efficient scheme to enhance energy efficiency and spatial diversity in wireless body area fading channels

[14, 26]. However, there has been very little research work on the incremental relay-based routing protocol approach in in-body WBAN communication systems [20].

2.6 WBANs for promising applications

The number of chronic disease patients rise rapidly every year worldwide and is expected to increase to 360 million by 2030 based on the World Health Organization survey [28]. Yuce *et al.* [4] illustrated that the most common infectious diseases, as well as chronic diseases, can be cured or prevented if they are detected in the early stage. The IEEE 802.15.6 standard brings a technical standard forward intended for WBANs to support numerous improvements in the quality of life in many areas including medical applications and non-medical applications. Table 2.4 illustrates the categorization of applications of body area communications.

2.6.1. Medical applications

The fast growth in the global population will most likely lead to a significant shortage of medical clinicians and nurses in future years [1]. WBANs have a high potential to offer various affordable solutions for monitoring the health parameters of elderly and vulnerable people without disturbing their daily activities. In [4], the authors reported that the future healthcare information system could be facilitated through a few implanted sensors and a small central coordinator or smartphone; this could enable the transfer of information or timely feedback to health professionals under abnormal situations [14].

WBAN healthcare systems are supposed to provide proactive wellness management and concentrate on early detection and prevention of diseases. Employing WBANs in remote telemedical applications allows for the continuous monitoring of a patient’s

Table 2.4 Categorization of applications of body area communications.

Medical WBAN	Non-medical	Entertainment
Cardiovascular diseases	ECG	emotion Detection
Glucose sensor	blood pressure	social networking
Endoscopy capsule	medical devices control	video streaming share
Pacemaker	temperature	secure authentication

physiological signals attributes such as blood pressure, heartbeat and body temperature. Moreover, the measurement of numerous vital signs for patients is required around four to six times in one day regarding ECG, blood pressure and temperature [27]. For instance, a formal procedure of routine of chronic illness patient visits is required to monitor the health progress, whereas WBANs are able to offer biosensors that can be employed to track the various kinds of physiological or biochemical parameters anytime and anywhere [28].

2.6.2. Non-Medical applications

Non-medical WBANs techniques can be used in many areas such as real-time streaming and entertainment applications [5]. The architecture that captures body motion for medical evaluation also can be applied to capture human body motion or movement for a 3D video game or real-time audio streaming. WBANs can also achieve emotion detection by measuring simple physical manifestations. Fear conditioning can be detected when heart rate and respiration rate are significantly increased [28]. Human emotional status can be obtained through monitoring emotion associated physiological signals such as ECG, electromyography (EMG), blood pressure and so forth.

WBANs also support entertainment applications including fitness, social networking and sports training. Appliances such as cell phones, smartwatches, etc., can be operated as devices integrated into WBANs [14] which then provide benefits in terms of athletic training plans via heart rate monitoring and muscle fatigue variability analysis. Also, WBANs can transmit real-time feedback to game players to prevent training injuries and improve performance [33-34].

References

[1] B. Latré, B. Braem, I. Moerman, C. Blondia, and P. Demeester, "A survey on wireless body area networks," *Wireless Networks*, vol. 17, no. 1, pp. 1-18, 2011.

[2] B. Alghamdi and H. Fouchal, "Wireless body area network platforms evaluation," in *IEEE International Wireless Communications and Mobile Computing Conference (IWCMC)*, Sardinia, Italy, pp. 1348-1352, 2013.

[3] A. Liberale, E. Dallago, and A. L. Barnabei, "Energy harvesting system for wireless body sensor nodes," in *IEEE Biomedical Circuits and Systems Conference (BioCAS) Proceedings*, Lausanne, Switzerland, pp. 416-419, 2014.

[4] M. R. Yuce, P. C. Ng, and J. Y. Khan, "Monitoring of physiological parameters from multiple patients using wireless sensor network," *Journal of Medical Systems*, vol. 32, no. 5, pp. 433-441, 2008.

[5] R. Cavallari, F. Martelli, R. Rosini, C. Buratti, and R. Verdone, "A survey on wireless body area networks: technologies and design challenges," *IEEE Communications Surveys & Tutorials*, vol. 16, no. 3, pp. 1635-1657, 2014.

[6] S. Ullah, H. Higgins, B. Shen, and K. S. Kwak, "On the implant communication and MAC protocols for WBAN," *International Journal of Communication Systems,* vol. 23, no. 8, pp. 982-999, 2010.

[7] J. Abouei, J. D. Brown, K. N. Plataniotis, and S. Pasupathy, "Energy efficiency and reliability in wireless biomedical implant systems," *IEEE Transactions on Information Technology in Biomedicine,* vol. 15, no. 3, pp. 456-466, 2011.

[8] Y. Liao, M. S. Leeson, and M. D. Higgins, "Analysis of PC and SGA models for an ultra wide-band ad-hoc network with multiple pulses," in *IEEE International Workshop on Computer Aided Modelling and Design of Communication Links and Networks (CAMAD),* Guildford, UK, pp. 246-250, 2015.

[9] Q. Fang, S. Y. Lee, H. Permana, K. Ghorbani, and I. Cosic, "Developing a wireless implantable body sensor network in MICS band," *IEEE Transactions on Information Technology in Biomedicine,* vol. 15, no. 4, pp. 567-576, 2011.

[10] K. Y. Yazdandoost, "UWB loop antenna for in-body wireless body area network," in *European Conference on Antennas and Propagation (EuCAP),* Gothenburg, Sweden, pp. 1138-1141, 2013.

[11] S. Ullah, M. Mohaisen, and M. A. Alnuem, "A review of IEEE 802.15. 6 MAC, PHY, and security specifications," *International Journal of Distributed Sensor Networks,* vol. 2013, pp. 1-12, 2013.

[12] A. Rangarajan, "Review: Emerging Trends in Healthcare Adoption of Wireless Body Area Networks," *Biomedical Instrumentation & Technology,* vol. 50, no. 4, pp. 264-276, 2016.

[13] K. Takizawa *et al.*, "Channel models for wireless body area networks," in *Annual International Conference of the IEEE Engineering in Medicine and Biology Society (EMBC)*, Vancouver, Canada, pp. 1549-1552, 2008.

[14] Y. Liao, M. S. Leeson, M. D. Higgins, and C. Bai, "Analysis of in-to-out wireless body area network systems: towards QoS-aware health Internet of Things applications," *Electronics*, vol. 5, no. 3, p. 38, 2016.

[15] D. Kurup, G. Vermeeren, E. Tanghe, W. Joseph, and L. Martens, "In-to-out body antenna-independent path loss model for multilayered tissues and heterogeneous medium," *Sensors*, vol. 15, no. 1, pp. 408-421, 2014.

[16] F. Touati and R. Tabish, "U-healthcare system: state-of-the-art review and challenges," *Journal of Medical Systems*, vol. 37, no. 3, pp. 1-20, 2013.

[17] H. Cao, V. Leung, C. Chow, and H. Chan, "Enabling technologies for wireless body area networks: A survey and outlook," *IEEE Communications Magazine*, vol. 47, no. 12, pp. 84-93, 2009.

[18] M. K. Watfa, H. AlHassanieh, and S. Selman, "Multi-hop wireless energy transfer in WSNs," *IEEE Communications Letters*, vol. 15, no. 12, pp. 1275-1277, 2011.

[19] S. Ullah, B. Shen, S. Riazul Islam, P. Khan, S. Saleem, and K. Sup Kwak, "A study of MAC protocols for WBANs," *Sensors*, vol. 10, no. 1, pp. 128-145, 2009.

[20] N. Javaid, A. Ahmad, Y. Khan, Z. A. Khan, and T. A. Alghamdi, "A relay based routing protocol for wireless in-body sensor networks," *Wireless Personal Communications*, vol. 80, no. 3, pp. 1063-1078, 2015.

[21] E. Jovanov, C. C. Poon, G.-Z. Yang, and Y.-T. Zhang, "Guest editorial body sensor networks: from theory to emerging applications," *IEEE Transactions on Information Technology in Biomedicine,* vol. 13, no. 6, pp. 859-863, 2009.

[22] D. Rathee, S. Rangi, S. Chakarvarti, and V. Singh, "Recent trends in wireless body area network (WBAN) research and cognition based adaptive WBAN architecture for healthcare," *Health and Technology,* vol. 4, no. 3, pp. 239-244, 2014.

[23] K. S. Kwak, S. Ullah, and N. Ullah, "An overview of IEEE 802.15. 6 standard," in *International Symposium on Applied Sciences in Biomedical and Communication Technologies*, Roma, Italy, pp. 1-6, 2010.

[24] H. B. Li, K. Takizawa, B. Zhen, and R. Kohno, "Body area network and its standardization at IEEE 802.15. MBAN," in *IST Mobile and Wireless Communications Summit*, Budapest, Hungary, pp. 1-5, 2007.

[25] M. J. Lee *et al.*, "IEEE 802.15. 5 WPAN mesh standard-low rate part: meshing the wireless sensor networks," *IEEE Journal on Selected Areas in Communications,* vol. 28, no. 7, pp. 973-983, 2010.

[26] Y. Liao, M. S. Leeson, and M. D. Higgins, "A communication link analysis based on biological implant wireless body area networks," *Applied Computational Electromagnetics Society Journal,* vol. 31, no. 6, 2016.

[27] N. Bradai, L. C. Fourati, and L. Kamoun, "Investigation and performance analysis of MAC protocols for WBAN networks," *Journal of Network and Computer Applications,* vol. 46, pp. 362-373, 2014.

[28] S. Movassaghi, M. Abolhasan, J. Lipman, D. Smith, and A. Jamalipour, "Wireless body area networks: A survey," *IEEE Communications Surveys & Tutorials,* vol. 16, no. 3, pp. 1658-1686, 2014.

[29] M. Ameen, A. Nessa, and K. S. Kwak, "QoS issues with focus on wireless body area networks," in *IEEE International Conference on Convergence and Hybrid Information Technology*, Busan, South Korea, pp. 801-807. 2008.

[30] N. Bradai, S. Belhaj, L. Chaari, and L. Kamoun, "Study of medium access mechanisms under IEEE 802.15. 6 standard," in *Joint IFIP Wireless and Mobile Networking Conference (WMNC),* Toulouse, France, pp. 1-6, 2011.

[31] K. A. Ali, J. H. Sarker, and H. T. Mouftah, "Urgency-based MAC protocol for wireless sensor body area networks," in *2010 IEEE International Conference on Communications Workshops*, Cape Town, South Africa, pp. 1-6, 2010.

[32] S. Ullah *et al.*, "A comprehensive survey of wireless body area networks," *Journal of medical systems,* vol. 36, no. 3, pp. 1065-1094, 2012.

[33] D. M. Barakah and M. Ammad-uddin, "A survey of challenges and applications of wireless body area network (WBAN) and role of a virtual doctor server in existing architecture," in *International Conference on Intelligent Systems, Modelling and Simulation*, Kota Kinabalu, Malaysia, pp. 214-219, 2012.

[34] S. Akram *et al.*, "A fatigue measuring protocol for wireless body area sensor networks," *Journal of Medical Systems,* vol. 39, no. 12, pp. 1-15, 2015.

CHAPTER 3.

Design of a Wireless In-body WBAN model and Its Performance Evaluation

3.1 Introduction

Recent technological growth in wireless communication techniques, biosensors, and embedded computing systems has enabled various WBAN applications and services. A significant step to develop WBANs is the design and investigation of in-body communication systems. Implantable WBANs have a vast potential to revolutionise e-health services by treating many chronic diseases, detecting early neoplastic lesions, providing real-time health monitoring and so forth [1]. A typical implanted WBAN communication system is related to a combination of low power constraint in-body sensors, which are employed to acquire, process, and transmit different types of physiological parameters from inside the human body. An efficient implanted WBAN system requires in-body sensors with the following features: light weight, low energy consumption, miniature size and harmless to human health [2]. One of the main technical constraints on wireless in-body sensor networks is their limited power supply. Moreover, in-body devices and sensors are required to enable information transmission over a wide range of data rates. For example, some typical data rates of in-body sensors vary from few kbps in a glucose sensor to approximately 10 Mbps in a wireless capsular endoscope high-resolution image transmission [1, 3].

Animal testing and experiments are reported as potential approaches to achieving some promising results that can be employed to human beings [4]. However, based on the UK, European Union and other countries laws, 'no animal experiments can be conducted if there is a realistic alternative approach', and thus physical radio channel measurements in the in-body region are not possible [1, 4]. To date, there is very limited literature that investigates in-body propagation channel modelling and communication system performance evaluation. In wireless communication networks, electromagnetic wave propagation suffers from reflection, scattering and diffraction when signals are transported from the transmitter (Tx) to the receiver (Rx). It has been reported [5] that the transmitting signal energy drops off with d^n, where d and n represent the overall length of transmission distance and the path loss coefficient, respectively. Considering an in-body communication system, the human body acts as a communication channel where energy losses are primarily absorption by human tissues and organs, which result in health risks due to heat dissipation, body temperature increase, tissue damage, blood flow reduction and so forth [1, 6-7]. These remain a problem even though WBAN implanted devices are low-power. Once the majority of available power is concentrated in a small volume inside the human body, the SAR value may become very large, and thus the amount of radiation energy absorbed by the body tissue should be carefully examined when considering human safety issues [1, 8].

The dielectric properties of biological tissues are influenced by the operating frequency band. WBAN communication systems are mostly proposed in the MICS, ISM, and UWB frequency bands [2]. The MICS frequency band promises lower transmitting signal power attenuation. However, MICS band communication systems do not satisfy the requirements for high-speed transmission applications and their

antennas size are too big to operate in medical services [4]. The UWB band signal experiences significant power attenuation when propagating through the in-body area [4]. The UWB frequency band is a capable candidate for on-body communication systems due to its multi-path fading effect, and rapid information transmission rate. The UWB on-body communication system is introduced and studied in Chapter 6.

In this chapter, the globally available 2.4 GHz band is investigated because it is capable of supporting high data rates for in-body communication systems. A detailed review is presented of various typical human homogeneous tissues and of an advanced 3D computational human head model. PL models have been obtained using MATLAB Curve Fitting Toolbox, and the results show excellent agreement with the simulation results. Performance evaluation of the wireless in-body communication system is obtained concerning reliability, available transmission rates and coverage distance for a predetermined BER threshold based on a 3D human head model.

The rest of the chapter is presented as follows. In Section 3.2, dielectric parameters of various human tissues and the human head model are shown along with the PL simulation setups. The PL modelling work is demonstrated in Section 3.3. The evaluation of the communication system performance based on the multimodal imaging-based detailed anatomical (MIDA) human model is given in Section 3.4. Section 3.5 concludes this chapter.

3.2 Dielectric properties of the human body

3.2.1 Human tissue model

To investigate how the human body responds to electromagnetic waves, it is of significance to understand the dielectric properties of the human tissues, namely, conductivity, relative permittivity and loss tangent [9]. In homogeneous cases,

simulations for several typical tissues are demonstrated based on a flat phantom proposed in [8]. In the heterogeneous human body scenario, a comprehensive multimodal image-based human head was investigated, which is an advanced electromagnetic computational model published by Virtual Population Group [10].The dielectric parameters of human tissues are frequency dependent. Figures 3.1-3.3 show the conductivity, relative permittivity and loss tangent of multiple typical human tissues in a wide range of frequency from 1 to 10 GHz, respectively. The dielectric parameters of typical tissues including conductivity, relative permittivity and loss tangent are summarised in Table 3.1 [11]. A comprehensive database of the human tissues dielectric parameters can be found in the 'Nello Carrara' Institute of Applied Physics, a part of the Italian National Research Council [11]. They provide a web source for the body tissues dielectric properties from 10 Hz to 100 GHz. The real human body is irregularly shaped and is considered as a large heterogeneous object

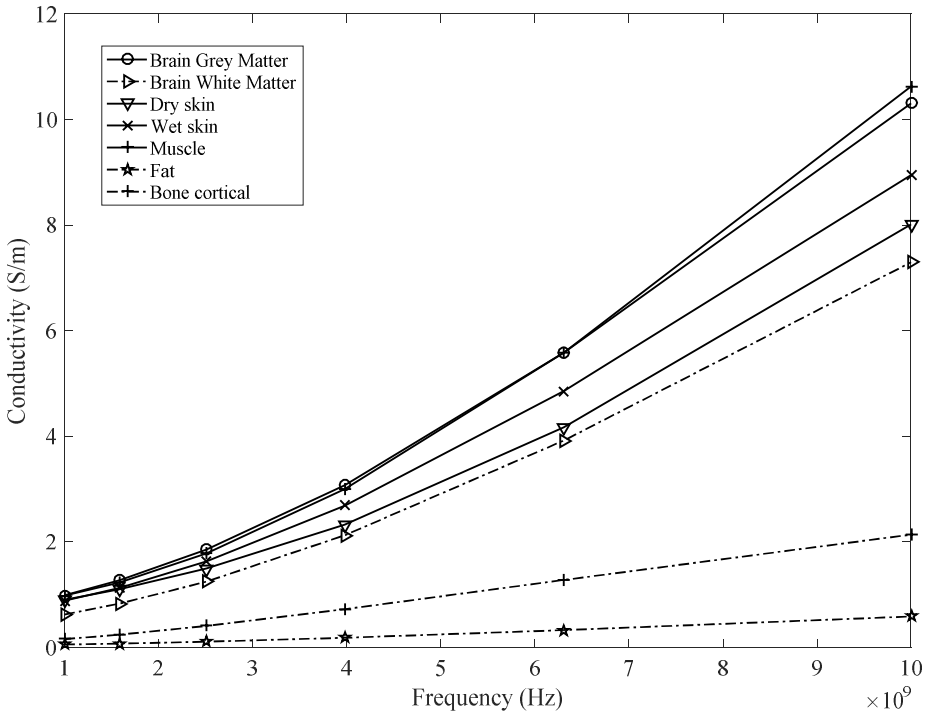

Figure 3.1 Conductivity of multiple human tissues.

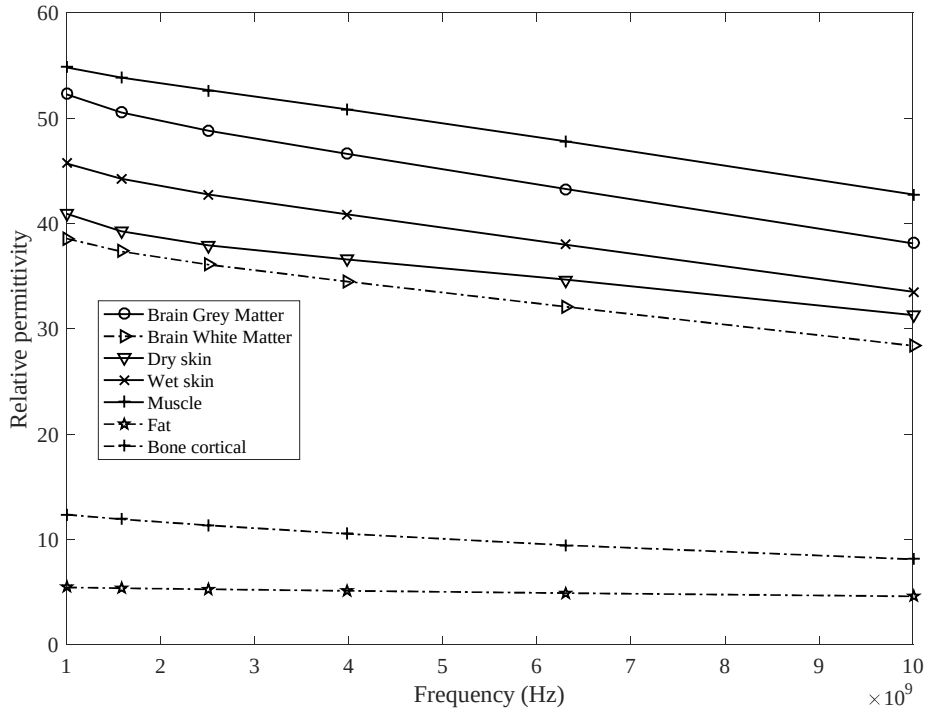

Figure 3.2 Relative permittivity of various human tissues.

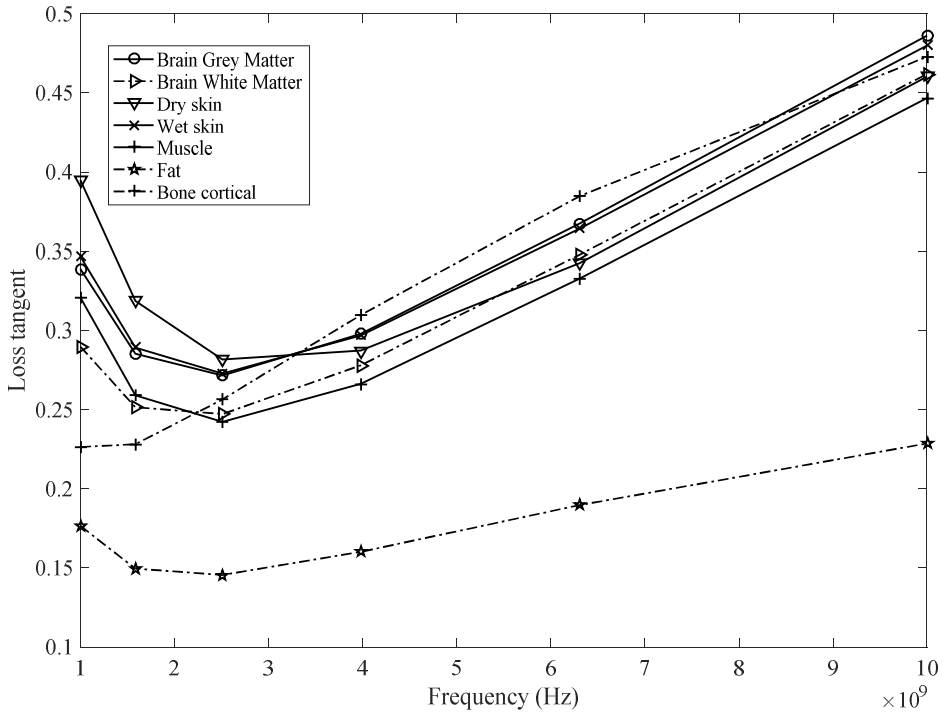

Figure 3.3 Loss tangent of various human tissues.

Table 3.1 Dielectric properties of typical tissues at 2.4 GHz.

Tissue	Conductivity (S/m)	Permittivity	Loss tangent
Air	0	1	0
Grey Matter	1.773	48.994	0.27104
White Matter	1.1899	36.226	0.24602
Skin Dry	1.4407	38.063	0.2835
Skin Wet	1.5618	42.923	0.27253
Muscle	1.705	52.791	0.24191
Fat	0.10235	5.2853	0.14503
Bone cortical	0.38459	11.41	0.25244
Blood	2.5024	58.347	0.2469
Liver	1.6534	43.118	0.2872
Kidney	2.3901	52.856	0.33868
Tooth	0.38459	11.41	0.25244
Heart	2.2159	54.918	0.30221
Retina	1.9967	52.698	0.28378
Tongue	1.7662	52.698	0.25102
Lung deflated	1.6486	48.454	0.25484

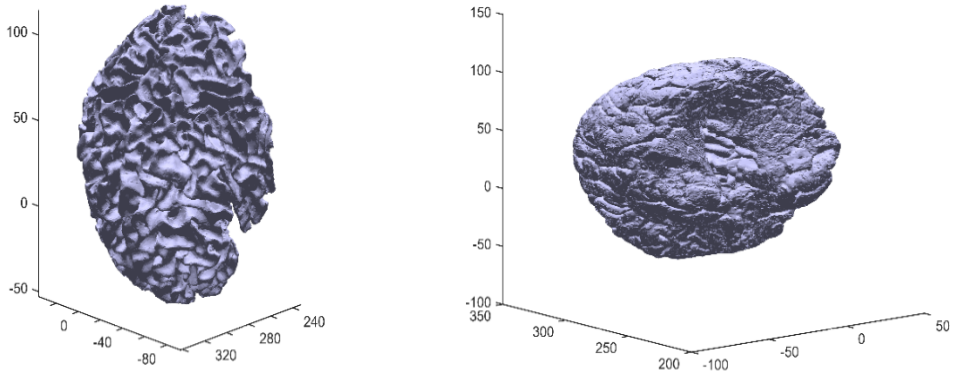

(a) (b)

Figure 3.4 Typical MIDA structures: (a) brain white matter, (b) brain grey matter (All dimensions in mm).

with dielectric properties that vary considerably with tissue types [1]. To analyse the in-body channel transmission characteristics, an advanced 3D computational human model is needed. A multimodal imaging-based detailed anatomical computational human head model 'MIDA' is taken into account. MIDA is a detailed anatomical computer model, including more than 150 types of human organs and tissues, with the highest resolution of 0.5 mm; it is thus more advanced and accurate than the Virtual Population models [12-13]. The advances of the MIDA model are not only available to computational modelling research but also can be applied to examine the safety issues of medical devices located in, on or around the head [10]. Figure 3.4 shows the selected structures of the MIDA human head model: brain white matter and grey matter.

3.2.2 PL simulation setup

First electromagnetic wave propagation in some typical homogeneous tissues at 2.4 GHz, are investigated. Dipole antennas are chosen for PL analysis due to the simple

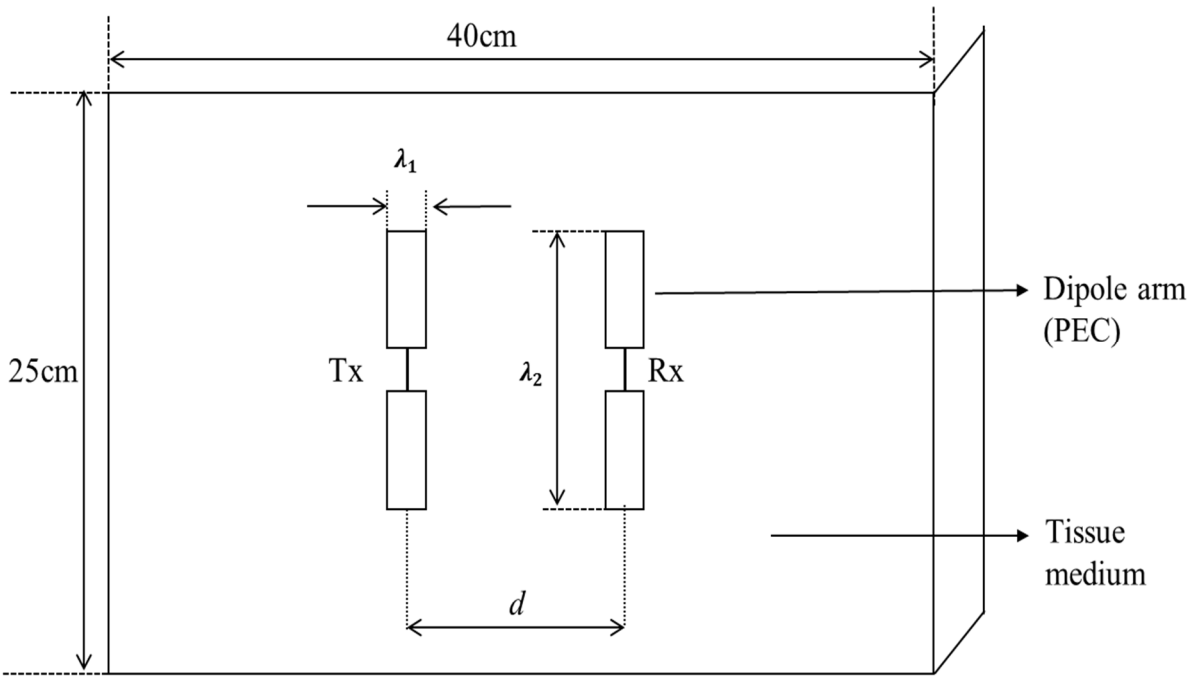

Figure 3.5 Simulation setup for the homogeneous tissue.

structures in free space communication channels, and the dimensions of such antennas are suitable to implant inside the human body by surgery for multiple medical applications. The simulation phantom for homogeneous tissues is shown in Figure 3.5; two arms of both the Tx and Rx antennas are both made of perfect electric conducting (PEC) material with a thickness λ_1 equal to 1 mm. The voltage source is selected for investigation and methods for all simulation cases are the same.

The length of the dipole antenna arms λ_2 is set to 6.25 cm so that the antenna is equal to a half wavelength for 2.4 GHz where the resonance occurs. The flat phantom shown in Figure 3.5 is beneficial to help the understanding and comparison of the PL between a series of homogeneous human tissues. The simulation setup for the MIDA human head model is shown in Figure 3.6. The Tx and Rx dipole antennas are both placed aligned inside the human head. The transmitting dipole is located and fixed in the skin layer while the receiving dipole moves horizontally from the reference point up to the

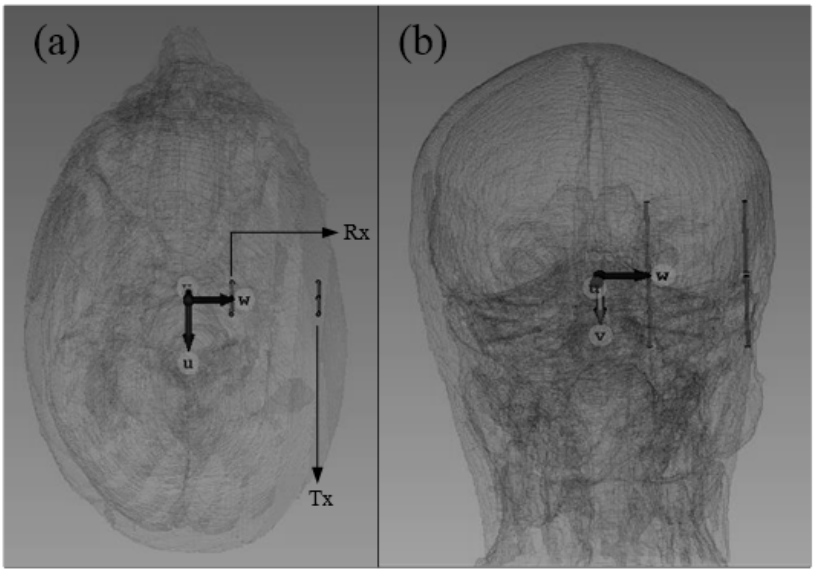

(a) (b)

Figure 3.6 MIDA model and dipole antennas, (a) Front view. (b) Side view.

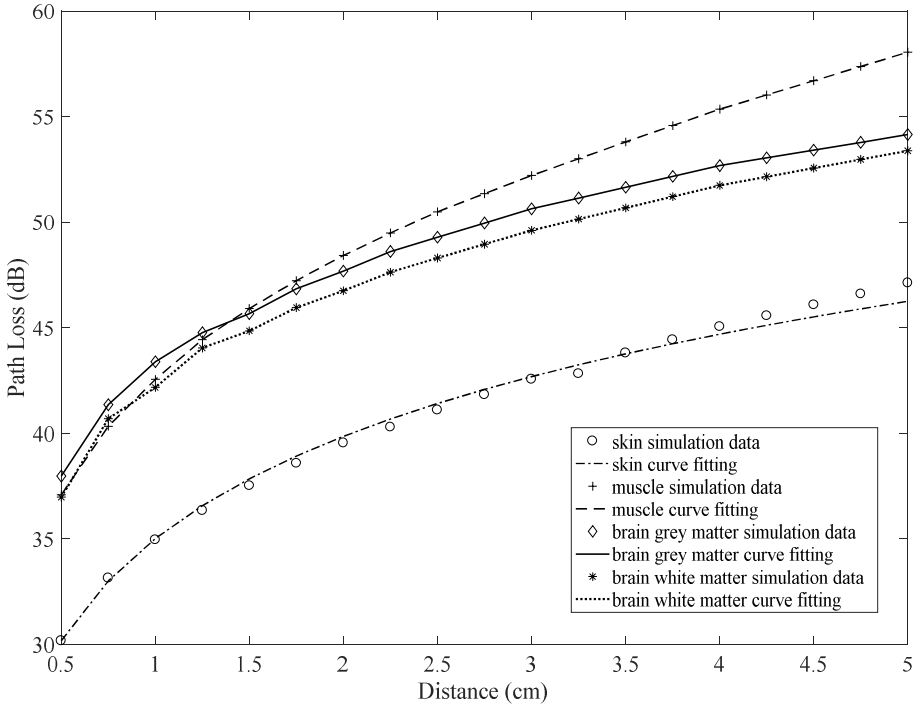

Figure 3.7 PL versus separation distance between antennas for homogeneous tissues. The solid curves are least square regression fits.

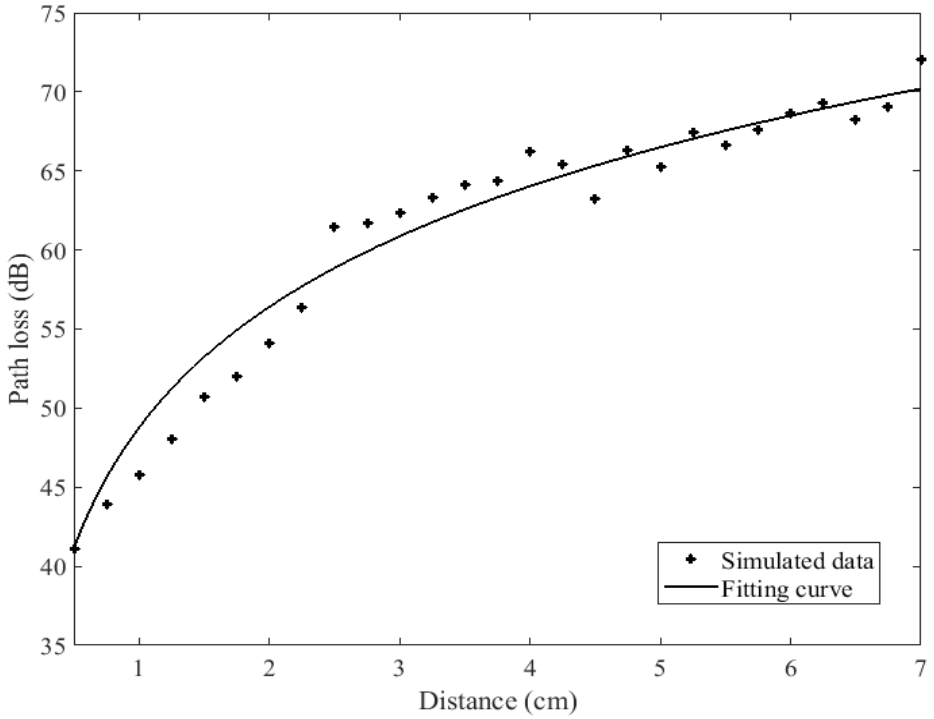

Figure 3.8 PL versus distance between antennas for heterogeneous MIDA human head model. The solid curve is least square regression fits.

deep head area with a distance up to 7 cm. The maximum grid step in both homogeneous and heterogeneous scenarios is set as 1 mm.

Figure 3.7 illustrates PL simulation results along with the corresponding curve fitting results for four human tissues, namely skin, muscle, brain grey matter and brain white matter. At the maximum communication distance (5 cm), muscle tissue achieves the highest PL value of approximately 57 dB, followed brain grey matter and brain white matter with the PL of the skin being lowest at around 46 dB. The simulated values are similar to existing results published in [5, 6], even though those outcomes are obtained by using insulated or helical antennas. Similarly, Figure 3.8 demonstrates the PL values for the heterogeneous MIDA model versus the distance. The least square fitting technique along with the MATLAB Curve Fitting Toolbox are used to evaluate the

accuracy of the heterogeneous MIDA human head PL values [14]. The determination coefficients R^2 are introduced to examine quality of the fit grade between PL values and the communication ranges. Table 3.2 demonstrates the specific parameters fitted using the least square fit method. Moreover, the statistical distribution of PL which fluctuates around the average PL is described by using $S(\mu, \sigma)$, which follows the log-normal distribution. The parameters μ and σ represent mean value, and the standard deviation also summarised in Table 3.2.

Table 3.2 PL models for human tissues and the MIDA model (d_{ref}=0.5 cm).

Tissue type	$PL_{dB}(d_{ref})$	n	$S(\mu, \sigma)$	R^2
Dry skin	30.17	1.608	(0, 1.534)	0.9941
Muscle	37.08	1.964	(0, 3.623)	0.9911
Grey matter	37.97	1.631	(0, 0.658)	0.9972
White matter	36.97	1.644	(0, 1.101)	0.9954
MIDA head model	42	2.6	(0, 1.745)	0.95

3.3 Human tissue safety

Wireless in-body communication systems create one or more electromagnetic field sources inside the human body. The distribution of the in-body devices/sensors is related to various parameters, such as the communication frequency, the dielectric properties of human tissues, the geometrical shape of the human body, and the antenna type of WBAN communications [1-2]. The safety evaluation of human tissue is

another key challenge in WBAN research because specific actual human head experiments are not possible. Electromagnetic radiation from an in-body sensor may cause SAR measurements or experiments for EM exposure in an energy absorption in the human body and potential interference with other implanted medical devices. Several biological effects of electromagnetic fields have been reported [1, 6-7]. One of the most important issues is the thermal effect due to the EM energy absorption by human tissues. Human body safety can be expressed regarding the SAR as averaged over any 10 grammes of tissue as [1]:

$$SAR = \frac{\sigma}{\rho}|E|^2 \tag{3.1}$$

where σ and ρ represent the conductivity and the mass density of human tissue respectively, and E denotes the electric field inside the human body. Safety guidelines for RF exposure have been proposed and recommended by several authorities and organisations. In this section, the simulated SAR values were compared with the latest SAR regulatory standards. The International Commission on Non-Ionizing Radiation Protection (ICNIRP) provides the SAR restrictions on whole body and localised tissue to prevent adverse biological effects between 10 MHz and 10 GHz, and the maximum of the average SAR of 10g contiguous tissue should be not more than 2 W per kg [1].

Table 3.3 SAR regulations from 10 MHz to 10 GHz.

Scenario	Average SAR	Localised SAR (head)
General exposure (unit)	0.4 W/kg	10 W/kg
Occupational exposure (unit)	0.08 W/kg	2 W/kg

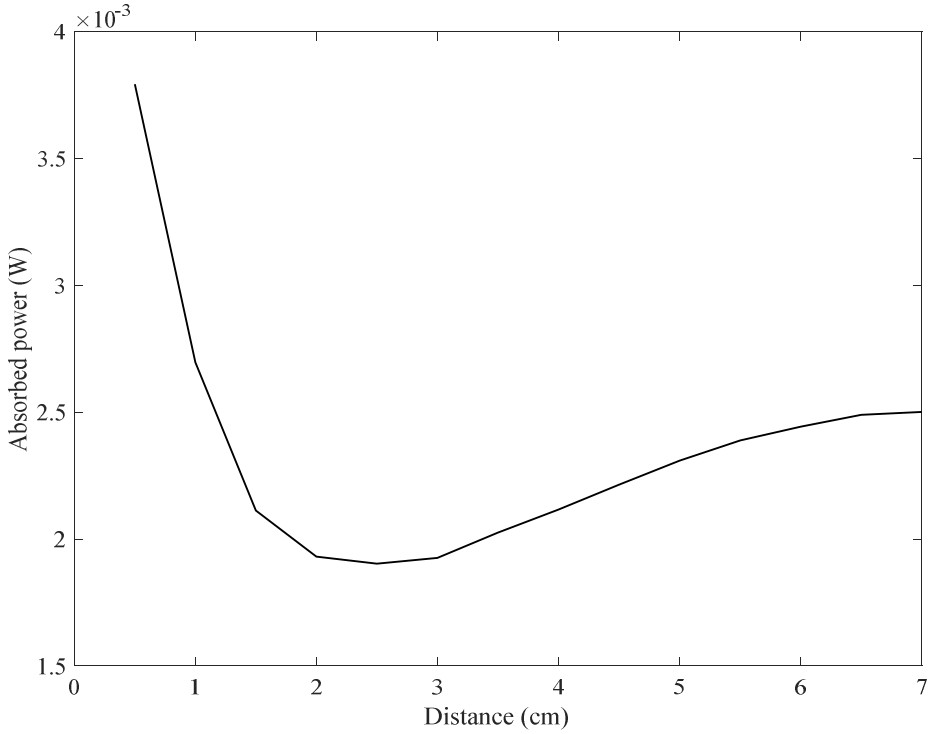

Figure 3.9 The absorbed power versus antenna separation distance.

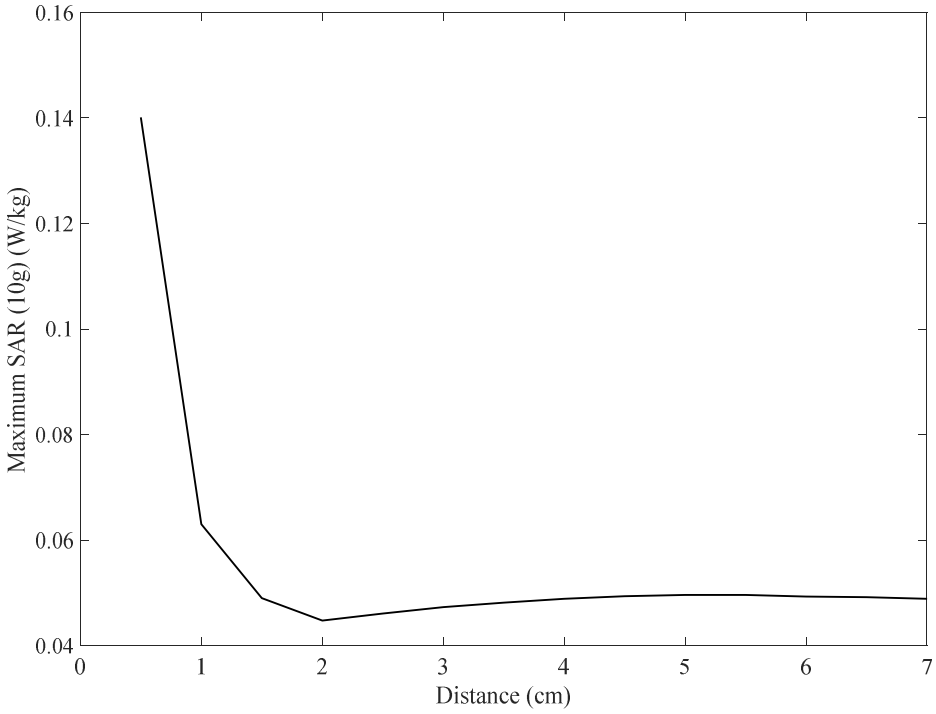

Figure 3.10 The maximum SAR 10g versus antenna separation distance.

Moreover, IEEE 802.15.6 standard regulates the average SAR value over 10g of tissue should not exceed 2W/Kg [4]. Table 3.3 summarises the SAR regulations for multiple scenarios.

Figure 3.9 illustrates the relationship between absorbed power and the communication distance. The maximum power is around 3.85 mW at the reference point d_{ref} (0.5 cm) while the minimum value 1.95 mW occurs at the approximate distance of 2.5 cm. The results demonstrate that the selected antenna type and the simulation approaches are appropriate and follow the safety advice of the ICNIRP and IEEE regulations. It can be seen further from Figure 3.10 that the maximum SAR 10g W/kg values vary with the antennas separating distance. Those values have been calculated by moving the Rx antenna location in the MIDA human head model. The maximum value is 0.14 W/kg at the 0.5 cm (skin tissue region) while the lowest SAR value is 0.045 W/kg at around 2 cm. The maximum SAR 10g W/kg and absorbed power results indicate that the antenna choice and simulation approaches are appropriate and satisfy the safety levels of the ICNIRP and IEEE standards. The detailed information regarding SAR calculation and comparison with the latest research work has been summarised in Appendix B.

3.4 Characterisation of the in-body communication system

There now follows an analysis of the implant WBAN including multiple factors: propagation loss, energy consumption, transmission rate, quality, transmission distance and so forth [1, 4-5]. The Rx receiving antenna movement begins at d = 5 mm from the transmitting antenna and the maximum separation range is 7 cm for the MIDA human model to minimise antenna coupling effects [8, 14]. In this chapter, a static human body model is assumed. In traditional communication systems, PL

represents signal energy attenuation in power or strength of an electromagnetic wave when it propagates via a certain environment. The Friis equation can describe the relationship between the average PL between the Tx and Rx as a function of the separating distance in the free space scenario [4]. The average PL can be expressed as:

$$PL_{dB}^{ave}(d) = PL_{dB}(d_{ref}) + 10n\log_{10}\left(\frac{d}{d_{ref}}\right), d \geq d_{ref} \quad (3.2)$$

where d_{ref}, $PL_{dB}(d_{ref})$ represent the reference distance and its corresponding PL value, respectively. The PL exponent *n* represents the standard PL exponent and is obtained applying the least square fit to the simulation data. The variable *d* is the separation distance between the Tx and Rx antennas. The IEEE 802.15.6 Group pointed out that this model is also applicable to describe the radio propagation in an implant to implant communication channel by adding a variable term to represent the random variations around the average path loss, which are caused by varying dielectric properties of the different tissues and organs [4]. In in-body communication systems, the shadowing effect may result in amplitude variation, which is defined as the difference between calculated PL values and the mean PL. An extended expression for in-body distance-based PL path loss model can be expressed in dB based on the Friis formula [8]:

$$PL_{dB}(d) = PL_{dB}(d_{ref}) + 10n\log_{10}\left(\frac{d}{d_{ref}}\right) + S_{dB} \quad (3.3)$$

where *S* represents the shadow fading effect. The shadow fading effect *S* expressed as:

$$S_{dB} = PL_{dB}(d) - PL_{dB}^{ave}(d) \quad (3.4)$$

In practical medical applications, the in-body communication path experiences different PL because the transmitting signal energy loss varies with the location of the

receiving antenna. A log-normal model is introduced to describe the MIDA heterogeneous scenario, and *S* then can be rewritten as [6, 8-9]:

$$p(S) = \frac{1}{\sqrt{2\pi}\sigma S} exp\left[-\frac{(\log_{10}(S) - \mu)^2}{2\sigma^2}\right] \tag{3.5}$$

where σ and μ denote mean and standard deviation of *S*, respectively. Here we take $\mu = 0$ and $\sigma = 1.079$. The average BER of the human head shadow fading channel can be expressed as [13-14]:

$$P_b(\bar{\gamma}) = \int_0^{\infty} P_0(\gamma) P(\gamma) d\gamma \tag{3.6}$$

where $\bar{\gamma}$ is the average signal-to-noise ratio. $P_0(\gamma)$ and $P(\gamma)$ represent the BER of the additive white Gaussian noise (AWGN) channel, and the probability density function (PDF) of γ, respectively. Multiple energy efficient modulation approaches are taken into account. BPSK and binary orthogonal PAM are selected to be used for the MIDA shadow fading channel model, and the channel performance is shown in Figure 3.11. In this Chapter, coherent BPSK technique is employed to demonstrate how to solve the Equation (3.6). The expression of the BPSK can be written as:

$$P_{0,AWGN}(\gamma) = \frac{1}{2} erfc\left(\sqrt{\gamma}\right) \tag{3.7}$$

where erfc(·) denote the complementary error function. Therefore the equation (3.6) of the BPSK modulation scheme can be rewritten as:

$$P_b(\bar{\gamma}) = \frac{1}{2}\sum_{n=1}^{N} erfc\left(\sqrt{\gamma}\right) \frac{1}{\sqrt{2\pi}\sigma\gamma_n} e^{-\frac{(\ln\gamma_n - \ln\bar{\gamma} + \frac{1}{2}(\frac{\ln 10}{10}\sigma_{dB})^2}{2\sigma^2}} (\gamma_n - \gamma_{n-1}) \tag{3.8}$$

The average BER performance of the in-body communication system can be achieved by numerical evaluation of the equation (3.8). Furthermore, the results regarding binary orthogonal PAM can be obtained in the same way [8]. The detailed information about CST parameter settings the essential steps in PL calculation approaches in MATLAB have been demonstrated in Appendix A.

According to previous published research on in-body communication systems [6, 8], a minimal BER performance of no less than 10^{-3} is needed for both BPSK and binary orthogonal PAM optimum receivers to promise acceptable communication. Thus, the predetermined threshold BER is selected as 10^{-3} for further investigation. It can be obtained from Figure 3.11 that the minimal required SNR value of binary orthogonal PAM is about 20.5 dB, while for BPSK it is around 17.5 dB. From the literature [3, 4, 9], it is established that the noise at the receiver side is AWGN and is primarily

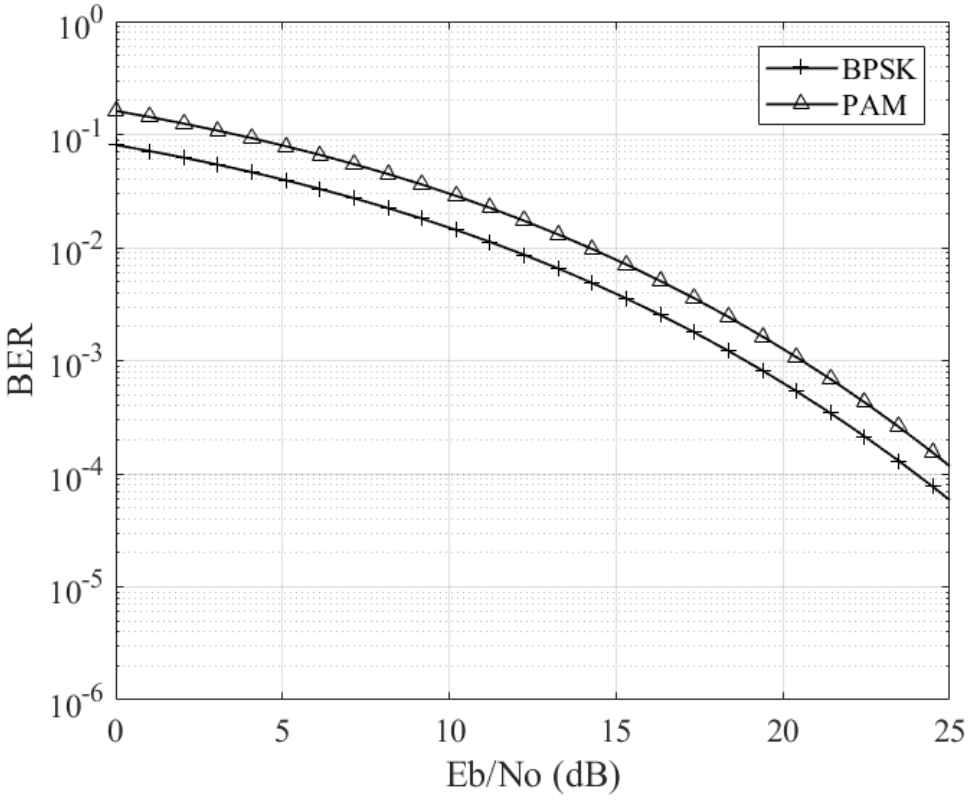

Figure 3.11 BER versus SNR for the MIDA human head channel.

contributed by thermal noise. The one-sided power spectral density of the noise in Joules is expressed as:

$$N_0 = k[T_a + (N_F - 1)T_0] \tag{3.9}$$

where T_a and T_b denote the temperature of the receiving dipole antenna noise and the transmission environment, respectively, k represents the Boltzmann constant and N_F is the receiver noise factor that can be defined via the noise figure in dB as $N_{F,dB} = 10\log_{10}(N_F)$. In this chapter, a typical value noise figure value of 3 dB is taken into account for further calculation. The SNR in dB can be stated as:

$$SNR_{dB} = P_{r,dBW} - 10\log_{10}(R_b) - N_{0,dB} \tag{3.10}$$

where $P_{r,dBW}$ and R_b mean the received power and communication transmission data rate, respectively. To analyse communication system reliability and quality, the system margin M_s is introduced for further investigation when a predetermined BER of 10^{-3} is selected. This system margin M_s should follow as [8, 16]:

$$M_s = SNR_{dB} - SNR_{min} \geq 0 \tag{3.11}$$

where SNR_{min} represents the minimal required SNR value that supports a reliable communication transmission in the predetermined BER scenario.

Figure 3.12 illustrates the achievable quality transmission range versus system margin calculated for various typical data transfer rates of 1 to 20 Mbps employing the BPSK and binary orthogonal PAM modulation methods. It can be obtained from Figure 3.12 that the wireless in-body communication system achieves a faster data rate at shorter distances. For example, the BPSK technique promises reliable data transmission at a distance of about 5.5 cm at 20 Mbps and affords around 7 cm at 10 Mbps; employing

1 Mbps could extend the communication distance to more than 10 cm. Similarly, the PAM method at those transmission data rates can achieve shorter ranges compared to BPSK. A 20 Mbps high-speed data rate can be transported for around 5 cm and a 1 Mbps low data rate covers around 10 cm distance with a reliable communication quality.

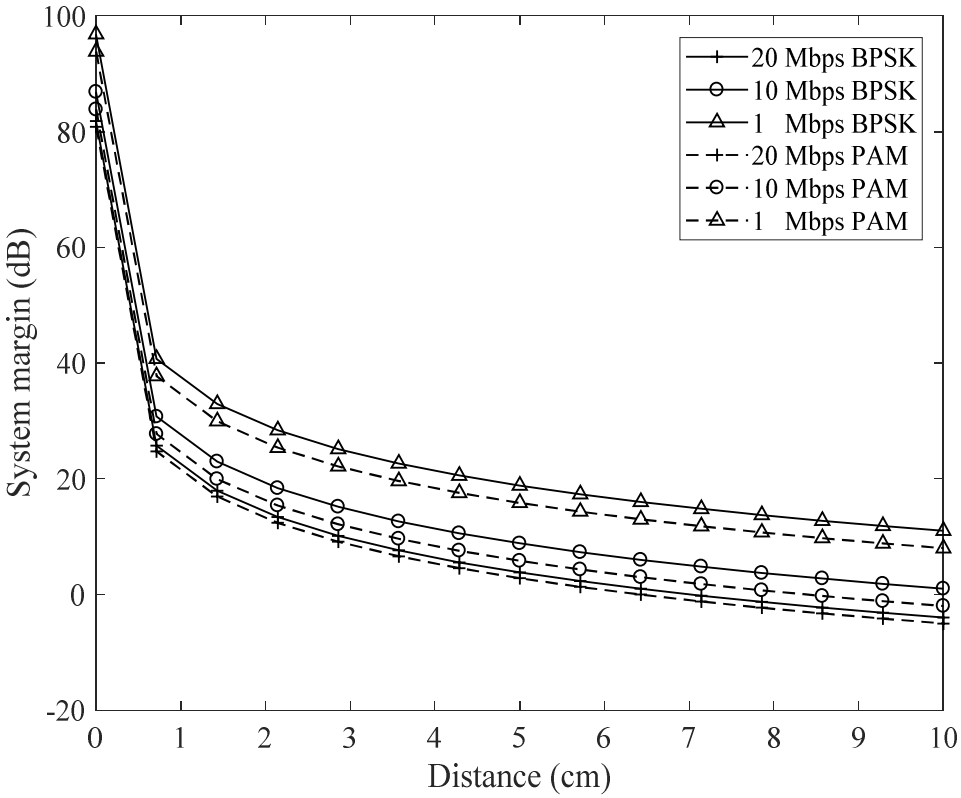

Figure 3.12 System margin versus distance at different data rates.

3.5 Summary

In recent years, implanted WBANs have begun to be considered as an essential approach for medical applications and services. This emerging technology has potential abilities to enable a wide range of assistance to patients, physicians, and researchers through real-time healthcare continuously monitoring, early detection of

Table 3.4 Simulation parameters for the link budget calculation in Chapter 3.

Simulation Parameter (unit)	Value
Frequency band (GHz)	2.4
Tx output power (μW)	25
Antenna gain (dBi)	0
Coding gain (dB)	0
Boltzmann constant (JK^{-1})	1.38×10^{-23}
BER (predetermined)	10^{-3}
Selected data rate (Mbps)	1, 10, 20
Selected transmission distance (cm)	7
SNR threshold (dB) (when BER=10^{-3})	17.5 (BPSK) 20.5 (PAM)
Noise figure (dB)	3 (typical value)

the disease and so forth. In this chapter, a review of the dielectric properties of human biological tissues has been demonstrated at first. PL has been derived based on several typical human tissues and the advanced computational human head model using the MATLAB Curve Fitting Toolbox. Additionally, a communication channel for the human cephalic area has been analysed using multiple modulation techniques. The BER performances have been obtained using various energy efficient modulation methods. Results show that using a high data rate (20 Mbps), binary orthogonal PAM is capable of 5 cm whereas BPSK only covers 5.5 cm. These results can be applied to future work regarding implantable brain-computer interface design and experimental validation.

The chapter has shown that the computational electromagnetics approach has been successfully used in demonstrating that high energy efficient modulation methods can support high data transmission scenarios healthcare applications. However, there exists a significant challenge for the proposed in-body communication system. Especially, in this model, the communication channel is only valid for the human brain region. Further research should be made to support healthcare services such as organ transplantation monitoring that are considered to be included in the human frontal thorax area [9, 17].

References

[1] S. Movassaghi, M. Abolhasan, J. Lipman, D. Smith, and A. Jamalipour, "Wireless body area networks: A survey," *IEEE Communications Surveys & Tutorials,* vol. 16, no. 3, pp. 1658-1686, 2014.

[2] H. Cao, V. Leung, C. Chow, and H. Chan, "Enabling technologies for wireless body area networks: A survey and outlook," *IEEE Communications Magazine,* vol. 47, no. 12, pp. 84-93, 2009.

[3] J. Y. Oh, J. H. Kim, H. S. Lee, and J. Y. Kim, "PSSK modulation scheme for high-data rate implantable medical devices," *IEEE Transactions on Information Technology in Biomedicine,* vol. 14, no. 3, pp. 634-640, 2010.

[4] R. Chavez-Santiago, *et al.*, "Propagation models for IEEE 802.15.6 standardization of implant communication in body area networks," *IEEE Communications Magazine,* vol. 51, no. 8, pp. 80-87, 2013.

[5] T. Kumpuniemi, T. Tuovinen, M. Hämäläinen, K. Y. Yazdandoost, R. Vuohtoniemi, and J. Iinatti, "Measurement-based on-body path loss modelling for

UWB WBAN communications," in *International Symposium on Medical Information and Communication Technology (ISMICT)*, Tokyo, Japan, pp. 233-237, 2013.

[6] M. Vallejo, J. Recas, P. G. del Valle, and J. L. Ayala, "Accurate human tissue characterization for energy-efficient wireless on-body communications," *Sensors,* vol. 13, no. 6, pp. 7546-7569, 2013.

[7] M. Barua, M. S. Alam, X. Liang, and X. Shen, "Secure and quality of service assurance scheduling scheme for WBAN with application to e-health," in *IEEE Wireless Communications and Networking Conference*, Cancun, Mexico, pp. 1102-1106, 2011.

[8] Y. Liao, M. S. Leeson, and M. D. Higgins, "A communication link analysis based on biological implant wireless body area networks," *Applied Computational Electromagnetics Society Journal,* vol. 31, no. 6, pp. 619-628, 2016.

[9] L. Martens, D. Kurup, W. Joseph, and G. Vermeeren, "In-body path loss model for homogeneous and heterogeneous human tissues," in *URSI General Assembly and Scientific Symposium*, Istanbul, Turkey, pp. 1-4, 2011.

[10] M. I. Iacono, *et al.*, "MIDA: a multimodal imaging-based detailed anatomical model of the human head and neck," *PloS One,* vol. 10, no. 4, p. e0124126, 2015.

[11] D. Andreuccetti, R. Fossi, and C. Petrucci, "An Internet resource for the calculation of the dielectric properties of body tissues in the frequency range 10 Hz-100 GHz," Available online: http://niremf.ifac.cnr.it/tissprop. Accessed 14th February 2017.

[12] M. I. Iacono, *et al.*, "A computational model for bipolar deep brain stimulation of the subthalamic nucleus," in *Annual International Conference of the IEEE Engineering in Medicine and Biology Society*, Chicago, USA, pp. 6258-6261, 2014.

[13] E. Neufeld, *et al.*, "Simulation platform for coupled modeling of EM-induced neuronal dynamics and functionalized anatomical models," in *International IEEE/EMBS Conference on Neural Engineering (NER)*, Montpellier, France, pp. 517-520, 2015.

[14] D. Kurup, W. Joseph, G. Vermeeren, and L. Martens, "Path loss model for in-body communication in homogeneous human muscle tissue," *Electronics Letters,* vol. 45, no. 9, pp. 453-454, 2009.

[15] B. Harris, P. Andrews, I. Marshall, T. Robinson, and G. Murray, "Forced convective head cooling device reduces human cross-sectional brain temperature measured by magnetic resonance: a non-randomized healthy volunteer pilot study," *British Journal of Anaesthesia,* vol. 100, no. 3, pp. 365-372, 2008.

[16] D. B. Smith, D. Miniutti, L. W. Hanlen, D. Rodda, and B. Gilbert, "Dynamic narrowband body area communications: Link-margin based performance analysis and second-order temporal statistics," in *IEEE Wireless Communications and Networking Conference (WCNC)*, Sydney, Australia, pp. 1-6, 2010.

[17] K. L. L. Roman, G. Vermeeren, A. Thielens, W. Joseph, and L. Martens, "Characterization of path loss and absorption for a wireless radio frequency link between an in-body endoscopy capsule and a receiver outside the body," *EURASIP Journal on Wireless Communications and Networking,* vol. 2014, no. 1, pp. 1-10, 2014.

CHAPTER 4.

Design of a Wireless In-to-out WBAN Communication System

4.1 Introduction

The rapid development of wireless communication technologies towards the health IoT is expected to bring increasingly attractive solutions, such as early diagnosis and treatment, organ transplantation monitoring and the like [1-2]. A proposed structure of the health IoT system is shown in Figure 4.1. A typical health IoT-based healthcare network consists of a smart gateway, a series of in-body and on-body sensors, and multiple communication paths that can continuous process and transfer human physiological signals to remote medical servers [2]. The health IoT technologies can be realised through health surveillance and remote telemedicine support systems, which are capable of transmitting real-time data collection, and visualisation via the Internet. Moreover, the large volume of collected medical data could help researchers in further studies such as the development of new healthcare products and the delivery of effective health education to people via the Internet [1-2]. To date, the majority of the research work has focused on on-body and off-body communication networks rather than in-body or in-to-out (I2O) body scenarios [3]. Moreover, some open research issues and technical challenges in the health IoT network are summarised in

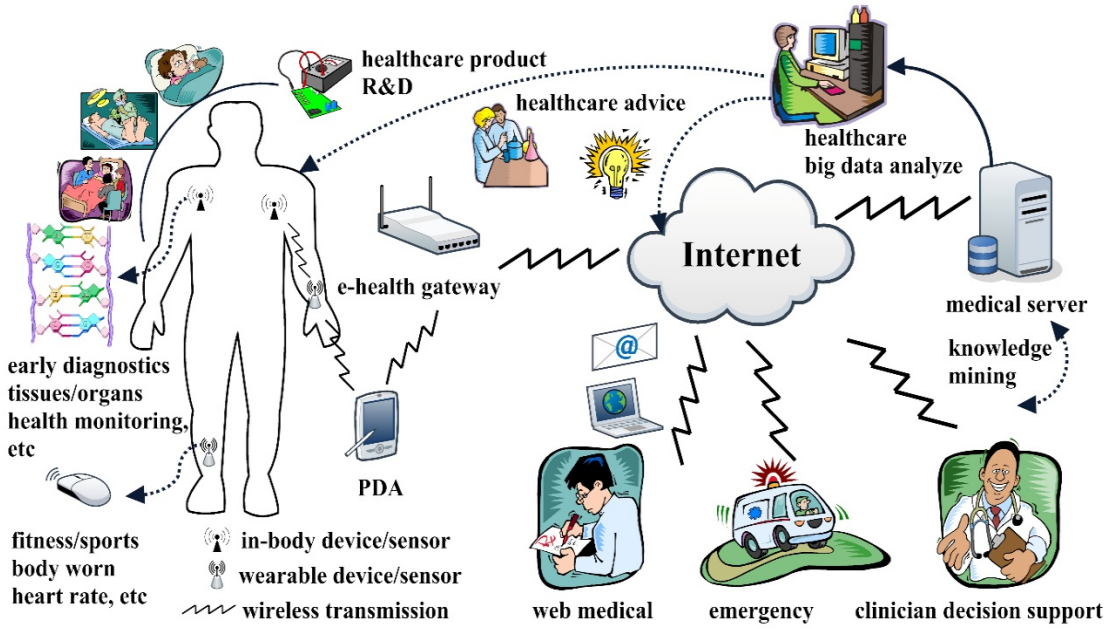

Figure 4.1 Demonstration of a typical structure of the health system.

Chapter 7.2 as part of the future work. In this Chapter, the main focus is on I2O WBAN network analysis and investigation. In-body and I2O WBAN systems differ from traditional wireless communication networks regarding propagation medium, transmission power restrictions and human body safety requirements. In [4], it is reported that more than 60% of the human intra-body area is composed of water and blood, and this may result in significant power attenuation when transmitting information through human tissues and organs. The key difference between I2O WBANs and the in-body communication networks is the transmission environment [5-6]. In the last chapter, a biological implant communication system for the human cephalic region was presented, where the in-body communication network covered a limited transmission distance. In this chapter, the I2O WBAN system is taken into account, which is a technique capable of supporting real-time medical data transmission from the in-body to the on-body region [6-7]. As shown in Figures 4.2

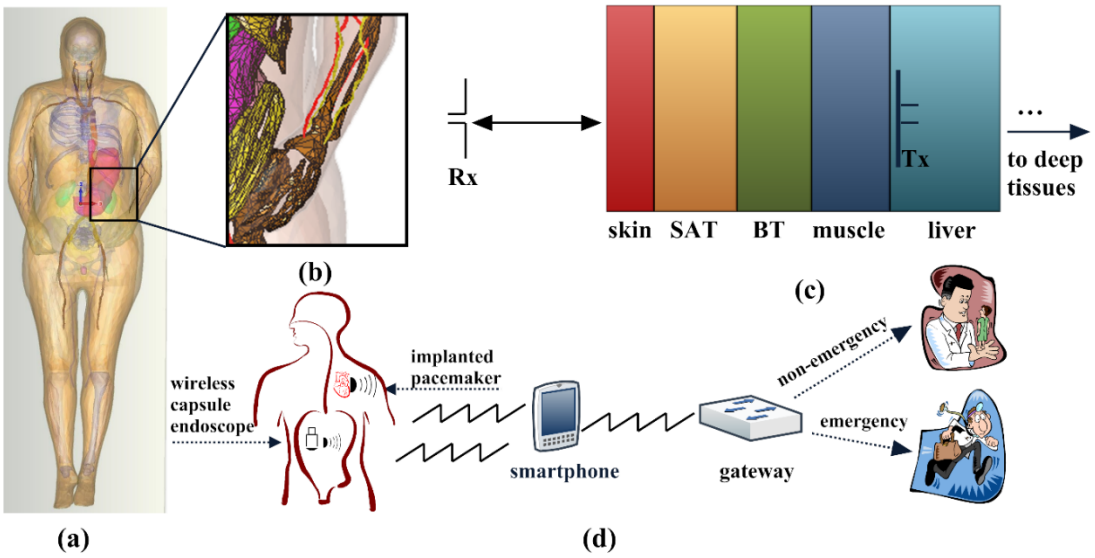

Figure 4.2 Demonstration of a typical structure of the health system. (a) the 3D human body model, (b) the cross section of the human frontal thorax, (c) an equivalent frontal thorax model, (d) a typical healthcare system.

(a) to (c), the I2O communication system can be the configured as a layer of air followed by a multiple-layer equivalent to the human body. Figure 4.2 (d) demonstrates several typical I2O WBAN applications including non-emergency and emergency situations. Concerning a personalised ubiquitous healthcare monitoring scenario, wireless implanted devices would significantly improve the comfort and mobility for patients when compared with existing wired connected medical devices [3]. RF techniques can offer longer transmission ranges, and interactive in-body sensor nodes communicate with on-body sensors wirelessly and efficiently [6]. The 2.45 GHz frequency is selected corresponding to the ISM band as this is a promising RF band to minimise the antenna size and it is compatible with other prospective communication methods.

Due to the technical constraints of in-body sensor batteries, improving the system performance of the communication module is a primary objective of the I2O WBAN

research [1, 6]. As discussed in Chapter 3, the in-body area is a lossy medium, which significantly attenuates the RF signals power when transmitting data inside the human body. To investigate the communication system performance between the sensors located inside and outside the human body, analysis of signal energy propagation loss is necessary for the development of the I2O path loss (PL) model. In this chapter, the PL model is obtained by using software from Computer Simulation Technology (CST) and an advanced 3D heterogeneous human model reported by [7]. The proposed PL model here is more accurate and achieves smaller deviation than those published in [7-9] because CST software employs the human tissues loss tangent properties in its simulations. Energy efficient digital modulation techniques are reported as a practical approach to overcoming the energy loss over the I2O communication channel caused by the heterogeneous intra-body environment [3]. Moreover, the transmitting power should comply with Federal Communications Commission (FCC) regulations and the specific absorption rate (SAR) must be lower than the safety guidance by the IEEE and ICNIRP as mentioned in the last chapter [10-11]. The performance of the I2O communication network with a series of data rates from 0.25 Mbps to 30 Mbps is discussed and investigated when utilising four selected modulation methods under the predetermined BER value of 10^{-3}.

The concept 'QoS' is widely reviewed and studied in communication networks. However, there is no consensus on its exact meaning. QoS handling for application-specific healthcare applications in wireless in-body and I2O communication systems remains a major research issue [12-13]. Analysis of the wireless in-body and I2O WBAN systems involves numerous typical QoS metrics regarding network throughput, available transmission range, system energy efficiency, network lifetime and so forth [1]. Also, it is important to note that the majority of medical applications

may demand one or multiple target-specific QoS metrics. For example, the data rate of in-body sensors varies from low data rate (a few kbps) in a pacemaker to relatively high data transfer speeds up to 10 Mbps in the wireless capsule endoscope and biomedical image processing [13]. Thus, the QoS mechanism, several application-specific QoS requirements and the most relevant QoS factors for service systems are discussed and summarised.

In this chapter, a simplified generic and accurate I2O WBAN PL model is obtained based on a multi-layer innovative 3D computational human body model by using CST electromagnetic solvers at 2.45 GHz. The simulated SAR values demonstrate that the I2O WBAN network satisfies the IEEE and other authorities' safety regulations. The BER and the system margin performance of the I2O communication system are presented by utilising the four selected energy efficiency modulation approaches.

The rest of this chapter is organised as follows: In Section 4.2, an introduction to the wireless I2O WBAN system is given. Followed by the simulation setting, PL modelling and the human safety evaluation are presented. Section 4.3 demonstrates the analysis of the proposed I2O communication system. Section 4.4 investigates the wireless I2O channel modelling and the system link budget. Section 4.5 presents the QoS issues and some research challenges. This chapter is concluded in Section 4.6.

4.2 Analysis of the I2O WBANs

4.2.1 System model

An I2O WBAN network covers various types of short-range communication links such as from in-body to on-body region [1]. Nodes in an I2O WBAN represent a sensor or device with communicating ability with other devices. The in-body sensor

Table 4.1 parameters of several tissues at 2.45 GHz.

Tissue	Relative Permittivity	Conductivity (S/m)	Loss tangent
Dry skin	38	1.46	0.2826
SAT	10.8	0.27	0.1452
BT	5.15	0.14	0.1953
Muscle	52.7	1.74	0.2419
Liver	43	1.69	0.2875

could be located either near the body surface (skin region) or in deep in the human body [1]. An on-body (wearable) device is usually placed on either the human body surface or up to a distance of 2 cm away from human skin surface and is capable of supporting wireless healthcare monitoring of a person anytime and anywhere [2]. Smartphones are considered to perform as communication gateways that visualise health information in user-friendly interfaces and transmit the data to physicians via the Internet. Moreover, the gateway is in charge of gathering all the information collected from in-body and on-body sensors and providing user-friendly interaction with the patients [1, 13].

4.2.2 Simulation settings

Biomedical antenna design in in-body WBAN is affected by many factors, such as body movement, posture and ageing. Literature about in-body antenna design research can be found in [8]. This chapter mainly focuses on the I2O WBAN communication channel design and investigation. Since it is difficult for researchers to test their results

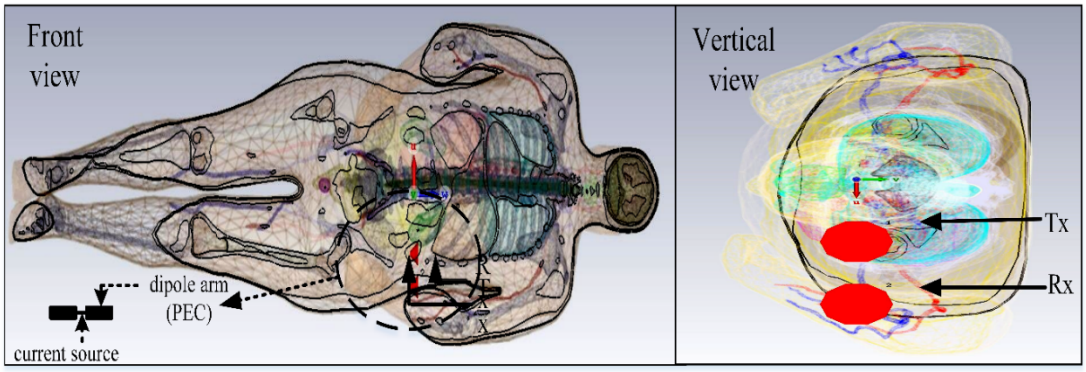

Figure 4.3 The front and vertical views of the 3D computational human model.

on an actual human body, the proposed human body model reported in [7] provides an alternative approach to analysis the performance of future I2O WBAN systems. The configuration, including a layer of air followed by layers equivalent to the frontal thorax of an adult, is as shown in Figure 4.2 (c). This advanced heterogeneous 3D human body model contains dry skin, subcutaneous adipose tissue (SAT), breast tissue (BT), muscle and liver are proposed, with thicknesses are 2 mm, 5 mm, 1 mm, 10 mm and 10 mm, respectively. The dielectric properties of those tissues are given in Table 4.1 [14]. The computational human body model in both front and vertical views is illustrated Figure 4.3.The simulation setup is in accordance with the methods proposed in [6], the transmitting antenna is located in the liver area with a length of 3.9 cm, while the receiving antenna is placed in a lossless medium (air) at a distance of 2 cm from the human body surface with a length of 6.12 cm ($\lambda/2$), where λ means the free space wavelength at 2.45 GHz. Moreover, both the Rx and Tx antennas are set in the aligned direction, with a thickness of 2 mm and made of perfect electric conducting (PEC) material. A current source is employed for simulations and the approaches are the same for all the cases.

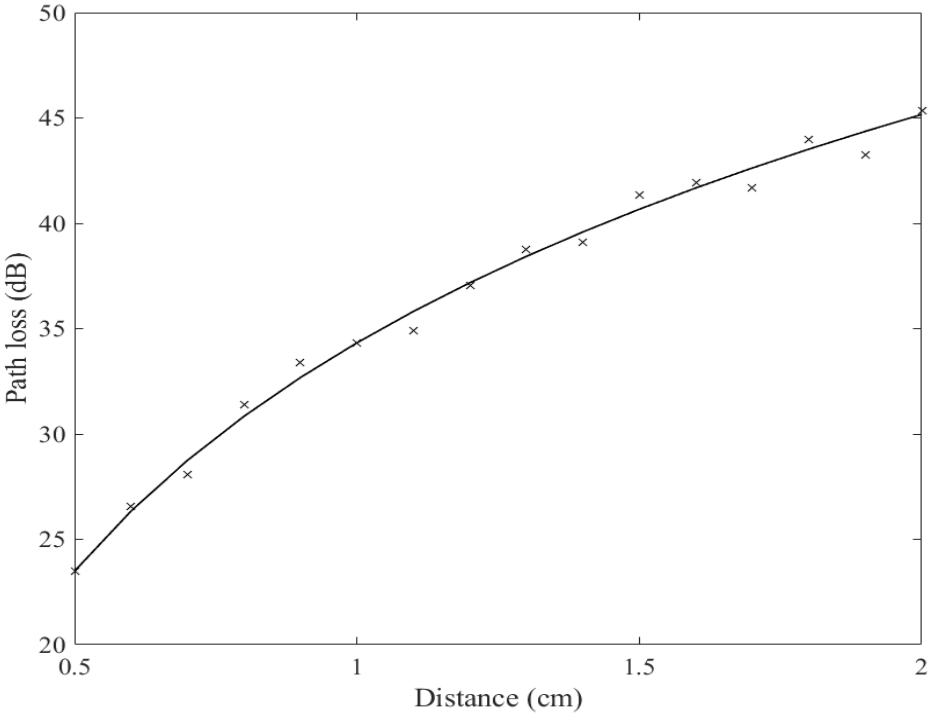

Figure 4.4 Path loss versus the communication distance.

4.2.3 I2O channel PL model

The statistical PL model, describing the I2O channel between an in-body sensor and an on-body sensor at a distance of *d*, can be stated in dB as [7]:

$$PL(d) = PL(d_{ref}) + 10n \log_{10}\left(\frac{d}{d_{ref}}\right) + S_{dB}, d \geq d_{ref} \quad (4.1)$$

where d and d_{ref} denote the separating distance between the Tx and Rx, and the reference distance (set as 0.5 cm in this chapter), respectively. $PL(d_{ref})$, $PL(d)$ represent the PL value at the reference distance d_{ref} and d, respectively. The parameter n is the path loss exponent which depends on the propagation medium. S is the shadow fading effect, which follows a normal distribution with a zero mean and a standard deviation σ_s, which represents the shadow fading strength degree [8].

Table 4.2 PL simulation results.

Parameter (unit)	Value
n	3.6
d_{ref} (cm)	0.5
σ_{dB} (dB)	2.93
$PL_{dB}(d_{ref})$ (dB)	23.49

The PDF function of the shadow fading effect *S* can be written in dB as:

$$P_{S_{(dB)}} = \frac{1}{\sqrt{2\pi}\sigma_s} \exp\left(-\frac{S_{dB}^2}{2\sigma_{log}^2}\right) \tag{4.2}$$

In a similar way to Chapter 3, a MATLAB least square fitting method has been implemented to yield a fitted PL as seen in Figure 4.4. The derived PL model has an exponent equal to 3.6, and the $PL(d_{ref})$ equals 23.49 dB, with a zero mean and a standard deviation of 2.93 dB. The results and the derived PL parameters are summarised in Table 4.2.

4.2.4 Safety analysis

As mentioned earlier, the signal propagation from the in-body to the on-body region leads to significant power attenuation. Biological effects and health risks may occur by exposure to RF electromagnetic fields. It has been reported in [4] that the RF signal energy absorption may lead to the body temperature increase inside the human body and tissue damage occur primarily if the body's inability to cope with the excessive

heat. As the I2O communications systems operate inside the human body and in the vicinity of the body surface, a safety investigation of the human body is of vital importance [1].

Table 4.3 Maximum SAR values for I2O communication model.

Location (unit)	SAR (1g)	SAR (10g)
5 mm	36.8 $mW \cdot kg^{-1}$	17.4 $mW \cdot kg^{-1}$
20 mm	31.5 $mW \cdot kg^{-1}$	19.3 $mW \cdot kg^{-1}$

According to the safety regulations of established international authorities and organisations such as the IEEE and the ICNIRP, the averaged SAR over 10 g of tissue should be less than 1.6 W per kg and 2W per kg, respectively [10-11]. An input power of 1 Watt (W) is provided to the in-body sensor, and the finite-difference time domain (FDTD) method employed with the 3D human body model. The maximum 1 g and 10 g SAR values for the proposed human body are given in Table 4.3 for the minimal distance (skin region) and maximum range (liver region). Results demonstrate that the SAR of the proposed human body model satisfies the IEEE and other authorities' regulations.

4.3 Analysis of the I2O communication system

4.3.1 The I2O communication channel

The human body is a lossy natural environment, which therefore leads to high attenuation for signal transmission. Due to the shadow fading effect, the instantaneous

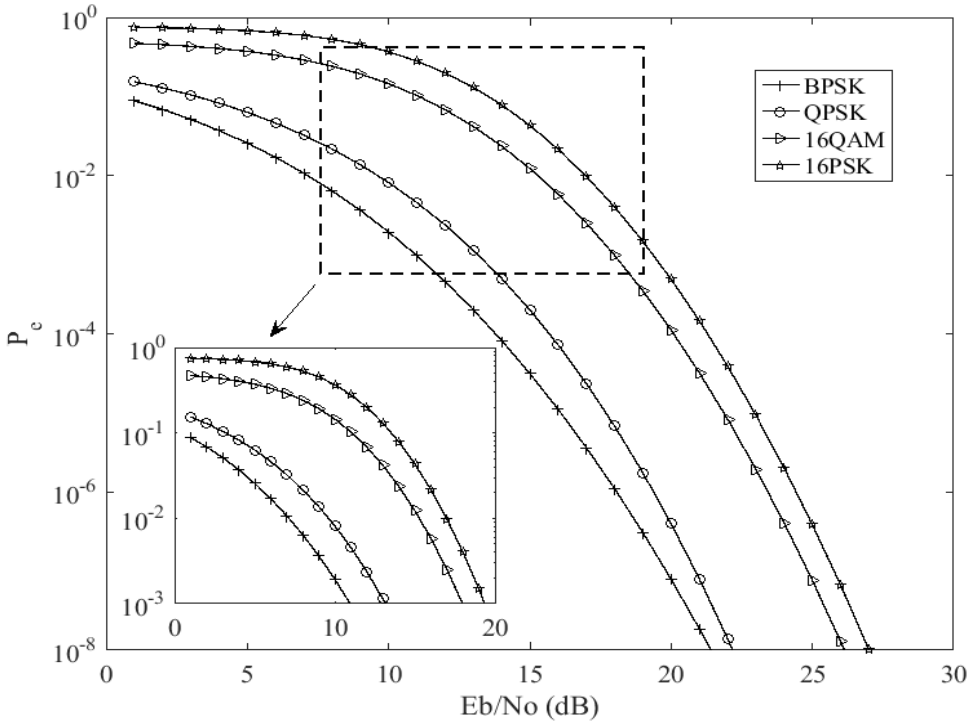

Figure 4.5 BER performance of four selected modulation techniques.

SNR is a random variable at the receiver output in an I2O WBAN channel. The received SNR values are no longer fixed, the bit error performance in optimum demodulation no longer applies. Therefore, average the bit error probability of the I2O shadow fading communication can be expressed as [15]:

$$P_e(\bar{\gamma}) = \int_0^{\infty} P_{b,AWGN}(\gamma)\, P_0(\gamma) d\gamma \tag{4.3}$$

where γ and $\bar{\gamma}$ denote the instantaneous and the average SNR values at the receiver side, respectively. $P_{AWGN}(\gamma)$ represents the BER performance in a AWGN channel, and $P_0(\gamma)$ means the PDF function of the instantaneous SNR at the receiver side.

The received power P_r can be expressed based on the PL and the transmitted power P_t:

$$P_r = \frac{P_t}{PL} \tag{4.4}$$

The received energy per information bit E_b is represented as:

$$E_b = \frac{P_r}{R_b} \tag{4.5}$$

where R_b denotes the data rate. Therefore the energy per bit to noise power spectral density ratio can be expressed as:

$$\frac{E_b}{N_0} = \frac{P_r}{N_0 R_b} = \frac{P_t}{R_b N_0 PL} \tag{4.6}$$

where N_0 denotes the noise power spectral density.

$$\ln\left(\frac{E_b}{N_0}\right) = \ln\left(\frac{P_t}{N_0 R_b PL}\right) = \ln\left(\frac{P_t}{R_b N_0}\right) - \ln(PL) \tag{4.7}$$

Since the PL is lognormal distribution as stated in equation (4.7), the term $\ln(E_b/N_0)$ can be obtained that follows a normal distribution once the data transmission rate R_b and the transmitted power P_t are fixed. Thus, the term E_b/N_0 follows a lognormal distribution.

$$P_0(\gamma) = \frac{1}{\sqrt{2\pi}\sigma\gamma} e^{-\frac{(\ln\gamma-\mu)^2}{2\sigma^2}} \tag{4.8}$$

where $\mu = \ln\bar{\gamma} - \frac{1}{2}\left(\frac{\ln 10}{10}\right)^2 \sigma_{dB}^2$, and $\sigma = \frac{\ln 10}{10}\sigma_{dB}$.

Detailed information on the selected modulation approaches can be found in [16-17]. Employing coherent BPSK modulation as a concrete demonstration, when [5]:

$$P_{AWGN}(\gamma) = \frac{1}{2} erfc\left(\sqrt{\gamma}\right) \tag{4.9}$$

where erfc(·) is the complementary error function and thus the equation (4.9) can be rewritten as:

$$P_e(\bar{\gamma}_m) = \frac{1}{2}\sum_{n=1}^{N} erfc\left(\sqrt{\gamma}\right)\frac{1}{\sqrt{2\pi}\sigma\gamma_n} e^{-\frac{(\ln\gamma_n - \ln\bar{\gamma}_n + \frac{1}{2}(\frac{\ln 10}{10}\sigma_{dB})^2}{2\sigma^2}}(\gamma_n - \gamma_{n-1}) \quad (4.10)$$

The average BER of the I2O communication channel can be obtained by numerical evaluation of equation (4.10). The same approach can be employed to the other selected modulation techniques. The statistical characteristic of E_b/N_0 is related to the shadowing effect of the proposed PL model. As discussed in Chapter 3, the AWGN noise is considered as the dominant noise source at the receiver side. The one-sided power spectral density of the thermal noise can be expressed as $N_0 = k[T_l + (N_F - 1)T_0]$ with k and N_F denote the Boltzmann constant and receiver noise factor, respectively [6, 18]. Similarly as Chapter 3 a typical noise figure value of 3 dB is employed in this chapter. The SNR values at the receiver side can be expressed in dB as:

$$SNR_{dB} = P_{r,dBW} - 10\log_{10}(R_b) - N_{F,dB} \quad (4.11)$$

Signal transmission via the I2O channel may suffer from high attenuation, so it is important to analyse the link budget to investigate the transmission quality and to design wireless communication systems for different scenarios. Two critical issues for the I2O WBAN systems are (i) energy consumption calculation for various predetermined BER communication links; (ii) the available transmission distances estimation when employing different transmission power.

Table 4.4 Parameters for the link budget investigation.

Simulation Parameter (unit)	Value
Frequency band (GHz)	2.45
Tx output power (μW)	1, 10, 25
Antenna gain (dBi)	0
Coding gain (dB)	0
Boltzmann constant (JK^{-1})	1.38×10^{-23}
BER (predetermined)	10^{-3}
Selected data rate (Mbps)	0.25, 5, 30
Selected distance (cm)	2
SNR (threshold) (dB) (when BER=10^{-3})	11 (BPSK) 13 (QPSK) 15.5 (16QAM) 18 (16PSK)
Noise figure	3 (typical value)

4.3.2 Analysis of the I2O link budget

The European Research Council recommends that the maximum transmission power should less than 25 μW in order to avoid human tissue damage [20]. In this chapter, typical transmitting power values 1, 10 and 25 μW are selected for further discussion. Given the high QoS requirements of healthcare communication systems, in agreement

with other I2O communication systems, a predetermined BER threshold of 10^{-3} is selected to ensure the communication performance is acceptable [5, 15]. As can be found in Figure 4.5, the threshold value SNR_{thr} for BPSK, QPSK, 16QAM and 16PSK are around 11 dB, 13 dB and 15.5 dB and 18 dB, respectively. The link budget simulation parameters are listed in Table 4.4.

The system margin M_s is an effective parameter that can estimate the reliability of communication network [6]. A communication channel with a negative link margin means that there is insufficient power to support data transmission and thus, it is critical to provide a suitable link to ensure that the communication system is reliable [6]. This parameter is given by determining the SNR that should exceed the threshold level (SNR_{thr}) as:

$$M_S = SNR_{dB} - SNR_{thr} > 0 \tag{4.12}$$

Figures 4.6-4.9 demonstrate the relationship between the system margin and the communication distance, with several typical data rates and numerous modulation approaches employing transmitter powers of 1 μW, 10 μW and 25 μW. Due to the constraints on the battery energy supply of the in-body sensor, trade-offs between transmitting power and communication channel quality should be taken into account [21].

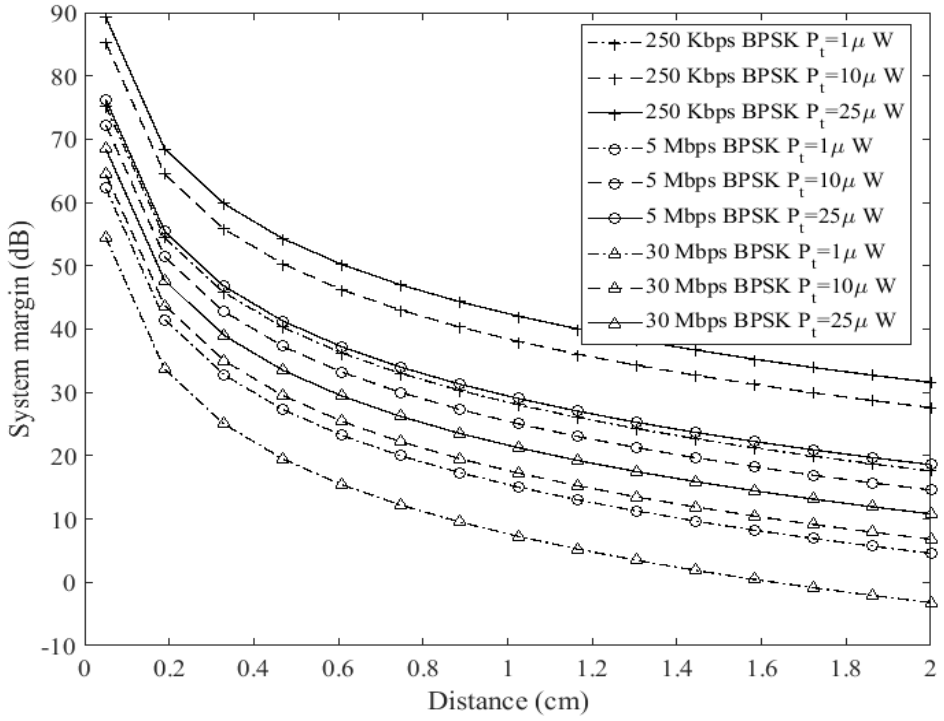

Figure 4.6 Link margin performance under BPSK modulation scheme.

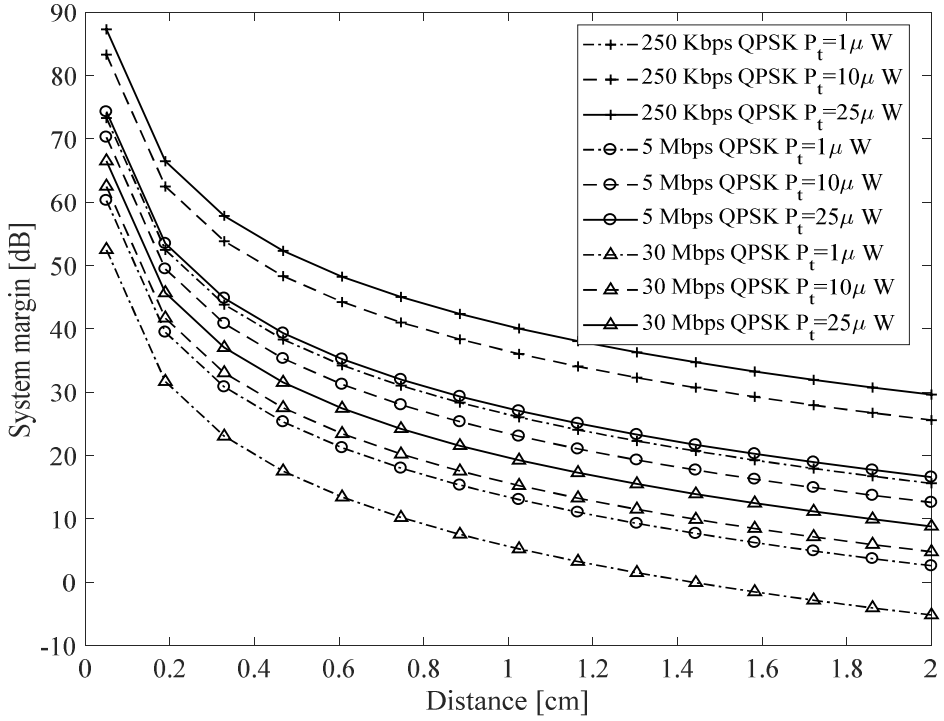

Figure 4.7 Link margin performance under QPSK modulation scheme.

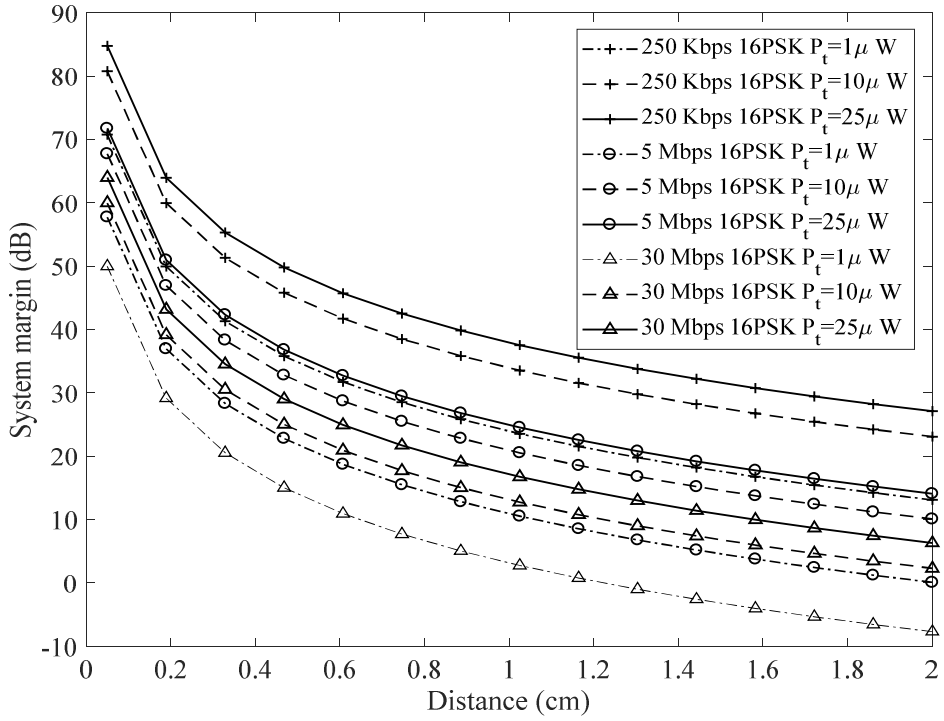

Figure 4.8 Link margin performance under 16PSK modulation scheme.

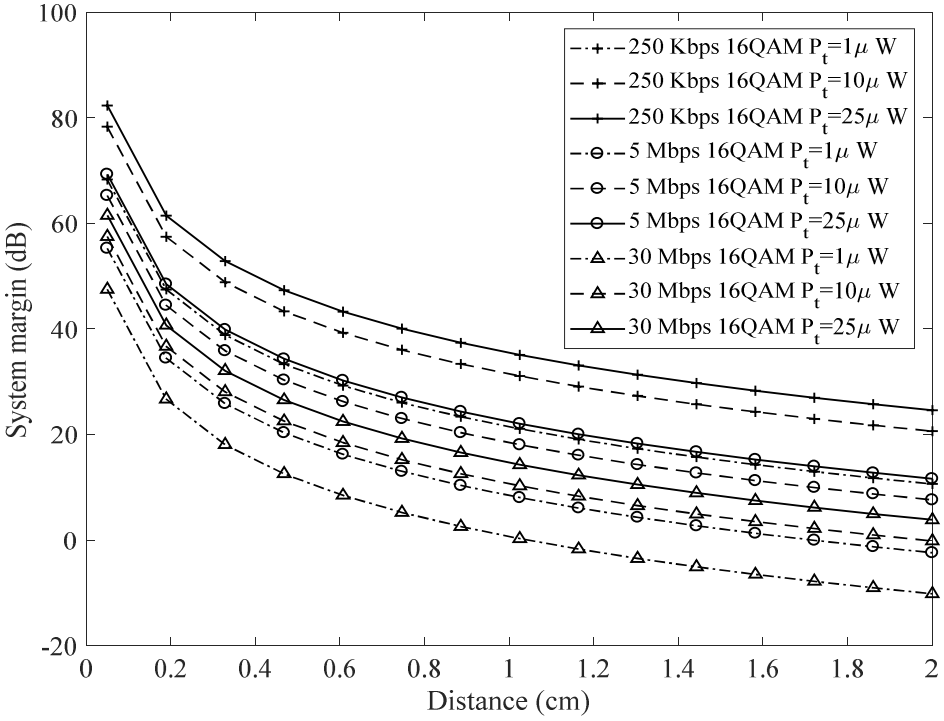

Figure 4.9 Link margin performance under 16QAM modulation scheme.

Results show that higher transmitting power can achieve longer communication distances for a certain data rate. The communication system can also cover longer distances by using lower transmission data rates when compared with higher data rates. For scenarios when under the same data rates and transmitting powers, the BPSK modulation scheme can achieve more reliable transmission than the other modulation schemes investigated. Furthermore, factors such as antenna orientations and body movements that account for energy losses should be taken into account and thus a fade system margin of a few dBs is required when designing real-time wireless medical systems to ensure the reliability of the information delivery [6, 21].

Table 4.5 QoS mechanism solutions.

Mechanism	Reliability	Real-Time Transmission	Energy Efficiency	Adaptability
Data collision	-	√	√	√
Data compression	-	-	√	√
Error control coding	√	√	√	√
Power control	√	√	√	√
Targeted ability	-	-	-	√

Table 4.6 Characteristics of multiple in-body and I2O WBAN scenarios.

Application	Energy consumption	BER	Operating distance	Lifetime	Data Rate
Pacemaker	Low	Low	Low	5-10 years	Few Kbps
Organ monitoring	Low	Moderate	Moderate	7–10 days	>100 Kbps
Glucose sensor	High	Moderate	Low	>1 week	Few Kbps
Capsule endoscope	High	High	Moderate	>24 h	~10 Mbps
Image processing	High	Very High	Low	>12 h	~10 Mbps

4.4 QoS analysis of WBANs

As different medical applications may demand different requirements, QoS support in the wireless in-body and I2O communication system is quite challenging [1-2]. Thus the QoS design challenges and issues for in-body and the I2O WBANs are discussed and analysed. The conclusions in this section can be employed to the in-body and I2O WBAN protocol design which is shown in Chapter 5.

4.4.1 Design challenges

In-body and I2O WBAN applications and services have specific network requirements to promise the system performance. Key requirements regarding the system level are listed as follows:

Signal propagation environment: Wireless in-body and I2O communication systems experience high path loss and energy loss due to tissue absorption that must be minimised and also obey the safety guidelines by authorities [1].

Network density: With the diversification of WBAN applications, different types of WBANs may be located inside or near the human body area. The IEEE 802.15.6 standardisation group expects up to 256 nodes per WBAN network [2].

Interference: Interference should be carefully considered when designing reliable wireless data transmission systems because a WBAN system may consist of a vast number of body sensors or people with numerous WBAN devices close to each other may experience interference.

Support for different data rates: Different WBAN applications may have different data rate requirements. Typically, medical applications request low data rate (around a few kbps) whereas non-medical services (such as multimedia) need high data rate of approximately up to 10 Mbps [1].

Compatibility: Bluetooth, WiFi, ZigBee and near field communication (NFC) have been proposed and investigated [3], and can support future WBAN technologies. Moreover, wireless in-body and I2O WBANs coexistence communication technologies, such as low-power WiFi, are also promising candidates for future medical applications design [22].

4.4.2 In-body and I2O WBAN QoS

The most important QoS metrics from the I2O communication system perspective involve network throughput, transmission distance, network lifetime and so forth [1].

Table 4.7 The QoS requirement of WBAN Applications.

QoS Requirement	WBAN requirements
Data rate	WBAN communication networks should cover from a few kbps up to 30 Mbps
Tolerance	around 3 seconds when sensor nodes either added or removed
Density	Less than 256 sensors
Mobility support	• Capable of reorganising the communication channels • Avoid data packet loss • Anti-interference when people moving
Latency	• Latency should be less than 125 ms for medical scenarios and not more than 250 ms for non-medical services. • Jitter should be less than 50 ms for all scenarios.
Compatibility	The network should be able to support that both the in-body, and on-body sensor nodes work together.

An in-body or I2O WBAN is required to analyse the application requirements and employ several QoS mechanisms [23]. Table 4.5 demonstrates the QoS mechanism solutions based on network conditions [3]. Optimisation of in-body and I2O communication systems that can realise the application-specific health IoT QoS requirements involves numerous elements [1]. The implanted devices battery lifetime for transplanted organs is the crucial factor, while the information transmission rate tends to be less of a critical issue. Reliable communication systems for glucose data

collected for diabetic patients would be the chief concern, and thus a lower predetermined BER value (say 10^{-6}) is required, which consumes more energy to improve system transmission quality. The significant features of some typical in-body and I2O WBAN applications are summarised in Table 4.6 [6, 24], coupled with the related QoS requirements in Table 4.7 [20-21].

4.5 Conclusions

In this chapter, an accurate I2O channel PL model for the 3D human I2O communication system at 2.45 GHz has been presented. Due to the technical constraints of the in-body sensor batteries, various high energy efficiency modulation schemes have been selected and investigated. The threshold SNR values of the proposed BPSK, QPSK, 16PSK and 16QAM modulation techniques are approximately 11 dB, 13 dB, 15.5 dB and 18 dB respectively when a satisfactory predetermined BER of 10^{-3} is selected. Results illustrate that the I2O WBAN network is enabled to achieve acceptable performance at relatively high data rates up to 30 Mbps at approximately 1.6 cm. Besides, it can offer a highly reliable I2O communication channel for longer ranges, at relatively lower data rates from 0.25 to 5 Mbps by utilising the BPSK technique. Analysis of the wireless in-body and I2O communication systems QoS issues regarding mechanism, conditions and several related factors are proposed and summarised. Finally, some design challenges are listed and discussed. The conclusions in this section can be applied to the I2O communication system protocols design which is analysed in Chapter 5.

References

[1] S. R. Islam, D. Kwak, M. H. Kabir, M. Hossain, and K.-S. Kwak, "The internet of things for health care: a comprehensive survey," *IEEE Access*, vol. 3, pp. 678-708, 2015.

[2] Y. J. Fan, Y. H. Yin, L. Da Xu, Y. Zeng, and F. Wu, "IoT-based smart rehabilitation system," *IEEE Transactions on Industrial Informatics*, vol. 10, no. 2, pp. 1568-1577, 2014.

[3] G. Vermeeren, E. Tanghe, A. Thielens, L. Martens, and W. Joseph, "In-to-out body path loss for wireless radio frequency capsule endoscopy in a human body," in *IEEE Annual International Conference of the Engineering in Medicine and Biology Society (EMBC)*, Orlando, USA, pp. 3048-3051, 2016.

[4] L. Galluccio, T. Melodia, S. Palazzo, and G. E. Santagati, "Challenges and implications of using ultrasonic communications in intra-body area networks," in *Annual Conference on Wireless On-demand Network Systems and Services (WONS)*, Courmayeur, Italy, pp. 182-189, 2012.

[5] J. Y. Khan, *Wireless body area networks: Technology, implementation, and applications*: Pan Stanford Publishing, 2011.

[6] Y. Liao, M. S. Leeson, M. D. Higgins, and C. Bai, "Analysis of in-to-out wireless body area network systems: towards QoS-aware health Internet of Things applications," *Electronics*, vol. 5, p. 38, 2016.

[7] D. Kurup, G. Vermeeren, E. Tanghe, W. Joseph, and L. Martens, "In-to-out body antenna-independent path loss model for multilayered tissues and heterogeneous medium," *Sensors*, vol. 15, no. 1, pp. 408-421, 2014.

[8] K. L. L. Roman, G. Vermeeren, A. Thielens, W. Joseph, and L. Martens, "Characterization of path loss and absorption for a wireless radio frequency link between an in-body endoscopy capsule and a receiver outside the body," *EURASIP Journal on Wireless Communications and Networking*, vol. 2014, pp. 1-10, 2014.

[9] D. Kurup, W. Joseph, G. Vermeeren, and L. Martens, "In-body path loss model for homogeneous human tissues," *IEEE Transactions on Electromagnetic Compatibility*, vol. 54, no. 3, pp. 556-564, 2012.

[10] A. Ahlbom *et al.*, "Guidelines for limiting exposure to time-varying electric, magnetic, and electromagnetic fields (up to 300 GHz)," *Health Physics*, vol. 74, no. 4, pp. 494-521, 1998.

[11] "IEEE standard for safety levels with respect to human exposure to radio frequency electromagnetic fields, 3 KHz to 300 GHz amendment," Available online: http://ieeexplore.ieee.org/servlet/opac?punumber=10830. Accessed 14th February 2017.

[12] Kathuria, M.; Gambhir, S. "Quality of service provisioning transport layer protocol for WBAN system, " In *Proceedings of the International Conference on Optimization, Reliability, and Information Technology (ICROIT)*, Haryana, India, pp. 222-228, 2014.

[13] J. Gubbi, R. Buyya, S. Marusic, and M. Palaniswami, "Internet of Things (IoT): A vision, architectural elements, and future directions," *Future Generation Computer Systems*, vol. 29, no. 7, pp. 1645-1660, 2013.

[14] D. Andreuccetti, R. Fossi, and C. Petrucci, "An Internet resource for the calculation of the dielectric properties of body tissues in the frequency range 10 Hz-

100 GHz," Accessed online: http://niremf.ifac.cnr.it/tissprop/. Accessed 14th February 2017.

[15] M. Cheffena, "Performance evaluation of wireless body sensors in the presence of slow and fast fading effects," *IEEE Sensors Journal*, vol. 15, no. 10, pp. 5518-5526, 2015.

[16] M. A. Hannan, S. M. Abbas, S. A. Samad, and A. Hussain, "Modulation techniques for biomedical implanted devices and their challenges," *Sensors*, vol. 12, no. 1, pp. 297-319, 2011.

[17] S. R. Kim and H.-G. Ryu, "Analysis and design of QAPM modulation based on multi-carrier using compressive sensing for low power communication," in *International conference on ICT Convergence*, Jeju, Korea, pp. 484-488, 2012.

[18] D. Anzai, S. Aoyama, M. Yamanaka, and J. Wang, "Impact of spatial diversity reception on SAR reduction in implant body area networks," *IEICE Transactions on Communications*, vol. 95, no. 12, pp. 3822-3829, 2012.

[19] Y. Nagata *et al.*, "Radiofrequency thermotherapy for malignant liver tumors," *Cancer*, vol. 65, no. 8, pp. 1730-1736, 1990.

[20] H. B. Elhadj, L. Chaari, and L. Kamoun, "A survey of routing protocols in wireless body area networks for healthcare applications," *International Journal of E-Health and Medical Communications*, vol. 3, no. 2, pp. 1-18, 2012.

[21] J. Elias, "Optimal design of energy-efficient and cost-effective wireless body area networks," *Ad Hoc Networks*, vol. 13, pp. 560-574, 2014.

[22] T. Hayajneh, G. Almashaqbeh, S. Ullah, and A. V. Vasilakos, "A survey of wireless technologies coexistence in WBAN: analysis and open research issues," *Wireless Networks*, vol. 20, no. 8, pp. 2165-2199, 2014.

[23] M. A. Yigitel, O. D. Incel, and C. Ersoy, "QoS-aware MAC protocols for wireless sensor networks: A survey," *Computer Networks*, vol. 55, no. 8, pp. 1982-2004, 2011.

[24] M. M. Monowar, M. M. Hassan, F. Bajaber, M. Al-Hussein, and A. Alamri, "McMAC: towards a MAC protocol with multi-constrained QoS provisioning for diverse traffic in wireless body area networks," *Sensors*, vol. 12, no. 11, pp. 15599-15627, 2012.

CHAPTER 5.

An Incremental Relay Based Routing Scheme for WBANs

5.1 Introduction

Due to recent developments in wireless communication technologies and intelligent integrated circuits, WBANs have attracted increasing attention in e-health applications and services [1]. A crucial role of WBANs is to provide accurate and reliable networking that interconnects implant devices and wearable devices inside, on or around the human body [2]. Wearable devices are reported as promising candidates to perform as an infrastructure for relaying data from implanted devices because of the high computational ability and convenience of power recharging. However, implant devices are categorised by strict requirements on low-power consumption, miniature size, reliable data transmission and data packet design [3]. The in-body sensor nodes are implanted inside the human body by surgery, and thus it is difficult to replace or recharge them. Additionally, the in-body sensor node should be capable of transmitting accurate medical data in a timely and reliable manner because every collected physiological signal in WBANs is of great significance [2]. As demonstrated in Figure 5.1, the in-body sensor nodes in e-health services should be able to support

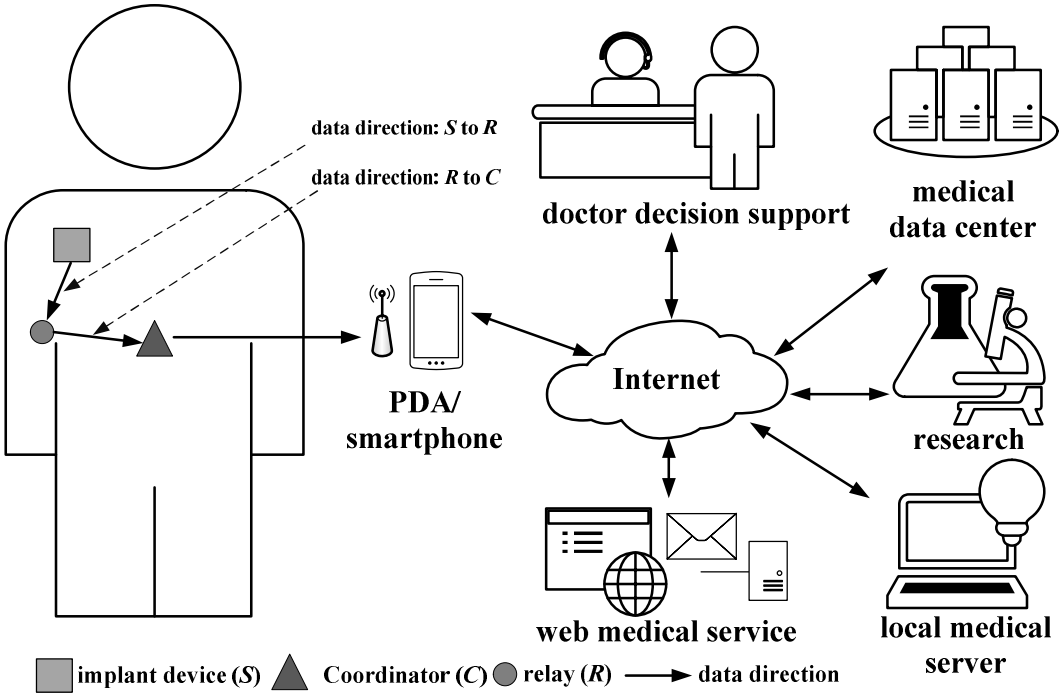

Figure 5.1 Demonstration of the information flows in a WBAN system.

various medical applications in an architecture with the use of IoT such as clinical decision support systems and medical data research [1,4]. Ahmad et al. [5] reported that scenarios in which the implant node *S* directly communicates with the external coordinator *C* or where data transmission between two in-body sensor nodes is not allowed due to the high power consumption. One effective approach to minimise an in-body WBAN system energy consumption is to decrease the overall transmission distance. The authors in [6] reported that a relay-based routing solution is an efficient method to realise energy savings. The in-body sensor node communicates with the relay node, which is responsible for forwarding and delivering data to the external coordinator. Thus, the overall communication distance is minimised and results in extending the in-body WBAN network lifetime. Moreover, the power consumption is significantly transferred from the in-body sensors to the wearable relays, which can be replaced and recharged easily. Ntouni et al. [7] reported that the energy consumption of in-body sensor nodes could be significantly reduced at the cost of relay nodes by

deploying the latter on patient's clothes. However, to date, the majority of the proposed WBAN routing protocols are specifically designed for wireless on-body WBAN systems [8-9]. Analysis and design of the in-body WBAN routing protocols is far more complicated. One of the major research challenges is the efficient energy utilisation of in-body sensor nodes. In addition, quality of service (QoS) support in in-body WBAN communication systems is another emerging research topic, which attracts attentions from both academics and industry specialists [9-10]. Akram et al. [11] pointed out that human natural dynamic movements would result in data packets dropping and increase the propagation delay. Liao et al. [4] stated that the design and implementation of implant WBAN communication systems need to consider a series of QoS metrics regarding network lifetime, throughput, and the propagation delay. Analysis of random data packet dropping due to the channel fading effect makes use of a stochastic uniform model with a probabilistic strategy in accordance with [12].

In this chapter, an advanced I2O WBAN PL model and a QoS-aware minimal power consumption model proposed in [10] are investigated when analysing signal energy attenuation from an implant device *S* to a relay node *R*. The mathematical models of the network lifetime, network throughput and delay are given along with multiple related constraint functions. An incremental relay-based routing technique for the wireless in-body sensor network is proposed and compared with the existing two-relay based protocol. Relays receive data from the in-body sensor nodes and forward the collected data to the external coordinator based on the assigned time division multiple access (TDMA) time slots. Simulation results are obtained regarding system stability period, network lifetime, energy consumption, throughput and propagation delay.

The rest of this chapter is organised as follows. In Section 5.1, an introduction to an advanced WBAN PL model and the network energy consumption model is presented.

Section 5.2 demonstrates the challenges of routing design in WBANs. Section 5.3 presents various selected QoS metrics mathematical models along with the relevant subjective functions. Section 5.4 shows the proposed protocol along with the demonstration of the communication data flow. The system performance analysis is demonstrated in Section 5.5. Section 5.6 concludes the chapter.

5.2 Challenges of routing design

WBAN network technologies offer numerous research challenges to both the industry and the academic communities. The technical difficulties include low capacity sensor battery, limited transmission range, energy management and so forth. Some critical technical challenges in wireless in-body WBANs routing design are summarised below [6-7]:

Communication link: The quality of the communication link between an in-body sensor and the corresponding relay varies as a function of transmission distance. The unstable communication channel may result in a higher delay and data packet loss.

Human safety and interference: The energy consumption of the in-body sensors needs to be minimised to ensure the people's health and security [3].

Power limitation: Due to the limitation of available energy resources in in-body WBAN systems, therefore, energy efficiency data routing protocols are needed to prolong in-body WBAN network lifetime.

Network topology: This must be considered to ensure maximum power consumption efficiency and minimise the propagation delay. Moreover, densely deployed WBAN systems may lead to high interference and incur human health risks. Thus, the total

number of the in-body sensors within the WBAN system needs to be carefully analysed.

5.3 System model

5.3.1 Path loss model

The transmission channel between an in-body transmitter node and a receiver node within a WBAN system is affected by numerous factors such as slow shadow fading and noise [12]. As presented in [4], the PL model can be expressed as:

$$PL_{dB}(d) = PL_{dB}(d_{ref}) + 10n\log_{10}(\frac{d}{d_{ref}}) + S_{dB}, d \geq d_{ref} \quad (5.1)$$

where d and d_{ref} denote the communication distance between a transmitter and a receiver, and the reference distance, respectively; n is the PL exponent and S denotes the shadow fading effect. Two typical application scenarios: deep implant to implant and implant to near surface are listed in Table 5.1 [4, 12]. In this chapter, the implant to near surface biological PL model is selected for further research.

Table 5.1 Parameters of numerous WBAN PL models.

Parameters (unit)	Deep implant to implant	Implant to near surface
$PL(d_{ref})$ (dB)	42	23.49
n	2.6	3.6
σ (dB)	1.745	2.93

5.3.2 Energy consumption model

The analysis of in-body and the I2O WBANs energy consumption is based on a flexible QoS communication model obtained by extending the literature [13-16]. The communication distance and the PL exponent are represented as *d* and *n*, respectively. The length of transmission packet is set as *k* and the required energy to be active is E_{elec}. Thus the minimal transmission energy consumption of the sensor node can be expressed as [10]:

$$E_{Tx}(d,k) = k\left(E_{elec} + E_{amp}dn\right) \tag{5.2}$$

where $E_{Tx}(d,k)$ and E_{amp} denote the minimal required energy consumption of the in-body sensor node and the amplifying circuit, respectively. The total energy consumption E_{total} constraints of a sensor node can be expressed as:

$$E_{total}(d,k) = E_{Tx}(d,k) + E_{Rx} \tag{5.3}$$

where the minimum energy consumption for the data receiving process can be expressed as $E_{Rx} = kE_{elec}$. Two commercially available WBAN transceivers, the nRF2401A and CC2420 are taken into consideration [17]. The relevant parameters of those transceivers are summarised in Table 5.2 [17].

5.4 QoS metrics modelling

5.4.1 Selected QoS metrics analysis

Definition of selected vital QoS metrics are listed below [4, 15]:

Stability period: The lifetime of the WBAN system until the first in-body sensor node is energy depleted.

Network Lifetime: The lifetime of the WBAN system until all in-body sensor nodes

Table 5.2 Radio parameters of nRF 2401A and CC2420.

Parameter (unit)	nRF2401A	CC2420
E_{Tx_elec} (nJ/bit)	16.7	96.9
E_{Rx_elec} (nJ/bit)	36.1	19.7
E_{amp} (nJ/bit/mn)	1.97	2.7
Tx current (mA)	10.5	17.4
Rx current (mA)	18	19.7

are energy depleted.

Network residual energy: The difference between initial network energy and consumed energy of all in-body sensor nodes during network operation.

Network Throughput: The number of information data packets successfully transmitted to the sink.

Delay: Time required for a signal to reach from in-body sensor node to the corresponding relay node. The delay will increase when the transmission distance becomes longer.

5.4.2 Network lifetime modelling

The number of in-body sensor nodes is *N* and the in-body WBAN network lifetime is T_{total}. One important target for the I2O WBAN is to maximise the network lifetime, which is formulated via linear programming as [4]:

$$\text{Objective function: Max } T_{total} = \sum_r t_r \tag{5.4}$$

where r and t_r represent the current round and summation of all rounds before all in-body sensors energy deplete, respectively. The energy consumption consists of data sensing E_{sen}, information transmission E_{trans}, data gathering E_{gat}, data processing E_{pro} and so forth. The residual energy of the in-body WBAN system after each round can be represented as E_i.

The other constraint functions are:

$$t_r \geq \frac{E_i}{\sum_i k\left(E_{sen}^i + E_{pro}^i + E_{trans}^i + nE_{amp}^i d_{SR}\right)}, \forall i \in N \tag{5.5}$$

$$E_o \geq E_i\,, \forall i \in N \tag{5.6}$$

$$E_i \to 0, \forall i \in N \tag{5.7}$$

$$\sum_i f_{SR} > \sum_r f_{RC}\,, \forall i \in N \tag{5.8}$$

where E_0 represents the in-body sensor node initial energy status. The constraint (5.5) defines the minimal energy consumption per round. Constraints (5.6) and (5.7) point out that current energy of the in-body sensor node E_i will gradually decrease after each round and can be regarded as dead when the energy is depleted. Constraint (5.8) illustrates that the information transmission directions should follow in-body sensor node *S* to a relay *R*, and then *R* forward the collected information to the coordinator *C*.

5.4.3 Network throughput modelling

Every piece of information within in-body WBANs is vital, and thus it is of great significance to increase the number of successfully transmitted data packets. The

linear programming model for the number of successfully received packets can be formulated as:

$$\text{Objective function: } \sum_{r} P_s \,, \forall r \in T \tag{5.9}$$

The aim of the objective function (5.9) is to maximise the number of successfully transmitted packets P_s.

Constraint functions are given as:

$$P_{SR} > P_{RC}, \forall S \in N, \forall R \in N \tag{5.10}$$

$$E_i \geq E_{Tx\_min} \tag{5.11}$$

$$P_{link} \geq P_{min} \tag{5.12}$$

Constraint (5.10) demonstrates that some information packets may be dropped when transmitting data from the in-body sensor R to coordinator C. Constraint (5.11) illustrates that the communication transmission channel fails once the remaining energy E_i is less than the minimal required transmission energy E_{Tx_min}. Constraint (5.12) states that the successfully probability of the transmission channel P_{link} should no less than the minimal required P_{min}.

5.4.4 Delay modelling

As demonstrated in equations (5.5) and (5.8), maximising the network lifetime will increase the delay. Moreover, high transmission signal energy attention leads to transmission link instability, which will cause higher data transmission delay. As reported in [4], propagation delay is the main factor in dealing with high data rate transmission scenarios. The mathematical model of the end to end delay τ_{SC} can be expressed in summary by:

$$\text{Objective function: } \tau_{SC} = \tau_S + \tau_{RC} \tag{5.13}$$

where the overall delay τ_{SC} consists of the nodal delay τ_S and the data transmission delay τ_{RC} from the relay node *R* to the coordinator *C*.

Subject to:

$$\tau_S \geq \tau_S^{Tx} + \tau_S^{queue} + \tau_S^{Proc} + \tau_S^{CC}, \forall S \in N \tag{5.14}$$

$$x \geq N \geq 0, \forall x \in Z^+ \tag{5.15}$$

$$P_{SR} \geq P_S \tag{5.16}$$

$$\gamma_S^{dep} \geq \gamma_S^{arr} \tag{5.17}$$

$$BER_i \geq BER_{pre} \tag{5.18}$$

$$Min\ d_{SR} \rightarrow d_{min} \tag{5.19}$$

where τ_S^{Tx}, τ_S^{queue}, τ_S^{Proc} and τ_S^{CC} represent the delay of information propagation, queuing, processing and channel capture, respectively [4, 8]. Constraint (5.14) states that the nodal delay consists of numerous factors such as information propagation, queuing, processing and channel capture. Constraint (5.15) states that if the number of in-body sensor nodes *N* is very large, the channel capture delay τ_S^{CC} will increase. Considering the limited packet handing ability at the receiver side, constraint (5.16) and (5.17) point out that the number of data packets should optimised, and the packet arrival rate γ_S^{arr} should less than the packet transmit rate γ_S^{dep}. Constraint (5.18) regulates that minimal BER so that it is no less than the predetermined BER as discussed in [4]. Constraint (5.19) shows that minimizing the overall transmission

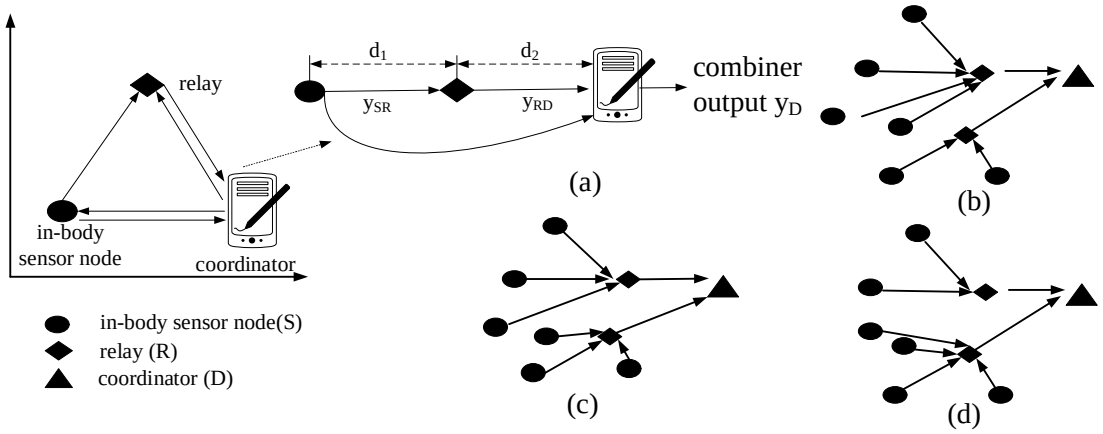

Figure 5.2 Demonstration of the relay based routing protocol. (a) a simple relaying model; (b)-(d) two-relay based routing protocols.

distance is an effective approach to save energy consumption and reduce the propagation delay. Due to the technical constraints and the fact that there is still no agreement for data packet superframe structures in in-body WBAN sensors, the propagation delay is defined as [18]:

$$\tau_S^{Tx} = \frac{d(S)}{c} \tag{5.20}$$

where c and $d(S)$ represent the speed of electromagnetic wave and the distance between an in-body sensor node to the corresponding relay node, respectively.

5.5 The proposed protocol

In this section, the data routing protocol for a wireless in-body sensor network is given to minimise the overall communication distance, subject to the acceptable QoS metrics as discussed before. The coordinator is deployed at the centre of the body, and the in-body sensor nodes are located at the predetermined positions. In accordance with [8], the number of relays is limited to two with coordinates (1.65, 0.75) and (0.9, 1.65). Demonstration of the multiple relay-based energy efficient routing protocols for in-

body WBAN systems is given in Figure 5.2. A simple relaying model is shown in Figure 5.2 (a). At the beginning stage, source noce *S* transmits the collected information data to a corresponding relay node *R* and the coordinator *D* at the same time. Afterwards, the relay node *R* received the data from *S* to *D*. Assuming the distance between S and R is d_1 and *R* to *D* is d_2. The transmitted information from *S* is defined as x_s and transmission medium characteristics of the *S* to *R* and *S* to *D* expressed as h_{SR} and h_{SD}, respectively. Therefore, the information data received at the corresponding relay node *R* (y_{SR}) and *D* (y_{SD}) from the in-body sensor node *S* can be written as: $y_{SR} = h_{SR}x_{SR} + N_{SR}$, $y_{SD} = h_{SD}x_{SD} + N_{SD}$, respectively. In this thesis, all simulation cases are in the same manner as proposed in [8-10], we employ a probabilistic method to calculate the total number of successfully transmitted packets, Moreover, as discussed earlier, no directly data transmission between the source node and the coordinator. Figures 5.2 (b)-(d) are two relay-based routing scenarios. The demonstration of the communication flow is shown in Figure 5.3. The first stage is the system initialization phase; every in-body sensor node is assigned a unique ID. The coordinator transmits an information message to inform all in-body sensor nodes with its location. Then each in-body sensor node communicates a data packet, which consists of its energy status and position. The coordinator compares the residual energy E_i of in-body sensor node with the minimised required energy as mentioned in equation (5.2). If $E_i \geq (5.2)$, the coordinator calculates the distance of the in-body sensor node with all relays. The corresponding relay is selected based on the minimum distance to the in-body relay node *S*. Relay nodes are selected in each round to route the data of the in-body sensor nodes. Relays are chosen according to the cost function proposed in [9]:

$$C(i) = \frac{d(i)}{R(i)} \tag{5.21}$$

where $d(i)$ and $R(i)$ represent the communication distance between the in-body sensor node *i* and the corresponding relay node, and the residual energy of the in-body node *i*, respectively. For the incremental relaying routing method, the corresponding relay nodes with the minimum values of $C(i)$ are selected in each round. The second relay node can be exploited to retransmit the data packet to the coordinator if the first relay transmission fails. An algorithm is given in Table 5.3 to handle the scenario when two in-body sensor nodes have the same cost function values.

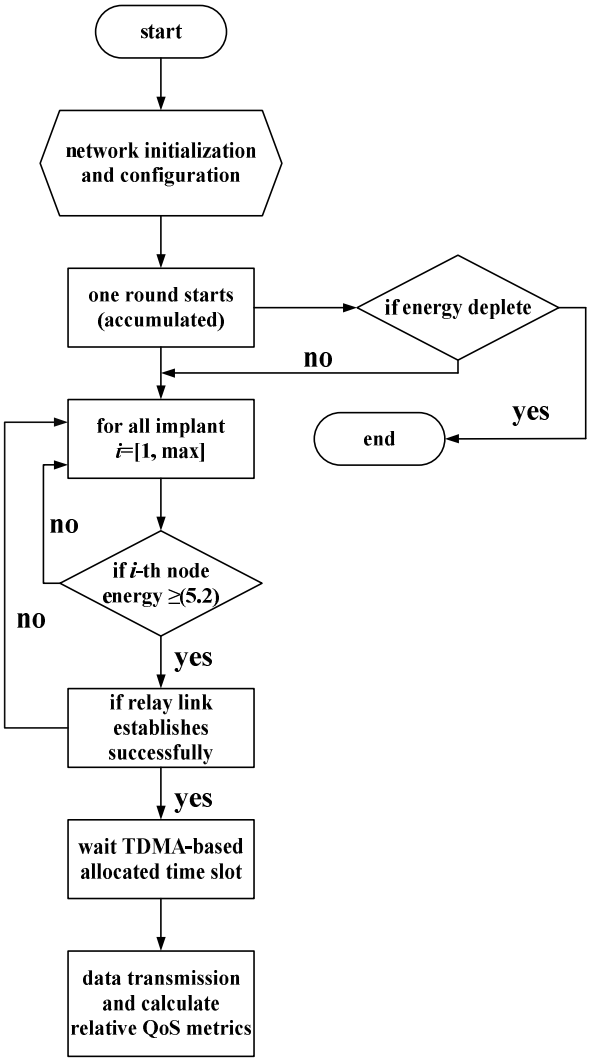

Figure 5.3 The demonstration of the routeing protocol.

Table 5.3 Proposed algorithm for a special case.

	Algorithm: A relay selection
1:	Routeing phase:
2:	if ($C(\beta) = C(\gamma)$) then
3:	$E_{total,min} = 2 \cdot E_{elec} + E_{amp} dn \leftarrow$ energy consumption
4:	if $E_{total,min}(\beta) > E_{total,min}(\gamma)$ then
5:	$C(\beta)$ = selected relay node
6:	Else
7:	$C(\gamma)$ = selected relay node
8:	end if
9:	end if

In the data scheduling phase, coordinator assigns time division multiple access (TDMA) time slots to the in-body sensor and its corresponding relay. Data transmission starts during the allocated time slot. Relay receives data from the in-body sensor node and forwards the collected data to the coordinator. The in-body WBAN system is regarded as dead when all in-body sensors are energy depleted.

5.6 Performance evaluation

In this section, the two-relay based and incremental relaying routing protocols are investigated. Analysis of the system performance employs the PL model and energy consumption model as described earlier in Section 5.3 and 5.4. The transmitting data packet size is set as 2000 bits as this is the maximum payload defined by the IEEE 802.15.6 standard [4]. It is assumed that all in-body sensor nodes are capable of transmitting information to the relay nodes and have the same initial energy of 0.5 Joules. Moreover, the half-duplex communication technique is employed, and the

coordinator does not support retransmission or feedback to the in-body sensor nodes under all conditions to avoid energy waste. As mentioned in Chapters 3 and 4, the transmitting information suffers random dropping caused by the channel fading effect and shadowing when an in-body sensor transmits collected data to the corresponding relay, and the relay delivers these to the coordinator. Thus, a uniform random model with a successful packet transmission probability of 0.7 is employed in all simulation cases in agreement with [18] to handle the packet loss situation. Coordinates of the in-body sensor nodes and the coordinator are listed in Table 5.4.

Table 5.4 The coordinates of in-body nodes and the coordinator.

Type	Node ID	x-coordinate	y-coordinate
In-body sensor node	1	0.2	1.6
	2	0.4	0.4
	3	0.3	0.1
	4	0.6	0.35
	5	0.7	1.5
	6	0.9	1.65
	7	1.65	0.75
	8	0.7	0.5
	9	0.7	0.3
	10	0.8	0.8
Coordinator		0.85	0.85

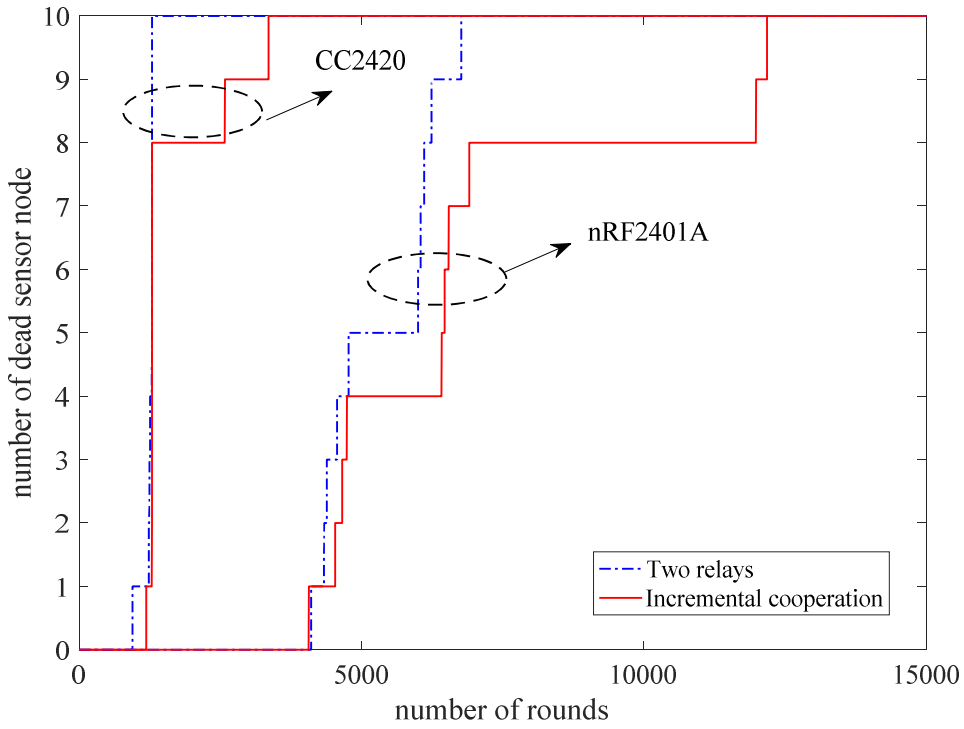

Figure. 5.4 Number of rounds versus the network lifetime.

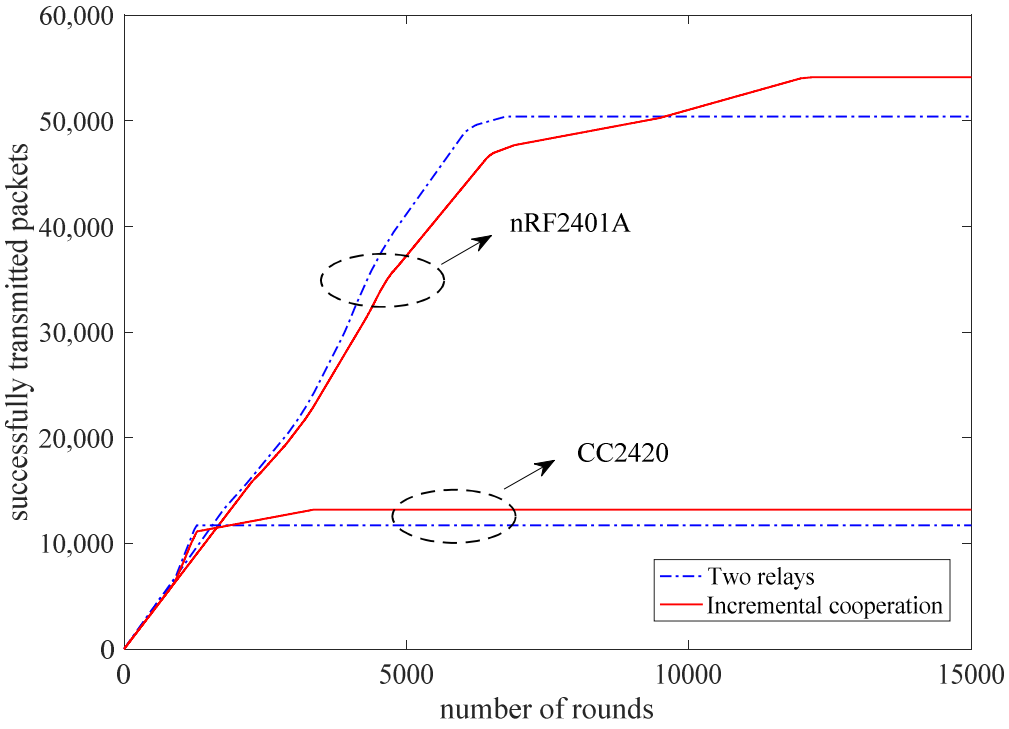

Figure. 5.5 Number of rounds versus the transmitted packets.

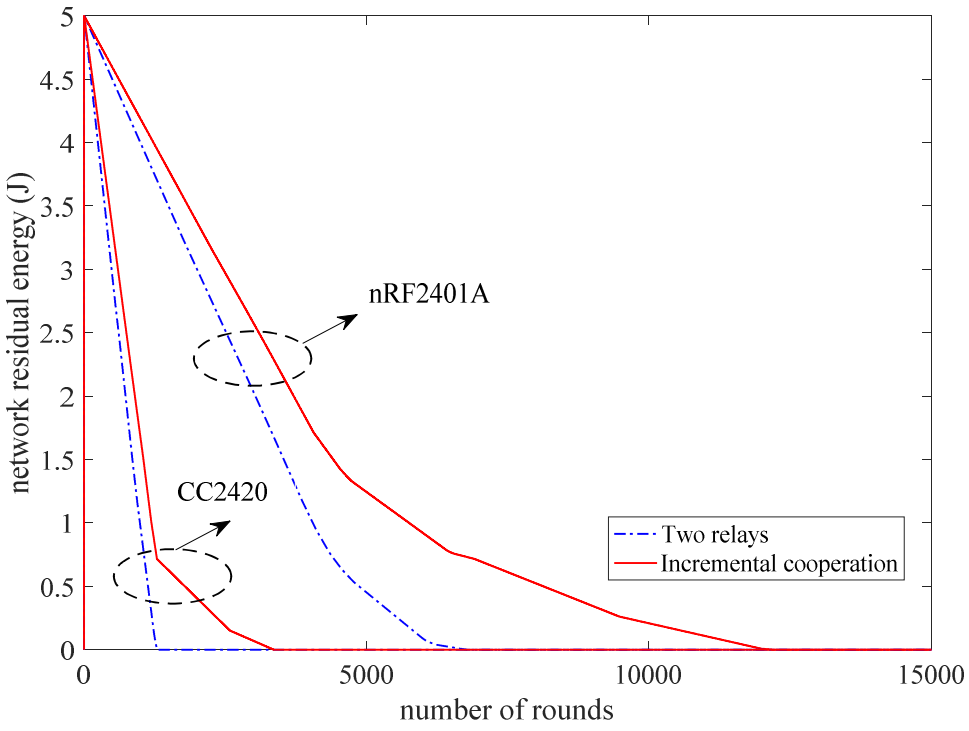

Figure. 5.6 Number of rounds versus the residual energy.

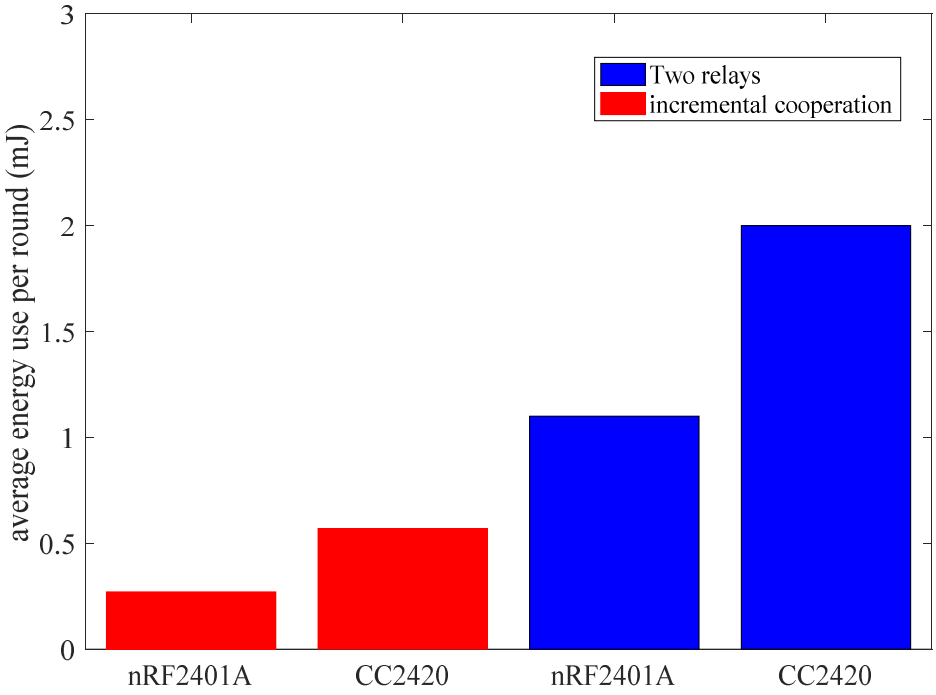

Figure 5.7 Average power consumption per round.

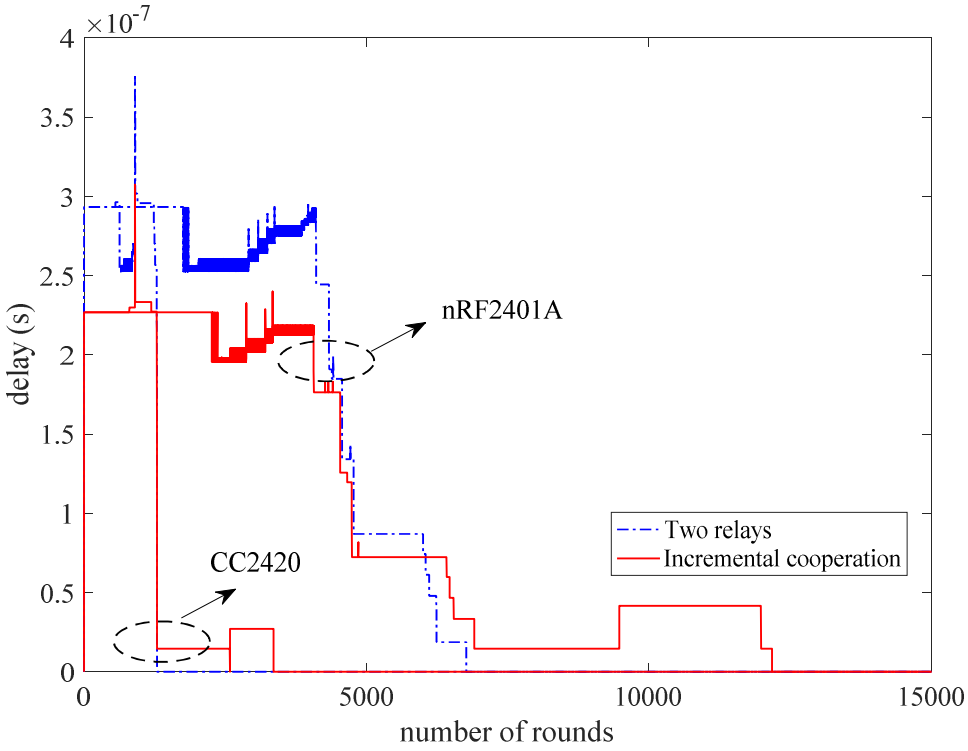

Figure. 5.8 Number of rounds versus the delay.

Figure 5.4 illustrates the comparison of the network lifetime of the incremental relaying and the two-relay cooperation routing protocols. It can be obtained that the incremental relaying scheme promises a longer stability period and entire network lifetime than two-relay routing technique when employing the same WBAN transceiver. The stability period of the two proposed routing protocols is nearly the same at approximately 4600 rounds when using the nRF2401A. The total network lifetime of the incremental relaying is around 12500 rounds when using the nRF2401A and 6500 rounds employing the CC2420, whereas the two-relay routing protocol supports approximately 3500 rounds and 1200 rounds, respectively.

As mentioned earlier, some information packets are dropped when in-body sensors transmit the sensed information to the relays due to the large size of the data packet, variation in the transmission routeing process and so forth [8]. It can be seen from

Figure 5.5 that the incremental relaying technique achieves a higher throughput than the two-relay based routing protocol when employing the same WBAN transceiver. When deploying the nRF2401A, the incremental relaying technique achieves more than 55000 packets while the two-relay based method achieves around 12000 packers. Similarly, the incremental relaying technique achieves more than 51000 packets, and the two-relay based method achieves around 11000 packets.

Figures 5.6 and 5.7 demonstrate the network residual energy and the average energy consumption per round, respectively. It can be obtained from Figure 5.5 that the nRF2401A based incremental relaying scheme achieves the highest network residual energy and promises the longest network lifetime. Figure 5.6 shows that the average energy consumption per round of the two-relay based routing protocol is approximately 1.2 mJ and 2.1 mJ when employing the nRF2401A and the CC2420 whereas the incremental relaying protocol consumes almost 0.35 mJ and 0.75 mJ when using the same WBAN transceivers. Vital reasons for the results may include that an alternative data transmission channel only starts to work once the first transmission channel fails and thus resulting in savings at the channel source.

Figure 5.8 presents the network delay for the two proposed data routing schemes. It shows that the two-relay scheme leads to a smaller delay performance than the incremental relay-based protocol after 5200 rounds while the two proposed techniques achieve nearly the same delay values when deploying the CC2420.

5.7 Conclusions

In-body sensor energy efficiency improvement and network lifetime extension are the most significant research challenges in WBANs for healthcare applications and services. In this chapter, an incremental relaying routing protocol for in-body WBAN

systems is presented and compared with the existing two-relay based routing technique. Moreover, the linear programming models of the network lifetime, throughput and propagation delay are given along with the relevant constraint functions. The proposed data routing protocol aims to minimise the transmission distance and achieve collision-free data packet transmission using a TDMA scheme. The results demonstrate that the proposed incremental relaying scheme achieves a longer network lifetime, higher energy efficiency and a larger number of successfully transmitted data packets. The two-relay based routing technique is thus a promising candidate for emergency data transmission in QoS-aware applications because it achieves higher transmission data rates than the incremental relaying routing method. The results obtained in this chapter can be employed in the analysis and design of wireless customised e-health applications and services.

References

[1] X. Lai, Q. Liu, X. Wei, W. Wang, G. Zhou, and G. Han, "A survey of body sensor networks," *Sensors,* vol. 13, no. 5, pp. 5406-5447, 2013.

[2] T. Hayajneh, G. Almashaqbeh, S. Ullah, and A. V. Vasilakos, "A survey of wireless technologies coexistence in WBAN: analysis and open research issues," *Wireless Networks,* vol. 20, no. 8, pp. 2165-2199, 2014.

[3] M. Seyedi, B. Kibret, D. T. Lai, and M. Faulkner, "A survey on intrabody communications for body area network applications," *IEEE Transactions on Biomedical Engineering,* vol. 60, no. 8, pp. 2067-2079, 2013.

[4] Y. Liao, M. S. Leeson, M. D. Higgins, and C. Bai, "Analysis of in-to-out wireless body area network systems: towards QoS-aware health Internet of Things applications," *Electronics,* vol. 5, p. 38, 2016.

[5] A. Ahmad, N. Javaid, U. Qasim, M. Ishfaq, Z. A. Khan, and T. A. Alghamdi, "RE-ATTEMPT: A new energy-efficient routing protocol for wireless body area sensor networks," *International Journal of Distributed Sensor Networks,* vol. 10, no. 4, p. 464010, 2014.

[6] N. Javaid, A. Ahmad, Y. Khan, Z. A. Khan, and T. A. Alghamdi, "A relay based routing protocol for wireless in-body sensor networks," *Wireless Personal Communications,* vol. 80, no. 3, pp. 1063-1078, 2015.

[7] G. D. Ntouni, A. S. Lioumpas, and K. S. Nikita, "Reliable and energy-efficient communications for wireless biomedical implant systems," *IEEE Journal of Biomedical and Health Informatics,* vol. 18, no. 6, pp. 1848-1856, 2014.

[8] N. Javaid, A. Ahmad, Q. Nadeem, M. Imran, and N. Haider, "iM-SIMPLE: iMproved stable increased-throughput multi-hop link efficient routing protocol for wireless body area networks," *Computers in Human Behavior,* vol. 51, pp. 1003-1011, 2015.

[9] N. Javaid, Z. Abbas, M. Fareed, Z. Khan, and N. Alrajeh, "M-ATTEMPT: A new energy-efficient routing protocol for wireless body area sensor networks," *Procedia Computer Science,* vol. 19, pp. 224-231, 2013.

[10] Y. Liao, M. S. Leeson, and M. D. Higgins, "Flexible quality of service model for wireless body area sensor networks," *Healthcare Technology Letters,* vol. 3, pp. 12-15, 2016.

[11] S. Akram *et al.*, "A fatigue measuring protocol for wireless body area sensor networks," *Journal of Medical Systems,* vol. 39, no. 12, p. 193, 2015.

[12] Y. Liao, M. S. Leeson, and M. D. Higgins, "A communication link analysis based on biological implant wireless body area networks," *Applied Computational Electromagnetics Society Journal,* vol. 31, no. 6, pp. 619-628, 2016.

[13] C. Chakraborty, B. Gupta, and S. K. Ghosh, "A review on telemedicine-based WBAN framework for patient monitoring," *Telemedicine and e-Health,* vol. 19, pp. 619-626, 2013.

[14] D. M. Barakah and M. Ammad-uddin, "A survey of challenges and applications of wireless body area network (WBAN) and role of a virtual doctor server in existing architecture," in *International Conference on Intelligent Systems Modelling and Simulation*, Nottingham, UK, pp. 214-219, 2012.

[15] D. Rathee, S. Rangi, S. Chakarvarti, and V. Singh, "Recent trends in wireless body area network (WBAN) research and cognition based adaptive WBAN architecture for healthcare," *Health and Technology,* vol. 4, pp. 239-244, 2014.

[16] M. M. Monowar, M. M. Hassan, F. Bajaber, M. A. Hamid, and A. Alamri, "Thermal-aware multiconstrained intrabody QoS routing for wireless body area networks," *International Journal of Distributed Sensor Networks,* vol. 10, no. 3, p. 676312, 2014.

[17] M. M. Sahndhu, N. Javaid, M. Imran, M. Guizani, Z. A. Khan, and U. Qasim, "BEC: A novel routing protocol for balanced energy consumption in wireless body area networks," in *International Wireless Communications and Mobile Computing* Conference, Dubrovnik, Croatia, pp. 653-658, 2015.

[18] M. M. Sandhu *et al.*, "Modeling mobility and psychological stress based human postural changes in wireless body area networks," *Computers in Human Behavior,* vol. 51, pp. 1042-1053, 2015.

[19] Y. Liao, M. S. Leeson, M. D. Higgins, and C. Bai, " An incremental relay based cooperative routing protocol for wireless in-body sensor networks," in *IEEE International Conference on Wireless and Mobile Computing, Networking and Communications,* New York, USA, pp. 1-6, 2016.

CHAPTER 6.

Design of a WBASN and Its Performance Analysis

6.1 Introduction

With the substantial and growing needs in ubiquitous healthcare communication systems and recent advances in low-power energy consumption techniques, a series of wireless communication technologies have been taken into consideration when providing long-term stability and high energy efficient in comprehensive healthcare networks [1]. The concept of a WBASN is derived from the WBAN. However, there exist numerous differences between WBASN and WBAN communication systems. WBASN sensors are fixed on a patient's clothes or located inside the human body and considered as stationary. Moreover, WBASN systems usually require additional sensors to account for possible data transmission failures whereas there are no redundant sensor nodes available for WBANs [2-3]. WBASN sensors are capable of monitoring human activities and collecting physiological signals in different scenarios such as hospital emergency units and community healthcare services. The data collected can be transmitted to the smart gateway and then forward to the medical staff via Internet. In addition, the data obtained can be applied to ubiquitous healthcare applications such as telemedicine development, clinical decision-making process and

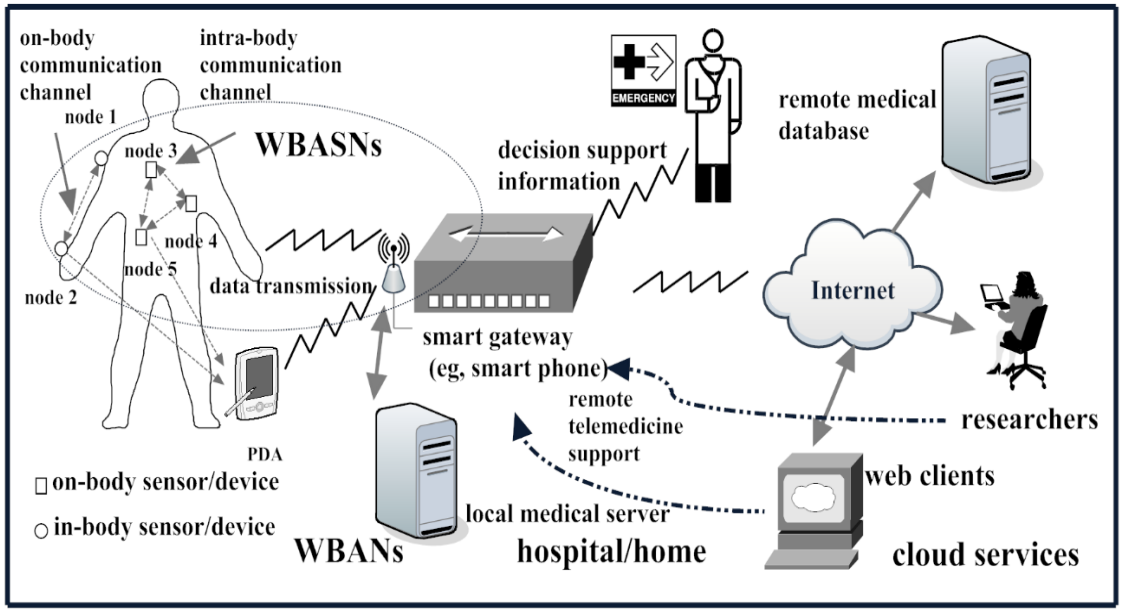

Figure 6.1 Illustration of a WBASN based IoT healthcare system.

even cloud computing for healthcare provision [4-6]. An illustration of a WBASN-based IoT healthcare system is shown in Figure 6.1. In [7], it was reported that in-body sensors are surgically implanted inside the human body and detect/collect multiple types of signals such as body temperature and pacemaker operation where the lossy nature environment of the human body might lead to significant signal energy attenuation. WBASN data transmission can be realised by several existing wireless communication technologies. For example, Bluetooth, Zigbee, wireless local area networks, cellular networks and ultra-wide band (UWB) [8-10]. Although the Bluetooth technique has been accepted and installed by more than 2 billion commercial use devices, it is only applicable to the human off-body region and this fact makes it inappropriate to employ in future smart healthcare and wellness applications [8]. Other emerging techniques such as Zigbee and cellular networks are only available to support low data rate applications (below circa 250 kbps) and are unable to support emergency medical services [9-10]. IEEE 802 is an international

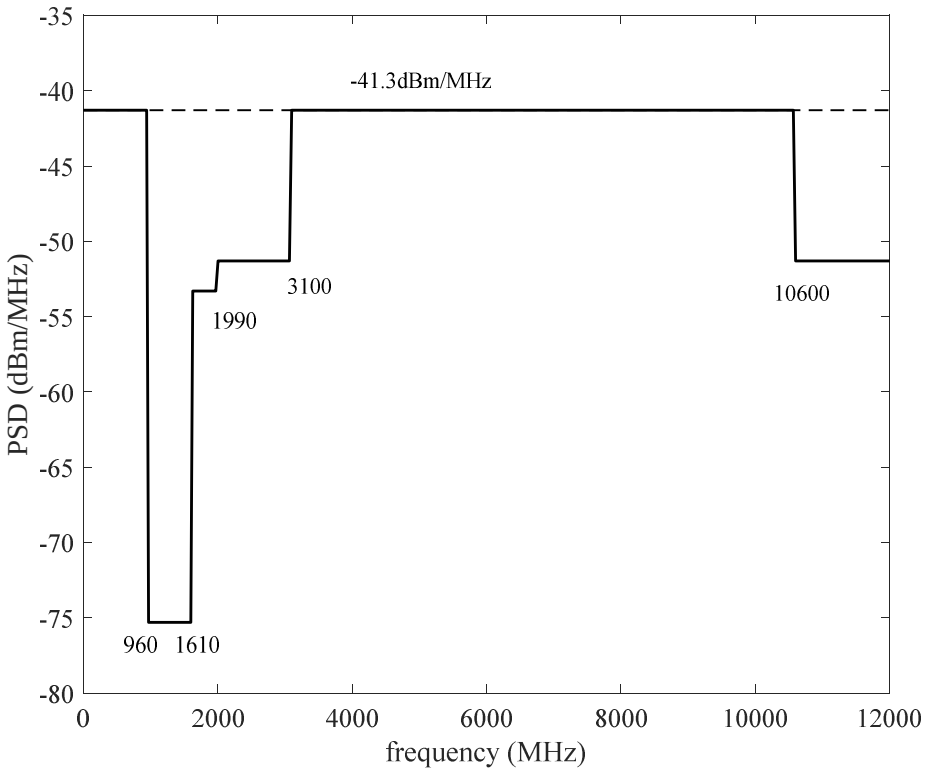

Figure 6.2 UWB emission limits proposed by FCC.

standardisation framework for various wireless communication technologies, including WBASNs, WBANs, wireless personal area networks (WPANs) and so forth [11-12]. In [11], the authors reported that IEEE 802.15.4 is not a suitable standard for dense sensor communication networks and is incapable of handling multi-user interference (MUI) when designing the future healthcare systems. The latest technical standard related to WBASN was published by the IEEE 802.15.6 Task Group in 2012 [12]. Among all proposed potential communication technologies by this global technology specification, ultra-wide band (UWB) technology was proposed as a potential approach for high data rate, short distance healthcare applications [12-13]. In [14], it was stated that the energy consumption of a single UWB body sensor is very low when compared to other commercially available devices. However, it should be

Table 6.1 Average power limits proposed by FCC for UWB devices.

Frequency (MHz)	EIRP (dBm)
0-960	-41.3
960-1610	-75.3
1610-1990	-53.3
1990-3100	-51.3
3100-10600	-41.3
Above 10600	-51.3

noted that the energy absorption of a vast number of UWB sensors simultaneously may lead to significantly energy absorption by the human body and raise safety concerns. The Federal Communication Commission (FCC) has allocated 7500 MHz of spectrum for the use of UWB sensors in the ranges of 3.1 to 10.6 GHz frequency band. The maximum power level ranges from 0 to 10.6 GHz are demonstrated in Figure 6.2, and the details of the corresponding average power limits for communication systems are summarised in Table 6.1.

To date, numerous communication approaches have been suggested to analyse the MUI effect in the UWB based WBASN systems by many researchers [16-18]. In this chapter, there are two widely used and highly energy efficient models that are selected and investigated. The standard Gaussian approximation (SGA) model was proposed

in [16] and denotes the MUI interference as an additive Gaussian noise with a uniform distribution. The results demonstrated that this technique is capable of providing accurate BER performance for high MUI effect scenarios. The pulse collision (PC) model was reported as one effective method of supporting the case of a large number of users WBASN systems and low data rate ad-hoc networks, which can overcome the interference among multiple asynchronous users in the WBASN network. According to [17], the MUI in PC model is studied based on the condition that interference is caused by collisions between various pulses from different transmitters.

In this chapter, the transmission of signals using pulse position modulation (PPM) in combination with time hopping (TH) coding is employed. Moreover, the system performance of the MUI has been evaluated based on the SGA and PC models. The results demonstrate that the performance of both the PC and SGA models will get worse as the data rate increases. A flexible QoS model for WBASNs is proposed, which can balance the probabilities of packet collisions and energy consumption. In addition, this model performs adequately to overcome MUI and achieves satisfactory date rates, which can be applied to future customised health monitoring design.

The rest of this chapter is arranged as follows. In section 6.1, the introduction of the UWB and the detailed background is presented. Section 6.2 shows the WBASN structure and the UWB radio characteristics. Section 6.3 represents SGA and PC models along with the system performance analysis; Section 6.4 illustrates a proposed flexible QoS WBASN system and the system performance, and finally, section 6.5 concludes this chapter.

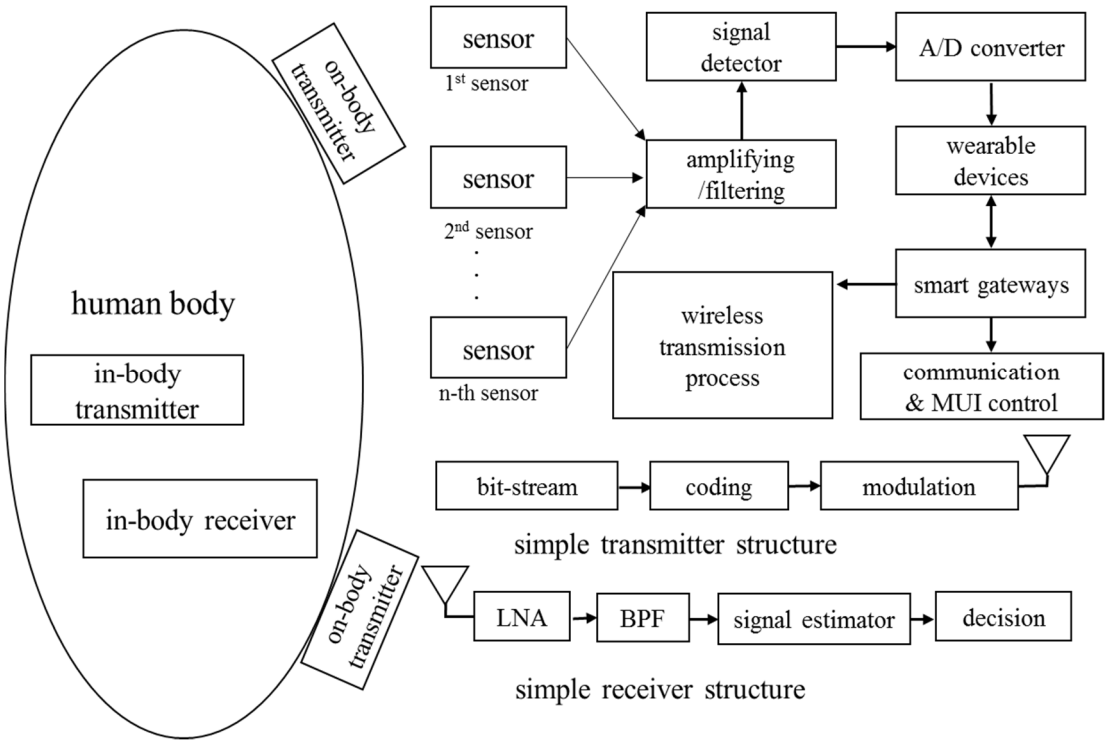

Figure 6.3 Demonstration of the sensor data information flows within a WBASN.

6.2 Analysis of the WBASN structures

6.2.1 WBASN structure

A WBASN system consists of a smart gateway, implanted sensors, on-body sensors and wireless communication channels that are capable of communicating patients' medical data to physicians and remote medical servers. Smartphones and other personal digital assistants are capable of collecting/gathering data from WBASN sensors and providing personalised user interface [1-3, 10], which make them possible to perform as the receiver (Rx) in future smart healthcare system design. However, due to the battery power restrictions, it is less likely that WBASN sensors can measure and transmit data continuously as wireless communication may lead to high-energy consumption [1]. The demonstration of the Tx, Rx and the data flows within the WBASN is shown in Figure 6.3. The detailed information concerning the signal sampling and processing can be found in [18].

6.2.2 UWB radio characteristics

As mentioned before, the TH coding technique is applied to handle emergency conditions and interference between emergency messages and normal data transmission. Also, the authors in [15] demonstrated that the PPM TH scheme transmission is reliable and stable, and thus there is no need to offer feedback information or request that the Tx retransmits data in another time slot as a result of information loss. The authors in [16] reported that multiple Gaussian pulse waveforms for medical implants and the second derivative pulse outperform other kinds of pulses under the FCC safety regulation. This second derivative Gaussian pulse waveform can be written as [15]:

$$p^2(t) = F_s(\alpha, f_0, t) - F_c(\alpha, f_0, t) \tag{6.1}$$

where:

$$F_s(\alpha, f_0, t) = G_{s1}(\alpha, f_0, t) G_{s2}(\alpha, f_0, t) \tag{6.2}$$

$$G_{s1}(\alpha, f_0, t) = \frac{4\pi t^2}{\alpha^4} - \frac{1}{\alpha^2} - \pi f_0^2 \tag{6.3}$$

$$G_{s2}(\alpha, f_0, t) = 4\pi e^{-2\pi(t/\alpha)^2} \sin(2\pi f_0 t) \tag{6.4}$$

$$F_c(\alpha, f_0, t) = \frac{4\pi f_0 t}{\alpha^2} \cos(2\pi f_0 t) \tag{6.5}$$

where f_0 and α denote the spectral moving factor and shaping factor, respectively.

Since PPM modulation may cause interference with other RF systems, therefore signal time-shifting is introduced. As demonstrated in Figure 6.4, the binary sequence data $b = (\cdots, b_0, b_1, \cdots, b_k, b_{k+1}, \cdots)$ is generated and transmitted. The channel coder adopts a repetition coder to introduce beneficial redundancy, and each bit is encoded

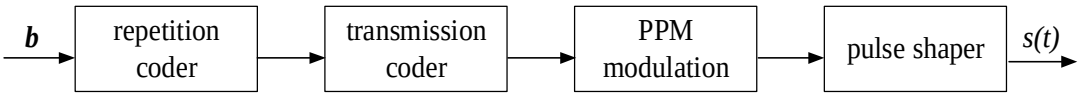

Figure 6.4 System model for an IR-UWB transmitter.

N_s times to improve the robustness of the transmission process. This process is followed by a transmission coder, then modulated by PPM and finally transmitted as a pulse train. The Tx signal is generated by independently and identically distributed (i.i.d.) random variables with the same probability for symbols '0' and '1'. The reference transmitter Tx transmits PPM signals to the corresponding Rx. The transmitted signal can be written as [15]:

$$s_1(t) = \sum_{j=-\infty}^{+\infty} \sqrt{E_s}\, p\left(t - jT_s - c_j T_c - \alpha_j \varepsilon\right) \tag{6.6}$$

where $p(t)$ and E_s represent the pulse waveform and the transmitted power for each pulse, respectively. T_s is the average pulse repetition period, and $c_j T_c$ is the time shift of the TH code. The terms ε and $\alpha_j \varepsilon$ represent the additional time shift and the time delay caused by the PPM modulation, respectively. The PPM modulation approach introduces an additional delay ε on all N_s pulses corresponding to a '1' bit. The subjective functions are given as $T_s \leq T_b / N_s$ and $\varepsilon \leq T_c - T_M$ where T_M is the duration of the waveform $p(t)$.

Similarly, the transmitted signal by the *n*-th UWB device can be expressed as:

$$s_{TX}^{(n)} = \sum_{j=-\infty}^{\infty} \sqrt{E_s}\, p\left(t - jT_s - c_j^{(n)} T_c - \alpha_j^{(n)} \varepsilon\right) \tag{6.7}$$

where $c_j^{(n)}$ and the $\alpha_j^{(n)}$ represent the TH code shift and the PPM shift of the *j*-th pulse, respectively.

6.3 Multi-user interference systems

MUI analysis is a significant issue in the design of the WBASN communication systems. As shown in Figure 6.5, in a realistic scenario the MUI effect may occur when the reference pulse collides with pulses emitted by other users within the same WBASN communions system. In this chapter, the performance of the PC model and the SGA model is presented, which can be employed as effective techniques to overcome the interference within WBASN systems.

6.3.1 SGA model

Multiple factors such as shadowing, diffractions and scattering may lead to a degradation in the communication link quality. All communication channels may also experience interference due to the propagation characteristics of the shared channel even if each link is perfect synchronised. The SGA technique is reported as an efficient method to model the MUI effect when deploying PPM TH multiple access (THMA) communication systems in the presence of asynchronous users [19]. Assuming the Tx and the Rx is perfectly synchronised, and the Rx has perfect knowledge of τ (delay). The received signal can be expressed as:

$$S_{Rx}(t) = r_u(t) + r_{mui}(t) + n(t) \tag{6.8}$$

where $r_u(t)$, $r_{mui}(t)$ and $n(t)$ denote the useful signal, MUI, and the thermal noise, respectively. The thermal noise and MUI noise at the Rx can be regarded as AWGN noise sources under the SGA hypothesis and the noise contributions to the decision

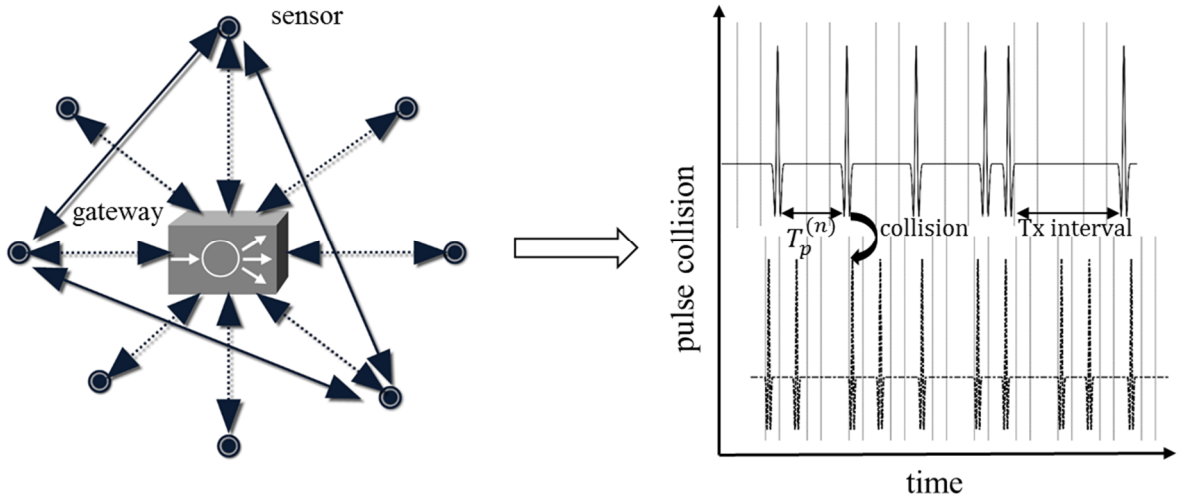

(a) (b)

Figure 6.5 (a) The sensors and a smart gateway within a WBASN; (b) pulse collision.

statistic are modelled as zero-mean Gaussian noise processes with variance σ_n^2 and σ_{MUI}^2, respectively. The total variance can be expressed as:

$$\sigma_{total}^2 = \sigma_{MUI}^2 + \sigma_n^2 \tag{6.9}$$

In accordance with [15], the IEEE 802.15.3a channel model is employed, and the received signal consists of both the desired transmitted signal and the AWGN noise. It is further assumed that there are N_s users within the same WBASN system, the BER performance of a binary PPM THMA based on the SGA model can be expressed as [16-17]:

$$BER = \frac{1}{2} erfc\left[\sqrt{\frac{\left(\left(\frac{E_b(1-R_0(\varepsilon))}{N_0}\right)^{-1} + \left(\left(\frac{(1-R_0(\varepsilon))^2}{\delta_M^2 R_b \sum_{n=2}^{N_u} \frac{E_{Rx}^{(n)}}{E_{Rx}}}\right)^{-1}\right)^{-1}}{2}}\right] \tag{6.10}$$

where E_{Rx} and $E_{Rx}^{(n)}$ denote the received energy per pulse for the referenced user and the n-th user, respectively. The term E_b represents the received energy per bit for the referenced user and can be expressed as $E_b = N_s E_{RX}^{(n)}$. The function $R_0(\varepsilon)$ is the autocorrelation function of the pulse waveform and N_0 is the power spectral density of the noise. σ_M^2 is the variance of the MUI and R_b is the data rate of the users. Considering multiple scenarios, where the number of users is 5, 10, 20, and 40 under data rates 10 Mbps and 20 Mbps. The Gaussian waveform shaping factor is set as 0.25 ns. The PPM shift and the pulse duration are both set as 0.5 ns. Figures 6.6 and 6.7 show the system performance of the SGA model at 10 Mbps and 20 Mbps based on the PPM THMA, respectively.

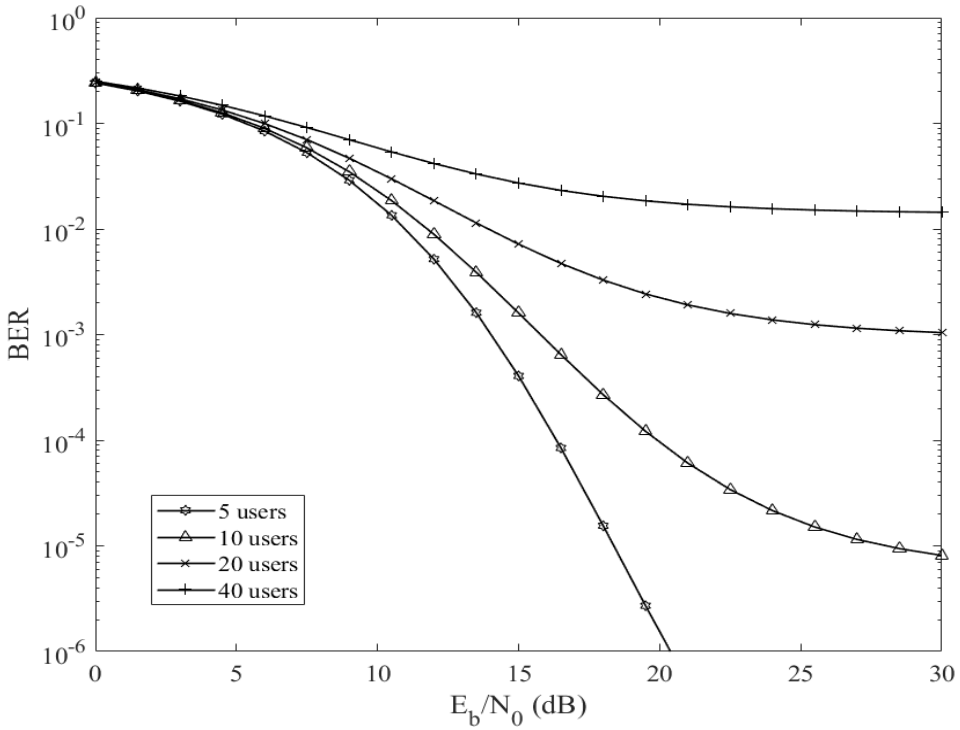

Figure 6.6 SGA model performance for a PPM THMA system at 10 Mbps.

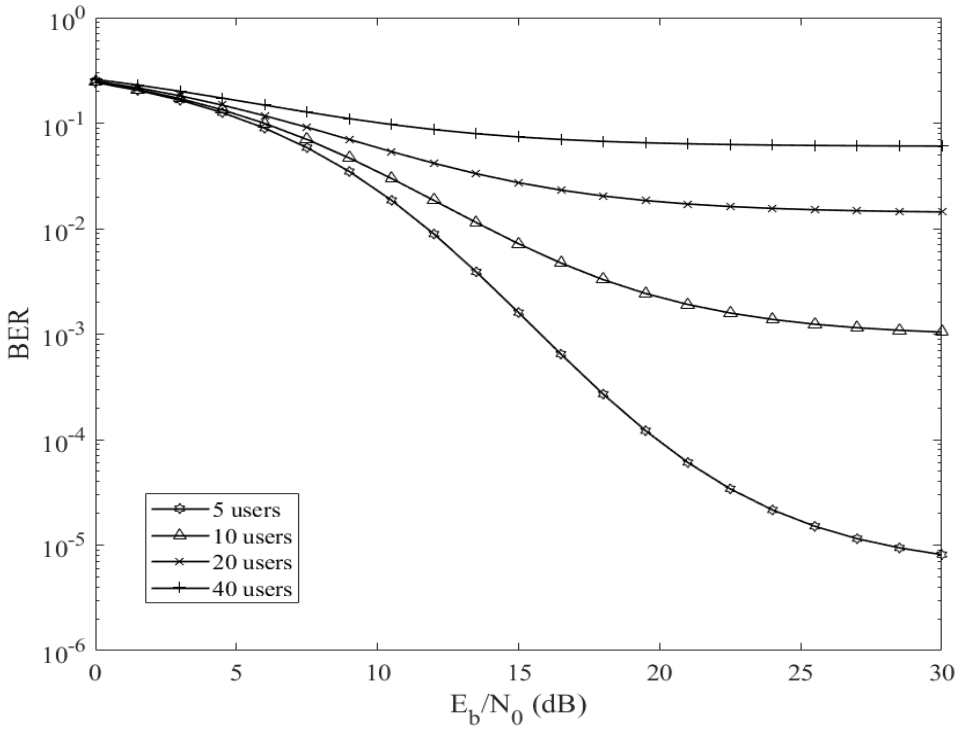

Figure 6.7 SGA model performance for a PPM THMA system at 20 Mbps.

It can be observed that the system performance degrades with higher data rates. Moreover, the larger number of users within the same WBASN system will result in worse performance, and SGA model cannot support a large number of users WBASN system (less than 40 users) under the relatively low data requirement 10 Mbps. Thus, SGA model is incapable of supporting high data rate WBASN system design in the context of large amount of users.

6.3.2 The pulse collision model

As demonstrated in [6], adjacent waveform overlaps between pulses belonging to different UWB sensors within the same WBASN system may result in significantly energy attenuation. In this subchapter, the pulse collision (PC) model is investigated to analyse the packet collision when the waveform overlaps on an MUI system by using PPM modulation scheme. Different effective pulse duration scenarios, from

70% to 100% of total energy of UWB pulse for taking overlap into simulation cases are considered with a 0.5 ns PPM shift. In a similar fashion to [16], it is assumed that the pulse collision is independent of pulse shape if the pulse duration remains same.

The system performance comparison between the PC and SGA models at bit rates of 10 Mbps and 20 Mbps is given in Figure 6.8 and 6.9, respectively. In accordance with [16], in both cases, the pulse waveform is selected as the second derivative Gaussian waveform. In the case of Figure 6.8, parameters are given as follows: N_s=2 and T_s =25ns. The parameters of Figure 6.9 are N_s =4 and T_s =25 ns. Figure 6.8 demonstrates that the BER performance under pulse collision depends on the effective pulse duration and system perform degrades with a higher numbers of collisions. It can be seen from Figure 6.9 that the system performance deteriorates as the data rate increases. The SGA technique shows unsatisfactory performance for a higher number

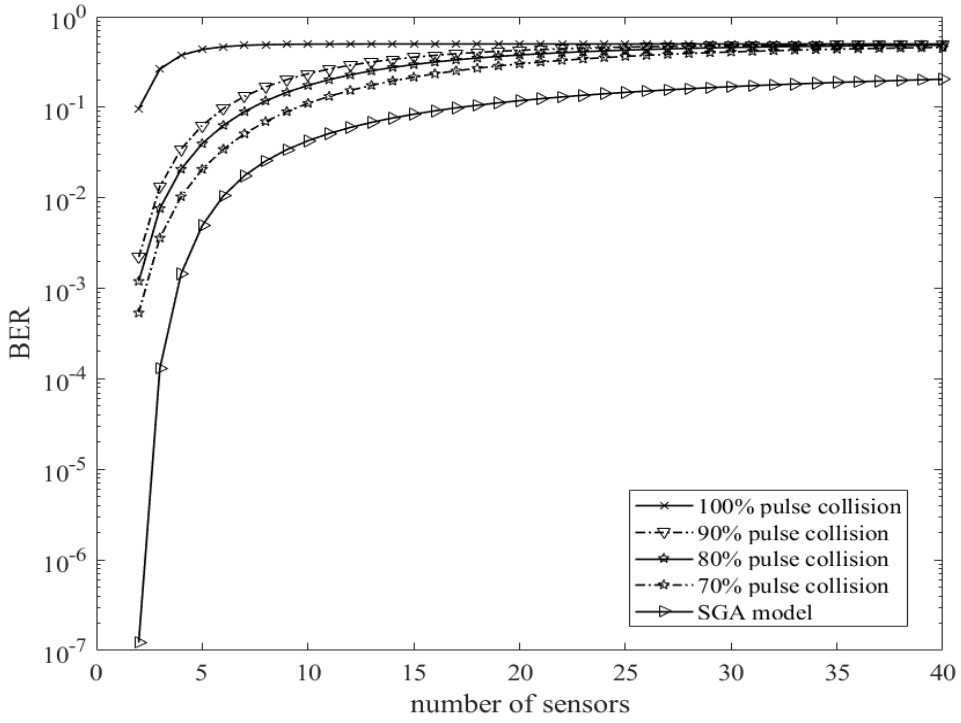

Figure 6.8 Comparison between PC and SGA models at a data rate 10 Mbps.

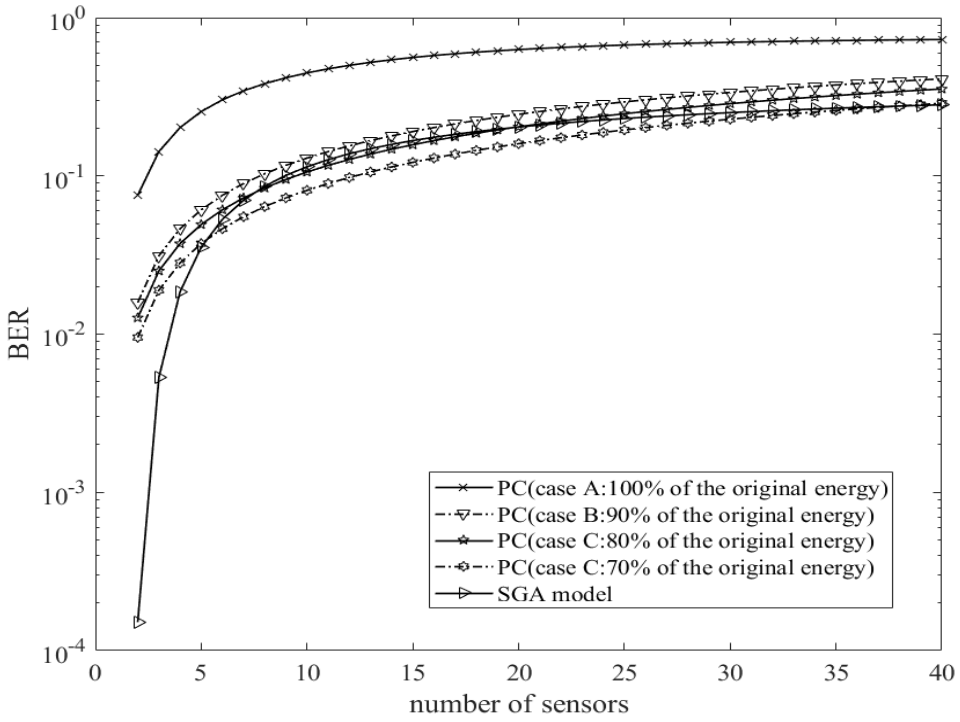

Figure 6.9 Comparison between PC and SGA models at a data rate 20 Mbps.

of UWB sensors when compared to the PC schemes. The results explain that the PC model outperforms the SGA model when using the same number of sensors for both 10 Mbps and 20 Mbps.

6.4 Design of the flexible QoS UWB based model

In [1-2], it was reported that one of the main technical challenges in WBASN systems is the energy efficiency. Therefore it is of importance to balance the power consumption and the number of sensors. It is assumed that the sensor nodes are capable of switching from ‘working mode’ to ‘sleep mode’ unless they are allocated to transfer a new data packet, and thus decreasing both energy consumption and the pulse collision probabilities. An ad hoc network methodology is introduced to achieve more accurate results. The MAC layer assigns unique time shift codes to priority emergency data that will not interfere with normal data transmission. A flexible energy

consumption model of a wireless communication system is given in Chapter 5 and assuming each patient has *N* sensors. Under the asynchronous UWB transmission scheme, the transmitted PPM THMA signal for *n*-th sensor of the *m*-th user can be defined as [6]:

$$S_{m(n)}(t) = \sum_{j=-\infty}^{+\infty} \sqrt{E_s} s(t) \tag{6.11}$$

where:

$$s(t) = p\left(t - jT_s^{(k)} - c_j T_c - nT_p^{(m)} - \alpha_j^{(n)} \sum_{k=0}^{\infty} \varepsilon^{(k)}\right) \tag{6.12}$$

where $p(t)$ and E_s denote the UWB waveform pulse and the pulse power, respectively. T_s and $c_j T_c$ represent the time interval between successive transmission with the *n*-th sensor and time shift that is caused by the TH code, respectively. As shown in Figure 6.5 (b), collisions may result in high energy loss when more than one sensor is transferring data simultaneously. To obtain more accurate results, an ad hoc network methodology is introduced to deal with this situation. Since Multiple pulses N_s for '1' bit scheme and various pulse transmission rates are employed to allow the gateway to identify patients; the BER performance can thus be denoted as:

$$BER = \sum_{i \geq [N_s/2]}^{N_s} P_1^i (1 - P_1)^{N_s - i} \tag{6.13}$$

where P_1 is the average error probability that caused by the pulse collision and leads to the random decision reception. The transmitted signal may collide with other transmitting pulses and lead to transmission failure. In this chapter, the data transmission process can be regarded as unsuccessful when more than half of its transmitting pulses are overlapped. P_1 can then be expressed as:

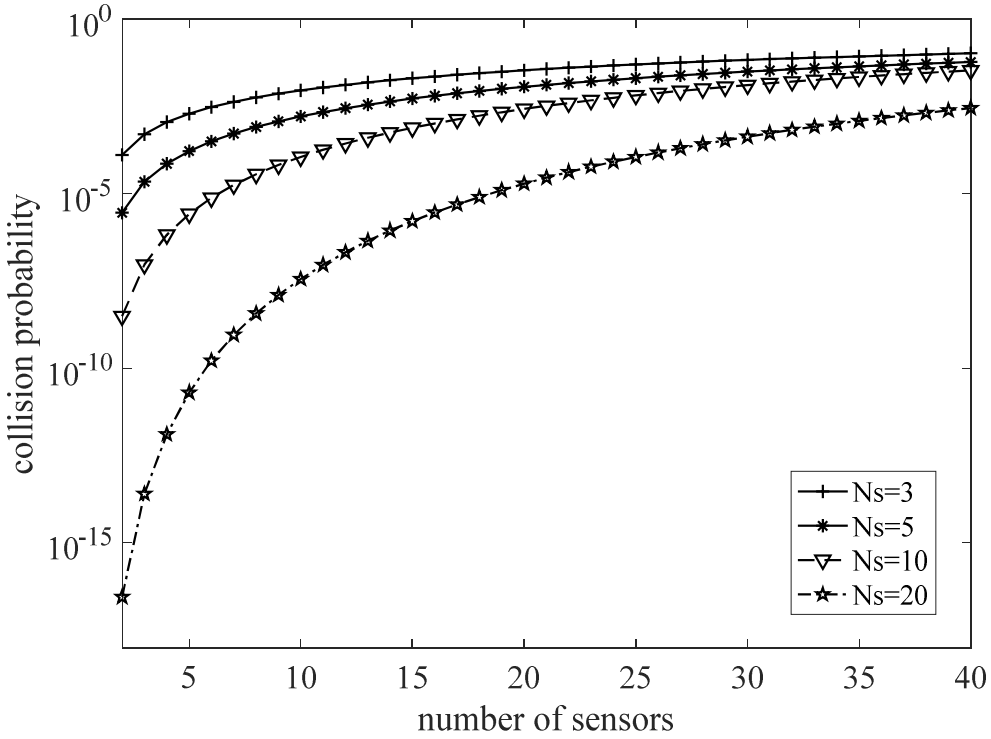

Figure 6.10 Collision probability versus a number of sensors under multiple N_s values when the data rate is 30 Mbps.

$$P_1 = \gamma P_2 \tag{6.14}$$

where $0 \leq \gamma < 1$. P_2 represents the average collision probability among N active users and may be expressed as:

$$P_2 = 1 - e^{-\left((N-1)\left(T_p^{(n)}/T_s\right)\right)} \tag{6.15}$$

where $T_p^{(n)}$ is the time interval between two successive pulses and T_s represents the pulse duration.

Figure 6.10 demonstrates that the collision probability versus the number of users for a series of N_s values under at a data rate of 30 Mbps. It illustrates that higher N_s values result in better performance and that the collision probability rises once the number of

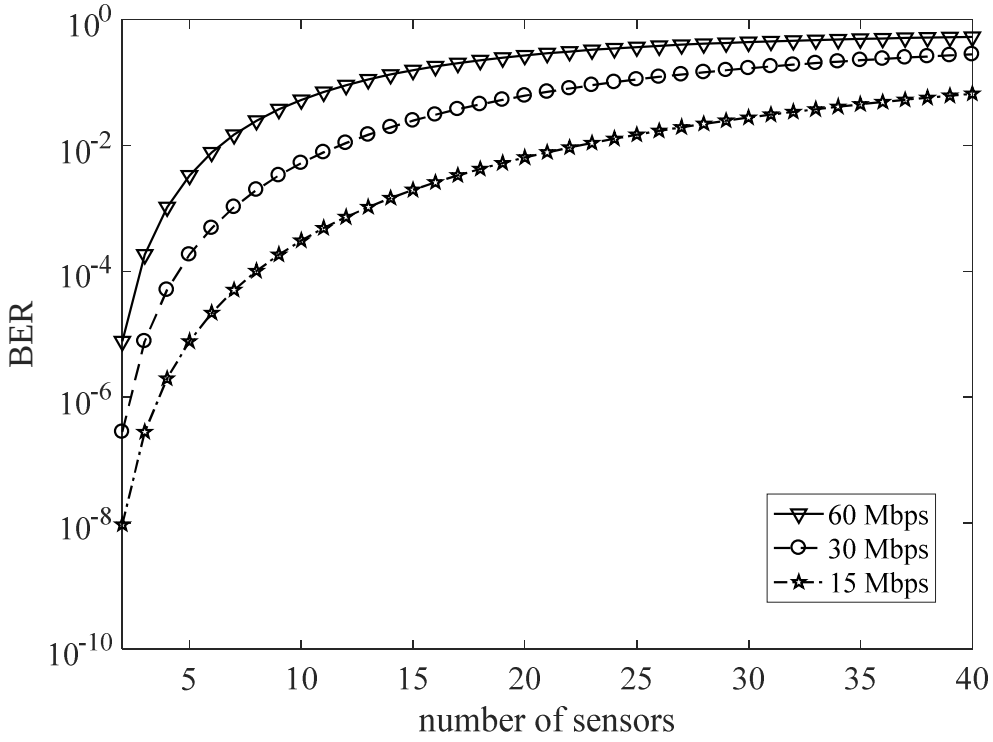

Figure 6.11 BER performance versus a number of sensors under multiple data rates when N_s is 10.

users increases. For the minimum acceptable collision probability of 10^{-3}, the proposed method can support approximately 30 sensors when N_s is 20 but fewer than 5 sensors when N_s is equal to 3. It should be noted that more energy will be wasted when one single information bit is transmitted with a large value of N_s. To balance the power consumption and the pulse collision probability of the UWB system, the N_S value is chosen as 10 for further investigation.

Figure 6.11 presents the BER performance versus the number of users when employing data transmission rates from 15 to 60 Mbps. The results indicate that the proposed wireless communication technique can support more users at lower data rates. Moreover, the system performance will get worse once the number of users increases. Specifically, the proposed WBASN system can support around 4 sensors at

a high data rate of 60 Mbps and more than 10 users at 15 Mbps. The proposed technique can balance system energy consumption and data rate when compared with the majority of the up to date research work in the WBASN area.

6.5 Conclusion

In this chapter, the introduction of the UWB technique and the FCC power regulations is given. The system performance of the proposed SGA and PC model using the second derivative Gaussian pulse waveform is obtained. The results demonstrate that the SGA model is incapable of supporting a higher number of users (around 40) when using the data rate 10 Mbps. Analysis of the PC model considers multiple effective pulse duration scenarios. The results illustrate that the PC model achieves lower BER performance under the same number of sensors when compared with the SGA model. Thus, this is an adequate technique that can be considered for the ad hoc network. Based on this, a flexible QoS WBASN model is proposed. This ad-hoc WBASNs network, with PPM modulation and TH techniques, has been modelled and the effect of the number of pulses employed has been studied in terms of both variable user numbers and different data rates. The number of pulses used clearly has an effect on the energy usage, and a value of 10 pulses per transmitted bit was found to be a good compromise between data transmission performance and energy cost. Using this number of pulses, for a collision rate of 10^{-3}, a bit rate of 15 Mbps permits almost 10 users to be accommodated but this falls to fewer than 5 when 60 Mbps is utilised. Thus, the system can achieve reasonable data transmission rates for adequate power consumption levels with a low collision probability. The obtained results show that the proposed WBASN system can promise a variety of BER performances under the multiple pulses per bit method. This approach can be employed to customised QoS

healthcare system design for application-specific monitoring systems regarding data rates and power consumption.

References

[1] J. Andreu-Perez, D. R. Leff, H. Ip, and G. Z. Yang, "From wearable sensors to smart implants –toward pervasive and personalized healthcare," *IEEE Transactions on Biomedical Engineering*, vol. 62, no. 12, pp. 2750-2762, 2015.

[2] M. Ameen, A. Nessa, and K. S. Kwak, "QoS issues with focus on wireless body area networks," in *International Conference on Convergence and Hybrid Information Technology*, Busan, Korea, pp. 801-807, 2008.

[3] N. Javaid, A. Ahmad, Y. Khan, Z. A. Khan, and T. A. Alghamdi, "A relay based routing protocol for wireless in-body sensor networks," *Wireless Personal Communications*, vol. 80, no. 3, pp. 1063-1078, 2015.

[4] A. Rghioui, A. L'aarje, F. Elouaai, and M. Bouhorma, "The internet of things for healthcare monitoring: security review and proposed solution," in *IEEE International Colloquium in Information Science and Technology (CIST)*, Tetouan, Morocco, pp. 384-389, 2014.

[5] J. Wan, C. Zou, S. Ullah, C. F. Lai, M. Zhou, and X. Wang, "Cloud-enabled wireless body area networks for pervasive healthcare," *IEEE Network*, vol. 27, no. 5, pp. 56-61, 2013.

[6] Y. Liao, M. S. Leeson, and M. D. Higgins, "Flexible quality of service model for wireless body area sensor networks," *Healthcare Technology Letters*, vol. 3, no. 1, pp. 12-15, 2016.

[7] E. Ibarra, A. Antonopoulos, E. Kartsakli, J. J. Rodrigues, and C. Verikoukis, "QoS-aware energy management in body sensor nodes powered by human energy harvesting," *IEEE Sensors Journal*, vol. 16, no. 2, pp. 542-549, 2016.

[8] M. Kumar, "Security issues and privacy concerns in the implementation of wireless body area network," in *International Conference on Information Technology*, Bhubaneswar, India, pp. 58-62, 2014.

[9] D. B. Arbia, M. M. Alam, R. Attia, and E. B. Hamida, "Data dissemination strategies for emerging wireless body-to-body networks based internet of humans," in *IEEE 11th International Conference on Wireless and Mobile Computing, Networking and Communications*, Abu Dhabi, UAE, pp. 1-8, 2015.

[10] D. E. Marcinko and H. R. Hetico, *Dictionary of Health Information Technology and Security*: Springer Publishing Company, 2007.

[11] W. W. Lee *et al.*, "A smartphone-centric system for the range of motion assessment in stroke patients," *IEEE Journal of Biomedical and Health Informatics*, vol. 18, no. 6, pp. 1839-1847, 2014.

[12] D. Bhaskar and B. Mallick, "Performance evaluation of MAC protocol for IEEE 802.11, 802.11 Ext. WLAN and IEEE 802. 15. 4 WPAN Using NS-2," *International Journal of Computer Applications*, vol. 119, no. 16, pp. 25-30, 2015.

[13] S. R. Islam and K. S. Kwak, "A comprehensive study of channel estimation for WBAN-based healthcare systems: feasibility of using multiband UWB," *Journal of Medical Systems*, vol. 36, no. 3, pp. 1553-1567, 2012.

[14] C. C. Poon, B. P. Lo, M. R. Yuce, A. Alomainy, and Y. Hao, "Body sensor networks: in the era of big data and beyond," *IEEE Reviews in Biomedical Engineering*, vol. 8, pp. 4-16, 2015.

[15] Y. Liao, M. S. Leeson, and M. D. Higgins, "Analysis of PC and SGA models for an ultra wide-band ad-hoc network with multiple pulses," in *IEEE International Workshop on Computer Aided Modelling and Design of Communication Links and Networks (CAMAD)*, Guildford, UK, pp. 246-250, 2015.

[16] D. Feng, S. Ghauri, and Q. Zhu, "Application of the MUI model based on packets collision (PC) in UWB ad-hoc network," in *International Conference on Networking, Sensing and Control*, Okayama, Japan, pp. 554-558, 2009.

[17] G. Giancola and M. G. Di Benedetto, "A collision-based model for multi user interference in impulse radio UWB networks," in *IEEE International Symposium on Circuits and Systems*, 2005, Kobe, Japan, pp. 49-52, 2005.

[18] A. Khaleghi, R. Chávez-Santiago, and I. Balasingham, "Ultra-wideband pulse-based data communications for medical implants," *IET communications*, vol. 4, no. 15, pp. 1889-1897, 2010.

[19] J. Fiorina, G. Capodanno, and M.-G. Di Benedetto, "Impact of time reversal on multi-user interference in IR-UWB," in *IEEE International Conference on Ultra-Wideband (ICUWB)*, Bologna, Italy, pp. 415-419, 2011.

[20] B. Otal, L. Alonso, and C. Verikoukis, "Highly reliable energy-saving MAC for wireless body sensor networks in healthcare systems," *IEEE Journal on Selected Areas in Communications*, vol. 27, no. 4, pp. 553-565, 2009.

CHAPTER 7.

Conclusions and Future Work

This thesis provides a communication framework for WBANs and numerous emerging research topics, which have great potential to be employed as capable techniques for healthcare system design. The 2.4 GHz and 2.45 GHz frequency bands are selected corresponding to the ISM band, as this is one efficient approach to reduce the antenna size, simplify the system architecture and interact with other wireless communication technologies for future medical system design such as Bluetooth, wireless local area network (WLAN) and WPAN. The basic system structure has been demonstrated and efficiently satisfies the requirements for in-body and I2O communications regarding data rate, transmission distance and data transmission reliability. In order to decrease in-body sensor power consumption and to lengthen the WBAN system lifetime, high energy efficient relay-based routing protocol design has been considered. TDMA is taken into account to promise data transmission from in-body sensor nodes to the nearby relays. This technique also can minimise the overall transmission distance within the WBAN and decrease the network energy consumption.

Another key research aim in this thesis is to design for extremely high data rate scenarios such as capsule application. One effective technique is to study and establish a flexible QoS-aware UWB communication model for WBASN. The results demonstrate that the proposed technique could balance power consumption and the

network performance when compared with the majority of the latest research literature in this area. Also, the system evaluation of this WBASN model has demonstrated that the feasibility of the wireless UWB path can achieve up to 60 Mbps data rate under satisfactory packet collision probability and power consumption. The research points proposed in this thesis can be used for future developments of telemedicine and ubiquitous healthcare service and heath IoT application design. The outcome of this work will inspire some emerging research subjects such as future smart healthcare system design and human body model experimental validation.

7.1 Concluding remarks

In Chapter 1, the background to WBAN, especially the existing ICT-based medical monitoring systems, and the current difficulties have been demonstrated. Moreover, this Chapter offers the research motivations, contributions and outline of the thesis.

In Chapter 2, a detailed description of the WBAN communications has been reported, including possible wireless communication technologies, the existing technical standards, available frequency bands, different types of human body communication channels. In addition, since traditional WSN techniques cannot specifically tackle the technical challenges associated with the human body, thus numerous research tasks have been listed. Moreover, different kinds of WBAN systems have been presented along with electromagnetic compatibility considerations. Finally, due to the safety concerns, the maximum transmitting power selection and SAR analysis have been considered based on IEEE 802.15.6 regulations.

In Chapter 3, the design of in-body WBAN communication system and the evaluation of the system performance are demonstrated. An appropriate in-body communication channel PL model is derived by employing the advanced computational

electromagnetics software CST and high-resolution 3D human cephalic model. The electromagnetic calculation results prove that SAR values follow safety guidelines proposed by IEEE and ICNIRP. Furthermore, a mathematical method has been suggested to derive the BER formulation of the in-body communication model. Then system performances have been obtained by employing binary orthogonal PAM and BPSK modulation schemes. The results show that the BPSK technique can cover 5.5 cm at a high data rate of 20 Mbps but this reduces to less than 5 cm when using binary orthogonal PAM. These results obtained can be applied to future in-body cephalic area medical device design.

In Chapter 4, the I2O WBAN communication system is given, which establishes a communication system employing the human frontal thorax region. An accurate statistical I2O WBAN PL model is derived based on the signal propagation between the transmitter and receiver by using CST electromagnetic solvers in conjunction with a 3D heterogeneous human model under safety constraints. The BER evaluation for the I2O communication channel using multiple efficient modulation techniques, namely BPSK, QPSK, 16QAM and 16PSK, is demonstrated. The link budget is then analysed based on a predetermined acceptable BER performance of 10^{-3}. The results show that higher transmitter power can facilitate longer communication distances when using the same modulation approaches. Moreover, the BPSK technique outperforms the others considered, supporting a data rate of 30 Mbps over approximately 1.6 cm. 16QAM only supports 1 cm when utilising the minimum transmitting power of 1 μW.

In Chapter 5, various routing protocol solutions have been proposed to minimise the WBAN energy consumption [19, 20]. Relay-based routing protocols are demonstrated as effective methods to decrease the overall transmission distance and reduce the in-

body sensor node power consumption [21]. The linear mathematic programming models of selected important QoS metrics are assumed along with the corresponding subjective functions. A reliable and energy-efficient incremental relaying routing protocol for WBAN communication system is proposed and compared with the existing two-relay routing protocol scheme. The improvement of the proposed protocol is that the second relay will only start to convey collected information packets from in-body sensors to the external coordinator unless the first relay node fails. The results proved that the proposed routing scheme achieves better performance in terms of network lifetime, a number of transmitted data packets, and average energy consumption than the two-relay based routing technique.

Followed by the network power consumption model proposed in Chapter 5, a flexible QoS-aware model for WBASN communication is presented in Chapter 6. PPM modulation technology is shown as an effective method to overcome multi-user interference in WBASNs. This UWB-based ad hoc network model is investigated as an operative candidate to support extremely high data rate, adaptive schedule MAC control, and energy efficient. Moreover, the solution is able to balance the collision probability and power consumption. The results obtained in this chapter can be employed in the analysis and design of wireless e-health high-speed short distance applications.

In Chapter 7, research conclusion remarks are presented. Moreover, numerous future research topics are demonstrated and can be considered as the inspiration for future work in WBAN application design. It is greatly believed that the outcome presented in this thesis will help WBAN communication system engineers and researchers to develop more accurate WBAN channel models and QoS-aware data routing protocols.

7.2 Future work

WBANs have tremendous potential in providing optimal and secure e-health applications and services with the satisfactory QoS performance under the architecture that implements the health IoT scenario [1-3]. However, WBANs are a very new topic, and there are still a lot of unaddressed problems and research challenges in this area. Among all current standard proposals for future smart healthcare services, the ISM frequency band is the most mature and widely accepted for both industry and research communities. Analysis of the coexistence issue of IEEE 802.15.6 technique and other technologies such as WiFi and Bluetooth in the context of multi-parameter physiological monitoring is of great significant in future research work [4-7]. Moreover, the MAC protocol plays a crucial role in offering QoS support and in prolonging network lifetime by optimising the packet collision performance along with energy consumption [8-9]. The current commonly used technology standard, the IEEE 802.15.4 protocol, employs slotted carrier sense multiple access/collision avoidance [10]. However, there exist numerous technical challenges to satisfy specific requirements such as it the fact that it cannot support priority-based channel access capability to support the emergency medical message transmission [11-13]. Thus, energy efficient priority-based MAC protocols that can support both emergency and regular data transmission routing scheme are necessary for future work.

Data security issues are considered as the highest priority in communication networks but there is surprisingly little work in this area for WBANs. The authors in [3, 14] pointed out that security specifications in WBANs related to a series of factors: energy consumption, computational capability, data rate and inherent security vulnerabilities, and the majority of traditional communication networks have been reported that are not appropriate for WBAN systems [15]. In addition, the coordinator should be

capable of supporting key distribution secure data management such as data encryption and decryption and capability to manage the number of users within the same WBAN system in a secure manner during data association process [16-17].

Owing to the legal provisions, WBAN model experimental validation constitutes another significant topic of future studies [17-18]. In this regard, biological experiments can be implemented by deploying advanced computational electromagnetic technique, and biological tissue-equivalent phantoms. Moreover, multi-disciplinary incorporation with body sensors to measure data information transmission in living animals is a capable method that can develop accurate WBAN communication models that could overcome the limitations of carrying out physical measurements in the human body [19-20].

References

[1] E. Borgia, "The Internet of Things vision: key features, applications and open issues," *Computer Communications,* vol. 54, pp. 1-31, 2014.

[2] S. Li, L. Da Xu, and S. Zhao, "The internet of things: a survey," *Information Systems Frontiers,* vol. 17, no. 2, pp. 243-259, 2015.

[3] Y. Liao, M. S. Leeson, M. D. Higgins, and C. Bai, "Analysis of in-to-out wireless body area network systems: towards QoS-aware health Internet of Things applications," *Electronics,* vol. 5, no. 3, p. 38, 2016.

[4] M. Patel and J. Wang, "Applications, challenges, and prospective in emerging body area networking technologies," *IEEE Wireless Communications,* vol. 17, no. 1, pp. 80-88, 2010.

[5] K. S. Kwak, M. Ameen, D. Kwak, C. Lee, and H. Lee, "A study on proposed IEEE 802.15 WBAN MAC protocols," in *IEEE International Symposium on Communications and Information Technology*, Incheon, Korea, pp. 834-840, 2009.

[6] T. Hayajneh, G. Almashaqbeh, S. Ullah, and A. V. Vasilakos, "A survey of wireless technologies coexistence in WBAN: analysis and open research issues," *Wireless Networks,* vol. 20, no. 8, pp. 2165-2199, 2014.

[7] Y. Kim, S. Lee, and S. Lee, "Coexistence of ZigBee-based WBAN and WiFi for health telemonitoring systems," *IEEE Journal of Biomedical and Health Informatics,* vol. 20, no. 1, pp. 222-230, 2016.

[8] S. Bhandari and S. Moh, "A priority-based adaptive MAC protocol for wireless body area networks," *Sensors,* vol. 16, no. 3, p. 401, 2016.

[9] S. Bhandari and S. Moh, "A survey of MAC protocols for cognitive radio body area networks," *Sensors,* vol. 15, no. 4, pp. 9189-9209, 2015.

[10] Y. Liao, M. S. Leeson, and M. D. Higgins, "Flexible quality of service model for wireless body area sensor networks," *Healthcare Technology Letters,* vol. 3, no. 1, pp. 12-15, 2016.

[11] S. Gambhir and M. Kathuria, "DWBAN: Dynamic priority based WBAN architecture for healthcare system," in *Computing for Sustainable Global Development (INDIACom),* New Delhi, India, pp. 3380-3386, 2016.

[12] M. Li, W. Lou, and K. Ren, "Data security and privacy in wireless body area networks," *IEEE Wireless Communications,* vol. 17, no. 1, pp. 51-58, 2010.

[13] M. Barua, M. S. Alam, X. Liang, and X. Shen, "Secure and quality of service assurance scheduling scheme for wban with application to ehealth," in *IEEE Wireless Communications and Networking Conference (WCNC)* , Cancun, Mexico, pp. 1102-1106, 2011.

[14] S. N. Ramli, R. Ahmad, M. F. Abdollah, and E. Dutkiewicz, "A biometric-based security for data authentication in wireless body area network (wban)," in *International Conference on Advanced Communication Technology (ICACT),* PyeingChang, Korea, pp. 998-1001, 2013.

[15] A. Lounis, A. Hadjidj, A. Bouabdallah, and Y. Challal, "Healing on the cloud: Secure cloud architecture for medical wireless sensor networks," *Future Generation Computer Systems,* vol. 55, pp. 266-277, 2016.

[16] R. Lu, X. Lin, and X. Shen, "SPOC: A secure and privacy-preserving opportunistic computing framework for mobile-healthcare emergency," *IEEE Transactions on Parallel and Distributed Systems,* vol. 24, no. 3, pp. 614-624, 2013.

[17] D. He and S. Zeadally, "Authentication protocol for an ambient assisted living system," *IEEE Communications Magazine,* vol. 53, no. 1, pp. 71-77, 2015.

[18] L. Mi, G. Bao, and K. Pahlavan, "Design and validation of a virtual environment for experimentation inside the small intestine," in *Proceedings of the International Conference on Body Area Networks*, Boston, USA, pp. 35-40, 2013.

[19] D. Anzai *et al.*, "Experimental evaluation of implant UWB-IR transmission with living animal for body area networks," *IEEE Transactions on Microwave Theory and Techniques,* vol. 62, no. 1, pp. 183-192, 2014.

[20] D. G. Reina, S. L. Toral, F. Barrero, N. Bessis, and E. Asimakopoulou, "The role of ad hoc networks in the Internet of Things: A case scenario for smart environments," in *Internet of Things and Inter-Cooperative Computational Technologies for Collective Intelligence*: Springer, pp. 89-113, 2013.

Appendix A.

Path Loss Analysis

Currently, numerous approaches have been employed in electromagnetics simulation approaches in WBANs. To the best of the author's knowledge, CST is one of the most convenient software and widely used in many literature [1-3]. However, different parameter settings, such as accuracy control, the number of mesh cells, antenna type, software selection, background definition, and boundary condition selection will significant influence the simulated results. The essential steps in using CST is listed below and the related simulation parameters are summarised in Table A.1. Table A.2 lists calculation approaches to obtain PL in frequency domain results.

The essential steps in CST are summarised as follows:

- The demonstration of the human body models is reported in [4-5].
- Import human head model into CST. The background and the boundary condition should carefully define. As in Chapter 3, the material is defined as 'normal'. Boundary conditions are selected as 'open' boundaries because they are more suitable and closer to practice.
- Check dielectric properties of tissues and organs. At the same time, define material density (Rho as shown in CST) as 1000 kg/m^3.
- Since the interest frequencies are 2.4 GHz in Chapter 3, we select the frequency range of simulation from 0 to 3.5 GHz.

- Mesh definition. (Single calculation consumes around 2 hours in Chapter 3 and 30 minutes in Chapter 4, respectively). It should be noticed that the higher accuracy control settings lead to a larger number of meshcells and consume longer simulation running time.

- Select power loss density/SAR in the CST.

- Select '-40 dB' in the CST solver. The number of mesh cells is approximately 29 million for the Chapter 3. The transmitting voltage (location is fixed) and the corresponding voltage (moves horizontally) can be obtained in CST in multiple locations using the same simulation methods.

- Click 'Post Processing' in CST and select 'averaging method' as IEEE C95.3 technical standard. Specific absorption rate (SAR) then can be calculated employing the software's IEEE C95.3 averaging method over 10g of tissue with 1 W input power.

- Import all simulation results into MATLAB for further investigation. The method of PL calculation in MATLAB is listed below.

All simulation cases in this thesis regarding PL calculation for 'in-body to deep tissue implant' and 'in-body to on-body' scenarios are implemented employing a 3D electromagnetic solver CST. The simulations are carried out using the implantable dipole antennas up to a distance of 7 cm as demonstrated in Chapter 3 and 2 cm in Chapter 4. The number of meshcells in Chapter 3 and 4 are 29 million and 7 million, respectively. Similarly as [7], an example of the sequences (in Chapter 3) of s_1 and s_2 is demonstrated in Figure A.1 where Tx and Rx separation distance is 0.5 cm. After the calculation approaches mentioned in the Table A.2, the frequency domain results

are obtained as shown in Figure A.2 where Tx and Rx separation distance is 0.5 cm. Path loss calculation at different distance can be followed in the same manner.

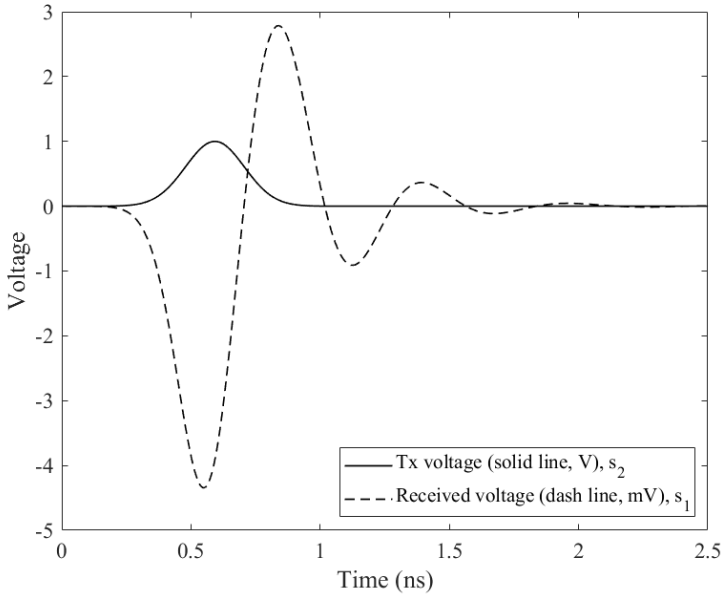

Figure A.1 An demonstration of sequences s_1 and s_2 (separation distance is 0.5 cm).

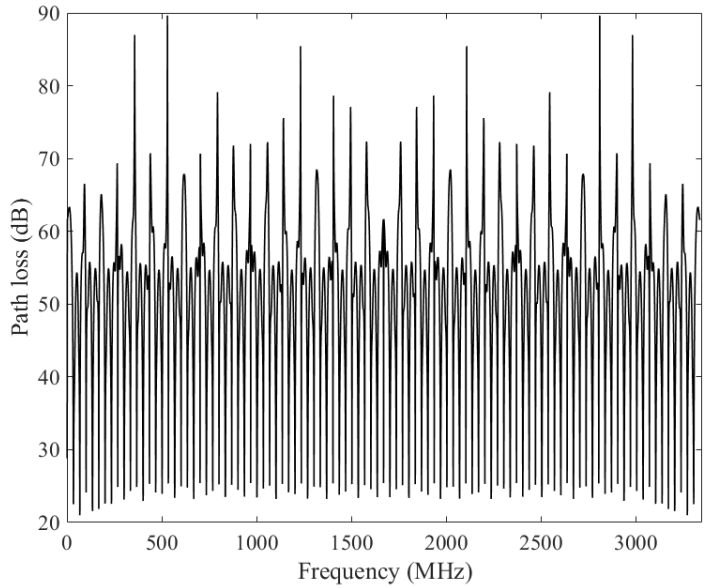

Figure A.2 An demonstration of frequency domain results (separation distance is 0.5 cm).

Table A.1 CST setting parameters in this thesis.

Parameter	Value (unit)	Brief description
Solver accuracy	-40 (dB)	High accuracy
Reference power in CST	1 (W)	In the same manner with [13-14].
Solver specials	Number of pulses =20	Default
Number of mesh cells (Chapter 3)	Around 29 million	Running time varies with the number of mesh cells and accuracy selection
Number of mesh cells (Chapter 4)	Around 7 million	In the same method with [16].
Boundary condition	Open	In the same method with [6]. Other methods reported [2, 7-8].
Material type	Normal	Define in CST
SAR calculation (10g)	2.4 (GHz)	Click 'Special' in CST. Averaging method select IEEE C95.3

Table A.2 PL value calculation in MATLAB.

Step	Brief description
Import obtained simulated values into MATLAB	Transform time-domain data to the frequency domain. Original signals are in time domain Define s_1 is the received voltage signal and s_2 is the transmitted voltage signal
Import s_1	s_1 signal is imported.
Import s_2	s_2 signal is imported
figure(); plot(20*log10(abs(fft(s1)./fft(s2))));	PL figure in frequency domain can be obtained.

Please note, different parameter settings, such as accuracy control, the number of mesh cells, antenna type, software selection, background definition, and boundary condition selection will significant influence the simulated results. We noticed that boundary condition method in intra-body communication system design consists of pyramidal microwave absorber [2], open boundary conditions [6], uniaxial perfect matching layer or perfectly matched layer [7-8]. In [13], the authors stated that the absorbing boundary condition employing a very high mode and a very high strength thickness with a minimum level of absorption at the outer boundary is 99.99%. Moreover, the majority of research literature do not present the accuracy control parameters, solver

specials and the number of meshcells [3, 9-12]. Therefore, in Appendix B, various key calculation results in the latest literature, such as SAR, PL exponent are listed for future research work.

A communication channel between transmitting antenna (Tx) and corresponding receiving antennas (Rx) can be obtained using a two-port linear network as reported in [8, 17]. Please note, a shift of the antenna resonance frequency may occur when located in a different transmission medium (or different tissues and body models), as demonstrated in [13], ISM band from 2.40 to 2.48 GHz, dipole antenna shows acceptable performance for intra-body region transmission. The output impedance of Tx is 50 Ω, and the Rx is 50 Ω, and thus PL can be defined as the ratio of the transmitted power to the received power in the two-port setup [8, 13, 17]. Assuming signal $s_1(t)$ of power P_{trans} is transmitted through an intra-body channel with corresponding received signal $s_2(t)$ of power P_{rec}, with the averaged over any random variations due to shadow fading effect. The PL of the communication channel can be seen as the value of the difference in dB between the transmitted and received signal power.

The path loss of the communication channel can be expressed as the ratio of the transmitted power to the received power:

$$PL|_{dB} = \frac{P_{trans}}{P_{rec}} \qquad (A.1)$$

Equation (1) can be rewritten as in dB as:

$$PL_{dB} = 10\log_{10}\frac{P_{trans}}{P_{rec}} \qquad (A.2)$$

To derive the PL model between the transmitting to receiving antenna as a function of distance, similar as [3], a semi-empirical formula based on the Friss formula can be expressed as:

$$PL_{dB}(d) = PL_{dB}(d_{ref}) + 10n\log_{10}\left(\frac{d}{d_{ref}}\right) + S_{dB} \qquad (A.3)$$

where $PL_{dB}(d_{ref})$ is the PL in dB at the reference distance d_0. n is the PL exponent, which equals to 2 in free space. Different reference distance d_0 values have been used in literature [1, 4, 12, 15] including 0.5 cm, 1 cm, 2.5 cm and even 10 cm in PL modelling work. In this thesis, we adopt 0.5 cm as the similar with [1]. In addition, numerous literature reported that PL exponent n is smaller than 2 both in measurement-based and simulation-based results. We summarise the latest PL model results in Appendix B.

References

[1]. M. Särestüniemi, T. Tuovinen, M. Hämäläinen, and J. Iinatti, "Finite integration technique for modelling of WBAN communication links in complex environments," in *International Symposium on Medical Information and Communication Technology (ISMICT),* Tokyo, Japan, pp. 154-158, 2013.

[2]. M. R. Basar *et al.*, "The use of a human body model to determine the variation of path losses in the human body channel in wireless capsule endoscopy," *Progress In Electromagnetics Research,* vol. 133, pp. 495-513, 2013.

[3]. A. Alomainy and Y. Hao, "Modeling and characterization of biotelemetric radio channel from ingested implants considering organ contents," *IEEE Transactions on Antennas and Propagation,* vol. 57, no. 4, pp. 999-1005, 2009.

[4]. M. I. Iacono *et al.*, "MIDA: a multimodal imaging-based detailed anatomical model of the human head and neck," *PloS One,* vol. 10, no. 4, p. e0124126, 2015.

[5]. Y. Liao, M. S. Leeson, and M. D. Higgins, "A communication link analysis based on biological implant wireless body area networks," *Applied Computational Electromagnetics Society Journal,* vol. 31, no. 6, pp. 619-628, 2016.

[6]. M. I. Jais *et al.*, "A novel 2.45 GHz switchable beam textile antenna (SBTA) for outdoor wireless body area network (WBAN) applications," *Progress In Electromagnetics Research,* vol. 138, pp. 613-627, 2013.

[7]. G. Noetscher, S. N. Makarov, and N. Clow, "Modeling accuracy and features of body-area networks with out-of-body antennas at 402 MHz," *IEEE Antennas and Propagation Magazine,* vol. 53, no. 4, pp. 118-143, 2011.

[8]. K. L. L. Roman, G. Vermeeren, A. Thielens, W. Joseph, and L. Martens, "Characterization of path loss and absorption for a wireless radio frequency link between an in-body endoscopy capsule and a receiver outside the body," *EURASIP Journal on Wireless Communications and Networking,* vol. 2014, no. 1, pp. 1-10, 2014.

[9]. A. F. Demir, Q. H. Abbasi, Z. E. Ankarali, M. Qaraqe, E. Serpedin, and H. Arslan, "Experimental characterization of in vivo wireless communication channels," in *IEEE Vehicular Technology Conference (VTC Fall),* Boston, USA, pp. 1-2, 2015.

[10]. C. Ong, J. Hee, T. See, and L. Ong, "Propagation studies of UWB transmission on human arm," in *Asia-Pacific Microwave Conference,* Macau, China, pp. 1-4, 2009.

[11]. R. Chávez-Santiago *et al.*, "Experimental path loss models for in-body communications within 2.36-2.5 GHz," *IEEE Journal of Biomedical and Health Informatics,* vol. 19, no. 3, pp. 930-937, 2015.

[12]. A. Stango, K. Y. Yazdandoost, F. Negro, and D. Farina, "Characterization of In-Body to On-Body Wireless Radio Frequency Link for Upper Limb Prostheses," *PloS One,* vol. 11, no. 10, p. e0164987, 2016.

[13]. D. Kurup *et al.*, "In-body path loss models for implants in heterogeneous human tissues using implantable slot dipole conformal flexible antennas," *EURASIP Journal on Wireless Communications and Networking,* vol. 2011, no. 1, p. 51, 2011.

[14]. D. Kurup, W. Joseph, G. Vermeeren, and L. Martens, "In-body path loss model for homogeneous human muscle, brain, fat and skin," in *Proceedings of the Fourth European Conference on Antennas and Propagation (EuCAP),* Barcelona, Spain, pp. 1-4, 2010.

[15]. A. Fort, C. Desset, J. Ryckaert, P. De Doncker, L. Van Biesen, and P. Wambacq, "Characterization of the ultra wideband body area propagation channel," in *IEEE International Conference on Ultra-Wideband,* Zurich, Switzerland, pp. 22-27, 2005.

[16]. D. Kurup, G. Vermeeren, E. Tanghe, W. Joseph, and L. Martens, "In-to-out body antenna-independent path loss model for multilayered tissues and heterogeneous medium," *Sensors,* vol. 15, no. 1, pp. 408-421, 2014.

[17]. D. Kurup, W. Joseph, G. Vermeeren, and L. Martens, "Path loss model for in-body communication in homogeneous human muscle tissue," *Electronics Letters,* vol. 45, no. 9, pp. 453-454, 2009.

Appendix B.

Comparison with Literature Results

Since there is no agreement in PL simulation parameter settings, we have compared our results with the latest literature in Appendix B. In this section, we list various results reported in the literature in this area. We hope this can help researchers for further investigation in this open research topic.

Table 2 summarises the PL models for numerous homogeneous tissue models [1-3], and Table 3 lists the PL for copious heterogeneous human body models reported in [4-12]. Moreover, Table 4 illustrates the latest results regarding SAR calculation and Table 5 shows noise figure values in WBANs. Apart from PL calculation, energy absorption is another a key parameter when designing the intra-body communication system. Generally, this issue is investigated by using SAR (unit in W/kg) and regulated by technical standards including the IEEE and ICNIRP to guarantee human body safety. In this section, numerous results regarding SAR calculation have been listed and compared with the results in this thesis. The authors in [13] demonstrated that the SAR values are related to the operating frequencies and human body models. Employing a power of 1 W, the 5 year-old human model achieves the highest SAR value (around 0.07 W/kg) whereas the adult head model obtains the minimal value (at 0.006 W/kg) at 2.4 GHz. When considering the whole-body model conditions, the Japanese female model is the highest (at around 0.072 W/kg) and the Korean body model is the smallest (around 0.035 W/kg), which are quite close to the results

proposed in Chapter 4. In [14], the results proved that the maximum 10g averaged SAR value is 0.183 W/kg when the input power is 1 W. In [15], the authors reported that the SAR value is 0.00041 W/kg when the delivered power is 1 W at 2.45 GHz. Similar results can be found in [16], the authors reported that the SAR values are related to the separating distance between the transmitter and receiver. The SAR values proposed in [16] range from 0.088 to 0.14 W/kg, which are quite similar to the results reported in Chapter 3. [17] illustrated that the maximum SAR (10g) value is 0.03762 W/kg when the input power is 1 W and the authors in [18] proved that the maximum 10g average SAR value for implantable applications is around 0.003367 W/kg at 2.4 GHz, which is slightly smaller than our results obtained in Chapter 3. The results in [19] demonstrated that the 10g volume averaged SAR is 0.13 W/kg where it is quite similar to our results. An experiment-based research [20] showed that 10g average SAR results are around 0.05 W/kg (body model) and approximately 0.045 W/Kg (body model+ bond plate), respectively. In addition, there is no agreement in noise figure calculation approaches [21-28]. To date, the majority research just assumes the noise figure value around 3 to 5 [22-25]. Some measurement-based work shows very small value 0.9 or very large value approximately around 6 [21, 27]. The IEEE 802.15.6 technical report stated noise figure is 8 for all communication scenarios [28]. we have listed noise figure values in WBANs in Appendix B for future research.

Table B.1 Comparison of different PL models (homogeneous cases).

Reference	$PL_{dB}(d_{ref})$	n	σ_{dB}
This thesis	(Dry skin) 30.17	1.608	1.534
	(Muscle) 37.08	1.964	3.623
	(Grey matter) 37.97	1.631	0.658
	(White matter) 36.97	1.644	1.101
Demir [1-2]	(Heart) 22.7	1.96	2.38
	(Posterior) 40.53	1.76	2.34
Roman [3]	(Skin) 56.81	3	0.16
	(Muscle) 57.69	3.17	0.18

Table B.2 PL values for heterogeneous human body models reported in the literature.

Reference	PL exponent *n*		
Chapter 3	2.6		
Alomainy [4]	Frequency	Measured	Simulated
	402 MHz	1.90	1.85
	868 MHz	2.00	1.90

	2.4 GHz	2.80	2.60
Demir [5]	Frequency	Measured	Simulated
	915 MHz	1.90	1.85
	2.4 GHz	2.80	2.60
Ong [6]	*n* ranges from 0.99 to 3.04		
Chávez-Santiago [7]	0.9		
Stango [8]	2.7		
Sard [9]	2.1		
Sayrafian-Pour [10]	Implant to on-body scenario		
	Deep tissue		4.26
	Near surface		4.22
	Implant to implant scenario		
	Deep tissue		6.26
	Near surface		4.99
Roman [11]	7.91 (child model) 7.10 (adult model)		
Zhao [12]	2.1-2.9 (female model) 2.4-3.4 (male model)		

Table B.3 SAR value averaged over 10g in literature.

Reference	SAR value (over 10g)
Conil [13]	0.07 W/Kg (5-year-old human model) 0.006 W/Kg (adult head model)
Agarwal [14]	0.072 W/Kg (Japanese Female model) 0.035 W/Kg (Korean body model)
Khan [15]	0.00041 Kg/W
Giman [16]	0.088 (at 60 mm) 0.14 (at 40 mm)
Hassan [17]	0.03762 W/Kg
Li [18]	0.003367 W/Kg
Zakaria [19]	0.13 W/Kg
Othman [20]	0.05 W/Kg (body model) 0.045 W/Kg (body model + bond plate)

Table B.4 Noise figure in literature.

Reference	Noise figure (dB)	Comments
This thesis	3	Typical value
Borton [21]	0.9	Experiment based result
Daoud [22]	1.1	2.45 GHz, measured
Kurup [23]	3.5	Implanted dipole antenna
Zakaria [24]	3.5	Simulated-based
Qiu [25]	4	Simulation-based
Oh [26]	5	Simulated-based
Wong [27]	6	Measured-based
Cheffena [28]	8	Noise figure values (implant-to-implant, implant-to-surface, surface-to-surface) all equal to 8

References

[1]. A. F. Demir *et al.*, "Anatomical Region-specific in vivo wireless communication channel characterization," *IEEE Journal of Biomedical and Health Informatics*, vol. PP, no. 99, pp. 1-1, 2016.

[2]. A. F. Demir, Q. H. Abbasi, Z. E. Ankarali, E. Serpedin, and H. Arslan, "Numerical characterization of in vivo wireless communication channels," in *IEEE MTT-S International Microwave Workshop Series on RF and Wireless Technologies for Biomedical and Healthcare Applications*, London, UK, pp. 1-3, 2014.

[3]. K. Lopez-Linares Roman, G. Vermeeren, A. Thielens, W. Joseph, and L. Martens, "Characterization of path loss and absorption for a wireless radio frequency link between an in-body endoscopy capsule and a receiver outside the body," *EURASIP Journal on Wireless Communications and Networking*, vol. 2014, no. 1, p. 21, 2014.

[4]. A. Alomainy and Y. Hao, "Modeling and characterization of biotelemetric radio channel from ingested implants considering organ contents," *IEEE Transactions on Antennas and Propagation*, vol. 57, no. 4, pp. 999-1005, 2009.

[5]. A. F. Demir, Q. H. Abbasi, Z. E. Ankarali, M. Qaraqe, E. Serpedin, and H. Arslan, "Experimental characterization of in vivo wireless communication channels," in *IEEE Vehicular Technology Conference (VTC Fall)*, Boston, USA, pp. 1-2, 2015.

[6]. C. Ong, J. Hee, T. See, and L. Ong, "Propagation studies of UWB transmission on human arm," in *Asia-Pacific Microwave Conference*, Macau, China, pp. 1-4, 2009.

[7]. R. Chávez-Santiago *et al.*, "Experimental path loss models for in-body communications within 2.36-2.5 GHz," *IEEE Journal of Biomedical and Health Informatics*, vol. 19, no. 3, pp. 930-937, 2015.

[8]. A. Stango, K. Y. Yazdandoost, F. Negro, and D. Farina, "Characterization of In-Body to On-Body Wireless Radio Frequency Link for Upper Limb Prostheses," *PloS One*, vol. 11, no. 10, p. e0164987, 2016.

[9]. A. Sard, Y. Hao, Y. Zhao, S. Lee, and G. Z. Yang, "Subject-specific analysis of the on-body radio propagation channel adopting a parallel FDTD code," in *Proceedings of the European Conference on Antennas and Propagation*, Barcelona, Spain, pp. 1-3, 2010.

[10]. K. Sayrafian-Pour, W.-B. Yang, J. Hagedorn, J. Terrill, and K. Y. Yazdandoost, "A statistical path loss model for medical implant communication channels," in *IEEE International Symposium on Personal, Indoor and Mobile Radio Communications*, Tokyo, Japan, pp. 2995-2999, 2012.

[11]. K. L. Roman, G. Vermeeren, A. Thielens, W. Joseph, and L. Martens, "Characterization of path loss and absorption for a wireless radio frequency link between an in-body endoscopy capsule and a receiver outside the body," *EURASIP Journal on Wireless Communications and Networking*, vol. 2014, no. 1, p. 21, 2014.

[12]. Y. Zhao, A. Sani, Y. Hao, S. Lee, and G. Yang, "A subject-specific radio propagation study in wireless body area networks," in *Loughborough Antennas & Propagation Conference*, Loughborough, UK, pp. 80-83, 2009.

[13]. E. Conil, A. Hadjem, F. Lacroux, M. Wong, and J. Wiart, "Variability analysis of SAR from 20 MHz to 2.4 GHz for different adult and child models using finite-difference time-domain," *Physics in Medicine and Biology*, vol. 53, no. 6, p. 1511, 2008.

[14]. K. Agarwal and Y.-X. Guo, "Interaction of electromagnetic waves with humans in wearable and biomedical implant antennas," in *Asia-Pacific Symposium on Electromagnetic Compatibility*, Taipei, Taiwan, pp. 154-157, 2015.

[15]. S. Khan, N. Ahmad, and M. Naeem, "The reduction rate at different frequencies," *Journal of Engineering and Applied Sciences,* vol. 34, no. 2, pp. 71-75, 2015.

[16]. F. N. Giman *et al.,* "Conformal dual-band textile antenna with meta surface for WBAN application," *Applied Physics A,* vol. 123, no. 1, p. 32, 2017.

[17]. S. Hassan and S. H. Shehab, "Evaluation of an ultra wideband (UWB) textile antenna in the vicinity of human body model for WBAN applications," in *IEEE International Conference on Electrical and Computer Engineering,* Dhaka, Bangladesh, pp. 195-198, 2015.

[18]. Z. Li, Y. Pang, J. Lin, J. Liu, S. Liu, and C. Li, "SAR computation and channel codeling of body area networks," in *International Conference on Biomedical Engineering,* Singapore, pp. 72-75, 2014.

[19]. D. Zakaria, F. Y. Zulkifli, and E. T. Rahardjo, "Implanted helical dipole antenna for UHF band applications," in *International Symposium on Antennas and Propagation,* Nagoya, Japan, pp. 1256-1259, 2012.

[20]. N. Othman, N. Samsuri, M. Rahim, and N. Elias, "SAR in the presence of conductive medical implant at 0.9, 1.8 and 2.4 GHz due to close proximity antenna," in *European Conference on Antennas and Propagation,* Davos, Switzerland, pp. 1-5, 2016.

[21]. D. A. Borton, M. Yin, J. Aceros, and A. Nurmikko, "An implantable wireless neural interface for recording cortical circuit dynamics in moving primates," *Journal of Neural Engineering,* vol. 10, no. 2, p. 026010, 2013.

[22]. M. Daoud, H. Mnif, and M. Ghorbel, "A low power low noise amplifier for 2.45 GHz ISM receiver for body area network," in *International Design & Test Symposium (IDT)*, Hammamet, Tunisia, pp. 296-301, 2016.

[23]. D. Kurup, G. Vermeeren, E. Tanghe, W. Joseph, and L. Martens, "In-to-out body antenna-independent path loss model for multilayered tissues and heterogeneous medium," *Sensors,* vol. 15, no. 1, pp. 408-421, 2014.

[24]. D. Zakaria, F. Y. Zulkifli, and E. T. Rahardjo, "Implanted helical dipole antenna for UHF band applications," in *International Symposium on Antennas and Propagation,* Nagoya, Japan, pp. 1256-1259, 2012.

[25]. Y. Qiu, Y. Chen, and D. Haley, "SNR estimation and decision making using hypothesis testing in energy-efficient adaptive modulation," in *Annual International Symposium on Personal, Indoor, and Mobile Radio Communication,* Tokyo, Japan, pp. 1949-1953, 2014.

[26]. J. Y. Oh, J. H. Kim, H. S. Lee, and J. Y. Kim, "New modulation scheme for high data rate implantable medical devices," in *International Symposium on Communications and Information Technology*, Incheon, Korea, pp. 1464-1467, 2009.

[27]. A. C. W. Wong *et al.*, "A 1 V 5 mA multimode IEEE 802.15. 6/Bluetooth low-energy WBAN transceiver for biotelemetry applications," *IEEE Journal of Solid-State Circuits,* vol. 48, no. 1, pp. 186-198, 2013.

[28]. M. Cheffena, "Performance evaluation of wireless body sensors in the presence of slow and fast fading effects," *IEEE Sensors Journal*, vol. 15, no. 10, pp. 5518-5526, 2015.